

แอดไมเซิลและแอดโซลูบิลไเซชันด้วยสารลดแรงตึงผิวที่สามารถเกิดปฏิกิริยาโพลีเมอร์ไรซ์ได้บนพื้นผิวออกไซด์



นางสาวเอมมา อาสนจินดา

ศูนย์วิทยทรัพยากร  
จุฬาลงกรณ์มหาวิทยาลัย

วิทยานิพนธ์นี้เป็นส่วนหนึ่งของการศึกษาตามหลักสูตรปริญญาวิทยาศาสตรดุษฎีบัณฑิต

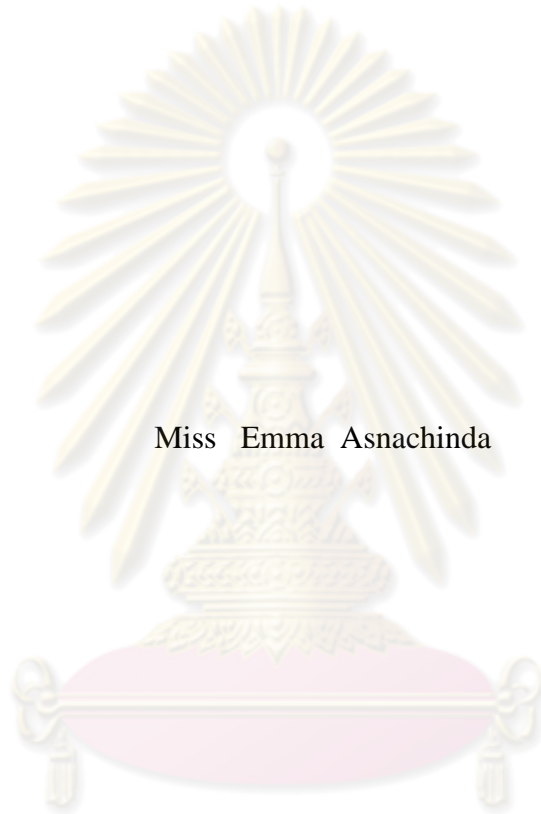
สาขาวิชาการจัดการสิ่งแวดล้อม (สหสาขาวิชา)

บัณฑิตวิทยาลัย จุฬาลงกรณ์มหาวิทยาลัย

ปีการศึกษา 2552

ลิขสิทธิ์ของจุฬาลงกรณ์มหาวิทยาลัย

ADMICELLES AND ADSOLUBILIZATION  
USING POLYMERIZABLE SURFACTANTS  
ONTO SOLID OXIDE SURFACE



Miss Emma Asnachinda

ศูนย์วิทยทรัพยากร  
จุฬาลงกรณ์มหาวิทยาลัย

A Dissertation Submitted in Partial Fulfillment of the Requirements  
for the Degree of Doctor of Philosophy Program in Environmental Management

(Interdisciplinary Program)

Graduated School

Chulalongkorn University

Academic year 2009

Copyright of Chulalongkorn University

THESIS TITLE ADMICELLES AND ADSOLUBILIZATION USING  
POLYMERIZABLE SURFACTANT ONTO SOLID OXIDE  
SURFACE

By Miss Emma Asnachinda

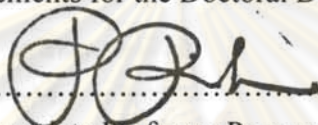
Field of Study Environmental Management

Thesis Advisor Associate Professor Sutha Khaodhiar, Ph.D.

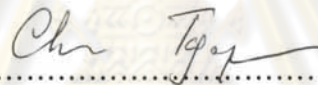
Thesis Co-advisor Professor David A. Sabatini, Ph.D.

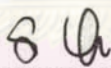
---

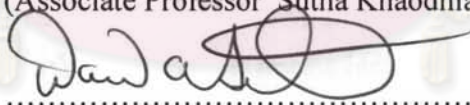
Accepted by the Graduated School, Chulalongkorn University in Partial  
Fulfillment of the Requirements for the Doctoral Degree


 ..... Dean of the Graduated School  
(Associate Professor Pornpote Piumsomboon, Ph.D.)


THESIS COMMITTEE


 ..... Chairman  
(Chantra Tongcumpou, Ph.D.)

 ..... Thesis Advisor  
(Associate Professor Sutha Khaodhiar, Ph.D.)

 ..... Thesis Co-advisor  
(Professor David A. Sabatini, Ph.D.)

 ..... Examiner  
(Punjaporn Wechayanwiwat, Ph.D.)

 ..... Examiner  
(Patiparn Punyapalakul, Ph.D.)

 ..... External Examiner  
(Aranya Fuangswasdi, Ph.D.)

เอมมา อาสนจินดา : แอดไมเซลและแอดโซลูบิไลเซชันด้วยสารลดแรงตึงผิวที่สามารถเกิดปฏิกิริยาโพลีเมอร์ไรซ์ได้บนพื้นผิวออกไซด์. (ADMICELLES AND ADSOLUBILIZATION USING POLYMERIZABLE SURFACTANTS ONTO SOLID OXIDE SURFACE) อ.ที่ปรึกษาวิทยานิพนธ์หลัก : รศ. ดร. สุธา ขาวเจียร, อ.ที่ปรึกษาวิทยานิพนธ์ร่วม: PROF. DAVID A. SABATINI, PH.D., 133 หน้า.

ตัวกลางสำหรับการดูดซับที่เพิ่มประสิทธิภาพด้วยสารลดแรงตึงผิวควบคู่กับพื้นผิวชนิดต่างๆ ได้มีการพัฒนาผ่านกระบวนการดูดซับโดยการแอดโซลูบิไลเซชัน อย่างไรก็ตาม การสูญเสียสารลดแรงตึงผิวเกิดขึ้นได้จากกระบวนการดีสorption ซึ่งมีผลในแง่ลบต่อเสถียรภาพของตัวกลางดังกล่าว งานวิจัยนี้มีเป้าหมายในการลดปริมาณการสูญเสียของสารลดแรงตึงผิวบนตัวกลางที่ได้รับการเพิ่มประสิทธิภาพโดยการโพลีเมอร์ไรซ์แอดไมเซล (ชั้นหรือการเรียงตัวของสารลดแรงตึงผิวที่ถูกดูดซับบนตัวกลาง) ของสารลดแรงตึงผิวนั้น รวมไปถึงการพิจารณาความสามารถในการกำจัดสารอินทรีย์ปนเปื้อนโดยใช้กระบวนการของการดูดซับร่วมกับสารลดแรงตึงผิว งานวิจัยนี้ยังมีจุดประสงค์ในการพิจารณาการเกิดขึ้นของฟิล์มโพลีเมอร์ที่ได้จากกระบวนการแอดไมเซลโพลีเมอร์ไรเซชันโดยใช้เครื่องมือที่มีความสามารถวิเคราะห์ในระดับนาโนเมตรเรียกว่า Atomic Force Microscopy (AFM) นอกจากนี้การวิเคราะห์โดยใช้หลักของมุมสัมผัสบนพื้นผิววัด (Contact Angle Measurement) ยังมีส่วนช่วยในการพิจารณาฟิล์มดังกล่าวอีกด้วย สารลดแรงตึงผิวที่ใช้ในงานวิจัยนี้ได้แก่สารลดแรงตึงผิวแบบสองหัวที่สามารถเกิดปฏิกิริยาโพลีเมอร์ไรซ์ได้ โดยมีพันธะคู่อยู่ที่ส่วนหางของโครงสร้างสารลดแรงตึงผิวดังกล่าว นอกจากนี้ DTAB ซึ่งเป็นสารลดแรงตึงผิวแบบดั้งเดิมได้ถูกนำมาใช้เพื่อเปรียบเทียบความสามารถระหว่างสารลดแรงตึงผิวแบบสองหัวที่สามารถเกิดปฏิกิริยาโพลีเมอร์ไรซ์ได้นี้ด้วย จากผลการศึกษาพบว่าสารลดแรงตึงผิวแบบสองหัวที่สามารถเกิดปฏิกิริยาโพลีเมอร์ไรซ์ได้นี้ มีความสามารถในการดูดซับมากกว่าสารลดแรงตึงผิวที่เกิดจากมอนอเมอร์ของมันเองและสารลดแรงตึงผิวแบบดั้งเดิม ทั้งนี้ยังสามารถเข้าถึงประสิทธิภาพในการดูดซับสูงสุดได้ก่อนโดยใช้ความเข้มข้นของสารลดแรงตึงผิวน้อยกว่า ในการศึกษากระบวนการแอดโซลูบิไลเซชันของสารลดแรงตึงผิวได้มีการนำสไตรีนและฟีนิลเอทานอลมาใช้เพื่อเป็นตัวแทนของสารอินทรีย์ที่มีขั้วอ่อนและสูงตามลำดับ จากการศึกษาพบว่าแอดโซลูบิไลเซชันจะมีค่ามากที่สุดเมื่อประสิทธิภาพการดูดซับของสารลดแรงตึงผิวบนพื้นผิวของของเหลวและของแข็งมีค่ามากที่สุดและโครงสร้างของสารลดแรงตึงผิวนั้นมีการเรียงตัวแบบสองชั้นอย่างสมบูรณ์ ทั้งนี้พบว่ากระบวนการโพลีเมอร์ไรซ์ไม่มีผลต่อประสิทธิภาพของแอดโซลูบิไลเซชันทั้งของสไตรีนและฟีนิลเอทานอลเลย โดยประสิทธิภาพในการแอดโซลูบิไลซ์ของสไตรีนจะเกิดขึ้นที่ส่วนกลางของโครงสร้างในแอดไมเซลเป็นหลัก เนื่องจากพื้นที่ในบริเวณนี้สามารถขยายตัวเพื่อรองรับโมเลกุลของสไตรีนที่เพิ่มขึ้นได้ ในทางกลับกัน กระบวนการแอดโซลูบิไลเซชันของฟีนิลเอทานอลมักจะเกิดขึ้นที่ส่วนพาลีเสด ซึ่งเป็นบริเวณที่อยู่ใกล้ส่วนหัวของสารลดแรงตึงผิว สำหรับการศึกษาเพื่อลดการสูญเสียของสารลดแรงตึงผิวพบว่า สารลดแรงตึงผิวแบบสองหัวที่สามารถเกิดปฏิกิริยาโพลีเมอร์ไรซ์ได้มีการสูญเสียน้อยกว่าสารลดแรงตึงผิวแบบอื่นที่นำมาทดลอง โดยจะเห็นได้ชัดว่ามีการสูญเสียของสารลดแรงตึงผิวจากตัวกลางดูดซับหลังจากได้ทำการล้างตัวกลางที่เพิ่มประสิทธิภาพโดยใช้สารลดแรงตึงผิวแบบดั้งเดิม

สาขาวิชา.....การจัดการสิ่งแวดล้อม.....

ปีการศึกษา 2552.....

ลายมือชื่อ..... เอ็มมา อาสนจินดา

ลายมือชื่อ.....อ.ที่ปรึกษาวิทยานิพนธ์หลัก.....

ลายมือชื่อ.....อ.ที่ปรึกษาวิทยานิพนธ์ร่วม.....

## 4889708320 : MAJOR ENVIRONMENTAL MANAGEMENT  
 KEYWORDS : POLYMERIZABLE SURFACTANT / ADMICELLE /  
 ADSORPTION / ADSOLUBILIZATION

EMMA ASNACHINDA : ADMICELLES AND ADSOLUBILIZATION  
 USING POLYMERIZABLE SURFACTANTS ONTO SOLID OXIDE  
 SURFACE. THESIS ADVISOR: ASSOC. PROF. SUTHA KHAODHIAR,  
 PH.D., THESIS CO-ADVISOR: PROF. DAVID A. SABATINI, PH.D.,  
 133 pp.

Various surfactant and solid surface systems have been evaluated for surface modification through surfactant adsorption and adsolubilization processes. However, surfactant-modified surfaces face the challenge of substantial losses due to desorption which negatively impacts the stability of that surfactant-modified surfaces. This research aims to minimize the amount of surfactant desorbed from the surface by polymerization of the admicelle (adsorbed surfactant aggregate/layer) including examining the ability of surfactant modified adsorbent to remove organic contaminant through the surfactant-based adsorption process. The objectives of this study extend to verify the presence of the polymer thin film formed via admicellar polymerization by atomic force microscopy (AFM) which allows the film to be studied at the nanometer scale. Along with the AFM examination, the contact angle of the admicellar-modified mica surface has been characterized to help examine these objectives. Surfactants used in this study were polymerizable gemini surfactant that is gemini surfactant containing a polymerizable group (double bond) in the tail structure. Furthermore, the comparison with conventional cationic non-polymerizable surfactant, DTAB, was additionally evaluated. Polymerizable gemini surfactant show higher surfactant adsorption than the monomeric and conventional surfactant. The polymerizable gemini surfactant also reached its maximum adsorption capacity at a lower aqueous surfactant concentration. Styrene and phenylethanol were selected to represent as weak and strong polar organic solutes in adsolubilization study, respectively. Adsolubilization reaches its maximum when surfactant adsorbed onto the solid-liquid interface with the complete bilayer formation and/or maximum adsorption. The impact of polymerization process on the adsolubilization of styrene and phenylethanol was not observed. Styrene increases its adsolubilization capacity to the core where it can expand to facilitate more solute molecules. In the other hand, phenylethanol adsolubilization was preferential related to the palisade region of admicelle structure. Lower desorption of gemini over non-gemini surfactant were observed, and increased stability of polymerized admicelles as reflected by their resistance to desorption. In addition, it was apparent that conventional surfactant bilayer readily desorbs during washing.

Field of Study : Environmental Management

Academic Year : 2009

Student's Signature เอมมา อสนาจินดา

Advisor's Signature Dr. Sutha Khaodhiar

Co-Advisor's Signature Dr. David A. Sabatini

## ACKNOWLEDGEMENTS

Financial support for this work was provided by the National Center of Excellence for Environmental and Hazardous Waste Management (NCE-EHWM), Chulalongkorn University, Thailand. In addition, financial support for this research was received from The 90<sup>th</sup> Years Anniversary of Chulalongkorn University (Ratchadphiseksomphot Endowment Fund), Chulalongkorn University. In addition, financial support for this research was received from the industrial sponsors of the Institute for Apply Surfactant Research (IASR), University of Oklahoma, including Akzo Noble, Clorox, Conoco/Phillips, Church & Dwight, Ecolab, Halliburton, Dow Chemical, Huntsman, Oxiteno, Procter & Gamble, Sasol and Shell. Also, funds from the Sun Oil Company Chair (DAS) at the University of Oklahoma helped support this research. We thank Prof. Tsubone from the Faculty of Science and Technology, and the Institute of Colloid and Interface Science, Tokyo University of Science, Japan. for providing us with the polymerizable surfactants samples for this research.

I appreciate very much the efforts of my advisors, Assoc. Prof. Sutha Khaodhiar, and Prof. David A. Sabatini for their encouragement, guidance, and the support provided throughout this study. I would like to thank Prof. Sabatini for his time and laboratory support at the University of Oklahoma, Norman, Oklahoma, USA. The appreciation would extend to Associate Prof. John H. O'Haver for his time guidance and laboratory support at the University of Mississippi, Oxford, Mississippi, USA. I would like to thank Dr. Chun Hwa See, and Miss Ramnaree Netvichian for their time, guidance, suggestion and valuable comments for this study. I would also like to thank the members of my committee, Dr. Chantra Tongcumpou, Dr. Patiparn Punyapalukul, Dr. Punjaporn Weschayanwiwat and Dr. Aranya Fuangswasdi, also my colleagues, Dr. Ampira Charoenseang and Miss Chodchanok Attaphong.

Finally, I am proud to dedicate this dissertation with respect to my beloved parents, Associate Prof. Pongpor and Pacharaporn, my sister and brother, Pongpanor and Dr. Pattarapong Asnachinda, and my beloved, Mr. Kitti Setavoraphan, for their love, encouragement, understanding, and their support through the years.

## TABLE OF CONTENTS

	<b>Page</b>
ABSTRACT (THAI).....	iv
ABSTRACT (ENGLISH).....	v
ACKNOWLEDGEMENTS.....	vi
TABLE OF CONTENTS.....	vii
LIST OF FIGURES.....	xi
LIST OF TABLES.....	xiii
LIST OF APENDIX FIGURES.....	xiv
LIST OF APENDIX TABLES.....	xv
<b>CHAPTER I : INTRODUCTION</b> .....	<b>1</b>
1.1 INTRODUCTION.....	1
1.2 OBJECTIVES .....	2
1.3 SCOPES OF THE STUDY.....	3
1.4 HYPOTHESES .....	3
<b>CHAPTER II : THEORETICAL BACKGROUNDS AND LITERATURE REVIEWS</b> .....	<b>5</b>
2.1 SURFACTANT PHENOMENA.....	5
2.2 ADSORPTION OF IONIC SURFACTANTS ONTO METAL OXIDE SURFACES.....	7
2.2.1 Surfactant Adsorption Phenomena.....	7
2.2.2 The Adsorption of Silicon Oxide Surface and its Structure ....	9
2.2.3 Influence Parameters of Surfactant Adsorption.....	10
2.2.3.1 Influence of Solution pH.....	10
2.2.3.2 Influence of Electrolyte Concentration.....	11
2.2.3.3 Influence of Temperature.....	11
2.3 ADSOLUBILIZATION OF ORGANIC SOLUTES.....	12
2.4 GEMINI SURFACTANT AND POLYMERIZABLE SURFACTANTS.....	14
2.4.1 Gemini Surfactant .....	14
2.4.2 Polymerizable Surfactant.....	15

	<b>Page</b>
2.4.3 Polymerizable Gemini Surfactant.....	15
2.5 DISPERSION STABILITY AND SURFACE MODIFICATION BY POLYMERIZABLE SURFACTANTS.....	16
2.6 ADMICELLAR POLYMERIZABLE AND ULTRATHIN POLYMER FILM.....	17
2.7 EFFECT PARAMETERS TO POLYMERIZATION OF SURFACTANTS.....	18
2.7.1 Dissolved Oxygen.....	18
2.7.2 Position of Polymerizable Group in the Surfactant Structure...	18
<b>CHAPTER III : RESEARCH METHODOLOGY.....</b>	<b>19</b>
3.1 MATERIALS.....	19
3.1.1 Surfactants.....	19
3.1.2 Organic Solutes.....	20
3.1.3 Adsorbent.....	20
3.2 EXPERIMENTAL SECTION.....	21
3.2.1 CMC Measurement.....	21
3.2.2 Surfactant Adsorption Study.....	21
3.2.3 Surfactant Polymerization Study.....	22
3.2.4 Adsolubilization Study.....	22
3.2.5 Surfactant Desorption Study.....	23
3.2.6 Surfactant Surface Characterization Study.....	23
3.3 ANALYTICAL METHOD.....	24
<b>CHAPTER IV : EFFECT OF IONIC HEAD GROUP ON ADMICELLE FORMATION BY POLYMERIZABLE SURFACTANTS.....</b>	<b>25</b>
4.1 ABSTRACT.....	25
4.2 INTRODUCTION .....	25
4.3 BACKGROUND .....	26
4.3.1 Polymerizable Surfactants .....	26
4.3.2 Gemini and Polymerizable Gemini Surfactants .....	27
4.4 HYPOTHESIS .....	28
4.5 MATERIALS AND ANALYTICAL SECTION .....	29



	<b>Page</b>
4.5.1 Materials.....	29
4.5.2 Analytical Method .....	30
4.5.3 Determination of the Adsorption Isotherm.....	30
4.5.4 Determination of the Surfactant Polymerization.....	31
4.5.5 Determination of the Effect of Polymerization on the Dispersion Stability of Silica.....	32
4.5.6 Determination of the Surfactant Desorption.....	32
4.6 RESULT.....	32
4.6.1 Adsorption Studies.....	32
4.6.2 Polymerization of Surfactants.....	34
4.6.3 Effect of Polymerization on the Dispersion Stability of Silica..	35
4.6.4 Surfactant Desorption Studies.....	37
4.7 DISCUSSION.....	40
<b>CHAPTER V : SATOMIC FORCE MICROSCOPY AND CONTACT ANGEL MEASUREMENT STUDIES OF POLYMERIZABLE SURFACTANT ADMICELLE ON MICA.....</b>	<b>42</b>
5.1 ABSTRACT .....	42
5.2 INTRODUCTION .....	42
5.3 EXPERIMENTAL SECTION .....	45
5.3.1 Materials .....	45
5.3.2 Atomic Force Microscopy.....	46
5.3.2.1 AFM Force Measurement.....	47
5.4 CONTACT ANGEL MEASUREMENT .....	47
5.5 SAMPLE PREPARATION.....	48
5.5.1 Characterization of Modified-mica Surface.....	48
5.5.2 Characterization of Styrene Adsolubilized in PG Aggregates Adsorbed on Modified-polymerize Mica Discs.....	48
5.5.3 Determination of Surfactant Desorption.....	49
5.6 RESULT AND DISCUSSION.....	50
5.6.1 Unmodified-mica.....	50
5.6.2 Adsorption of PG on Mica.....	52
5.6.3 Polymerization of PG on Mica.....	53
5.6.4 Adsolubilization of Styrene onto Polymerized-surfactant- modified Mica Surfaces.....	53

	<b>Page</b>
5.6.5 Desorption of PG on Mica.....	56
5.7 CONCLUSION.....	58
<b>CHAPTER VI : STYRENE AND PHNYLETHANOL ADSOLUBILIZATION OF POLYMERIZABLE GEMINI SURFACTANT</b>	<b>59</b>
6.1 ABSTRACT.....	59
6.2 INTRODUCTION.....	59
6.3 BACKGROUND.....	60
6.3.1 Adsolubilization of Surfactant onto Solid Oxide Surface.....	60
6.3.2 Polymerization of Surfactant.....	61
6.4 EXPERIMENTAL SECTION.....	62
6.4.1 Materials.....	62
6.4.2 Methods.....	64
6.4.2.1 Surfactant Adsolubilization.....	64
6.4.2.2 Measurements.....	64
6.5 RESULTS.....	65
6.5.1 Styrene Adsolubilization.....	65
6.5.2 Phynylethanol Adsolubilization.....	68
6.6 DISCUSSION.....	69
<b>CHAPTER VII : SUMMARIES, CONCLUSIONS AND ENGINEERING SIGNIFICANCE.....</b>	<b>70</b>
7.1 SUMMARIES.....	70
7.2 CONCLUSIONS.....	73
7.3 ENGINEERING SIGNIFICANCE.....	75
7.4 RECOMMENDATIONS AND FUTURE WORKS.....	76
<b>REFERENCES .....</b>	<b>77</b>
<b>APPENDICES.....</b>	<b>83</b>
APPENDIX A CMC Mesurements.....	84
APPENDIX B Surface Characterization.....	87
APPENDIX C Experimental Raw Data.....	93
APPENDIX D Publications and Conferences.....	131
<b>AUTHOUR BIOGRAPHY.....</b>	<b>133</b>

## LIST OF FIGURES

	<b>Page</b>
Figure 2-1 Example of surfactant micellization .....	6
Figure 2-2 Schematic presentation of typical surfactant adsorption isotherm...	9
Figure 2-3 The bilayer structure of surfactant admicells at the solid-liquid interface.....	12
Figure 2-4 Phenomena of solubilization and adsolubilization .....	13
Figure 2-5 A schematic represent of gemini surfactant. ....	14
Figure 2-6 Schematic of the polymerization for this research.....	18
Figure 4-1 The adsorption isotherm of PG, PM, and DTAB onto silica at electrolyte concentration of 1 mM NaBr, equilibrium pH of 6.5-7.5 and temperature of $25 \pm 2^\circ\text{C}$ .....	33
Figure 4-2 Zeta potential (o) and absorbance response (●) at the concentration of 80% CMC for polymerizable Gemini surfactant in a function of UV irradiation time.....	35
Figure 4-3 Zeta potential of surfactant-modified silica ; before polymerization of PG, PM, and DTAB. Electrolyte concentration; 1 mM of NaBr	36
Figure 4-4 Zeta potential of surfactant-modified silica ; after polymerization of PG, PM, and DTAB. Electrolyte concentration; 1 mM of NaBr	37
Figure 4-5 Zeta potential of surfactant-modified silica ; before polymerization and after washing of PG, PM, and DTAB. Electrolyte concentration; 1 mM of NaBr.....	38
Figure 4-6 Zeta potential of surfactant-modified silica ; after polymerization and after washing of PG, PM, and DTAB. Electrolyte concentration; 1 mM of NaBr.....	39

	<b>Page</b>
Figure 5-1 Schematic of the polymerization process for this research.....	45
Figure 5-2 Topography images of mica surfaces for unmodified mica (a), and images of PG adsorbed on mica before polymerization at NP1, 20% CMC (b), NP2, 80% CMC (c) with the presence of 1 mM NaBr electrolyte. ....	50
Figure 5-3 Topography (a and b) and Phase (c and d) images of styrene adsolubilized into polymerizes PG mica surface at the 80% CMC of PG concentration with the presence of 1 mM NaBr electrolyte for equilibrium state, SE2.....	55
Figure 5-4 Typical interaction forces between the tip and mica surface as a function of tip-surface separation for sample SE1 and SE2.....	56
Figure 5-5 Topographic images comparison of PG adsorbed on mica; a) NP2, before washing of non-polymerized surface at 80% CMC b) NP2W, after washing of non-polymerized surface at 80% CMC; Polymerized system; c) P2, before washing of polymerized surface at 80% CMC d) PW2, after washing of polymerized surface at 80% CMC with the presence of 1 mM NaBr electrolyte.....	57
Figure 6-1 Adsolubilization isotherms of styrene by PG, PM, and DTAB.....	65
Figure 6-2 The styrene admicellar partition coefficient ( $K_{adm}$ ) as a function of the styrene aqueous mole fraction ( $X_{aq}$ ) in DTAB, PM, and PG.....	67
Figure 6-3 The phenylethanol admicellar partition coefficient ( $K_{adm}$ ) as a function of the phenylethanol aqueous mole fraction ( $X_{aq}$ ) in DTAB, PM, and PG.....	69

## LIST OF TABLES

	<b>Page</b>
Table 3-1 The properties of surfactants used in this study.....	19
Table 3-2 Properties of organic solutes.....	20
Table 4-1 The properties of surfactant used in this study.....	30
Table 4-2 Experimentally determined maximum adsorption, molecule per area, and CMCs from adsorption isotherm for PG, PM and DTAB.	34
Table 4-3 Experimentally determined of desorption studies at plateau surfactant concentration for PG, PM and DTAB and after polymerization.....	40
Table 5-1 The properties of surfactants used in this study.....	46
Table 5-2 Summary of experimental set carried out in this research .....	49
Table 5-3 Summary of contact angle measurements.....	51
Table 6-1 The properties of surfactants used in this study.....	62
Table 6-2 Properties of organic solute.....	63
Table 6-3 Summary of adsolubilization capacities of the surfactant used in this study.....	68

ศูนย์วิจัยที่แพทย์  
 จุฬาลงกรณ์มหาวิทยาลัย

**LIST OF APPENDIX FIGURES**

	<b>Page</b>
Figure A-1 Interfacial surface tension of PG, PM, and DTAB at electrolyte concentration at 1 mM NaBr, equilibrium pH of 6.5-7.5 and temperature of $25\pm 2^{\circ}\text{C}$ .....	85
Figure A-2 FTIR spectra of polymerizable gemini surfactant as a function of polymerization time.....	88
Figure A-3 Example of section analysis.....	89
Figure A-4 Example of roughness analysis.....	90
Figure A-5 Given data from the Nanoscope V software determination of force curve using contact or tapping imaging mode.....	91

ศูนย์วิทยทรัพยากร  
จุฬาลงกรณ์มหาวิทยาลัย

## LIST OF APPENDIX TABLES

	<b>Page</b>
Table A- 1 Experimentally determined CMCs from surface tension, the minimum surface tension, and surfactant adsorption for PG, PM and DTAB .....	85
Table A-2 Ball part sizing of sample SE2.....	89
Table A-3 Surface tension measurement for polymerizable gemini surfactant (PG).....	93
Table A-4 Surface tension measurement for polymerizable monomeric surfactant (PM).....	93
Table A-5 Surface tension measurement for dodecyltrimethyl ammoniumbromide (DTAB).....	94
Table A-6 Adsorption of PG at 0.001 M NaBr, pH $7.0 \pm 0.5$ and temperature $25 \pm 2$ ° C .....	95
Table A-7 Summarizes: adsorption of PG with standard deviation.....	96
Table A-8 Adsorption of PM at 0.001 M NaBr, pH $7.0 \pm 0.5$ and temperature $25 \pm 2$ ° C .....	97
Table A-9 Summarizes: adsorption of PM.....	98
Table A-10 Adsorption of DTAB at 0.001 M NaBr, pH $7.0 \pm 0.5$ and temperature $25 \pm 2$ ° C .....	99
Table A-11 Summarizes: adsorption of DTAB .....	100
Table A-12 Styrene adsolubilization of DTAB at 0.001 M NaBr, pH $7.0 \pm 0.5$ and temperature $25 \pm 2$ ° C .....	101
Table A-13 Styrene adsolubilization of PG at 0.001 M NaBr, pH $7.0 \pm 0.5$ and temperature $25 \pm 2$ ° C .....	101
Table A-14 Styrene adsolubilization of PM at 0.001 M NaBr, pH $7.0 \pm 0.5$ and temperature $25 \pm 2$ ° C .....	102

	<b>Page</b>
Table A-15 Styrene adsolubilization of PG after polymerization at 0.001 M NaBr, pH $7.0 \pm 0.5$ and temperature $25 \pm 2$ ° C .....	102
Table A-16 Phenylethanol adsolubilization of DTAB at 0.001 M NaBr, pH $7.0 \pm 0.5$ and temperature $25 \pm 2$ ° C .....	103
Table A-17 Phenylethanol adsolubilization of PG before polymerization at 0.001 M NaBr, pH $7.0 \pm 0.5$ and temperature $25 \pm 2$ ° C .....	104
Table A-18 Phenylethanol adsolubilization of PG after polymerization at 0.001 M NaBr, pH $7.0 \pm 0.5$ and temperature $25 \pm 2$ ° C .....	105
Table A-19 Zeta potential measurement for PG before polymerization .....	106
Table A-20 Zeta potential measurement for PM before polymerization .....	106
Table A-21 Zeta potential measurement for DTAB before polymerization .....	107
Table A-22 Zeta potential measurement for PG after polymerization .....	107
Table A – 23 Zeta potential measurement for PM after polymerization.....	108
Table A – 24 Zeta potential measurement for DTAB after polymerization.....	108
Table A – 25 Zeta potential measurement for PG before polymerization and after washing.....	109
Table A – 26 Zeta potential measurement for PM before polymerization and after washing.....	109
Table A – 27 Zeta potential measurement for DTAB before polymerization and after washing.....	110
Table A – 28 Zeta potential measurement for PG after polymerization and after washing.....	110
Table A – 29 Zeta potential measurement for PM after polymerization and after washing.....	111
Table A – 30 Zeta potential measurement for DTAB after polymerization and after washing.....	111
Table A – 31 Summary of contact angle measurement result for PG .....	112
Table A – 32 Surface Roughness for PG.....	113
Table A – 33 Force curve result for sample SE1.....	117
Table A – 34 Force curve result for sample SE2.....	124
Table A-35 Summary of FTIR result for PG at variation of polymerization time..	130



# CHAPTER I

## INTRODUCTION

### 1.1 INTRODUCTION

Surfactant-modified adsorbents have been investigated for a number of applications. Various surfactants and solid surface systems have been evaluated for surface modification through surfactant adsorption and adsolubilization processes. Adsolubilization results from aggregation of surfactants at the solid-liquid interface which act as a two-dimensional solvent for organic solutes. The region between the surfactant head groups and the core region that is characterized by the penetration of water molecules has the potential to adsolubilize both polar and non-polar organic solutes. Surfactant-modified surfaces face the challenge of substantial losses due to desorption which is negatively impact the stability of that surfactant-modified surfaces. Gemini surfactants have reported to be more surface active compared to the corresponding monomeric and conventional surfactant, thereby requiring less raw materials for upscale production. Based on the effectiveness of gemini surfactants, polymerizable gemini surfactants show the capability of minimizing desorption of surfactant from the surface, thereby improving operating characteristics of the surfactant-modified media.

This research aims to minimize the amount of surfactant desorbed from the surface by polymerization of the admicelle (adsorbed surfactant aggregate/layer) including examination of the ability of surfactant modified adsorbents to remove

organic contaminants through the surfactant-based adsorption process. The formation of a polymeric thin film by admicellar polymerization is a process whereby in-situ monomer polymerization takes place inside of adsorbed surfactant bilayers on various substrates. The objectives of this research was to extend to verify the presence of the polymer thin film formed via admicellar polymerization by atomic force microscopy (AFM) which allows the film to be studied at the nanometer scale. Along with the AFM examination, the contact angle of the admicellar-modified mica surface has been characterized to help examine these objectives.

## 1.2 OBJECTIVES

The overall objectives of this study are to investigate the adsorption of polymerizable cationic gemini surfactant onto negatively charged solid oxide surface, to determine adsolubilization of organic solutes into admicelles, and to evaluate the desorption potential of polymerized admicelles. In this study, temperature, electrolyte concentration and pH of solution were set to constant. The specific objectives of this study are:

1. To compare the surfactant adsorption and the organic solute adsolubilization capacity of polymerizable gemini surfactant, polymerizable monomeric surfactant, and conventional surfactant.
2. To evaluate the stability of surfactant adsorbed on the solid oxide surface after polymerization of gemini and their monomeric surfactant in admicelles.
3. To evaluate the effect of polarity of organic solutes on the adsolubilization capacity.
4. To characterize the polymerized surface and determine the nature of surface.

### 1.3 SCOPES OF THE STUDY

This research intends to minimize the loss of surfactant from modified surfaces and to examine the ability of modified adsorbent material to adsorb organic solutes by polymerization of gemini surfactant. The adsorption of surfactant and the adsolubilization of organic solutes were conducted in batch experiments at room temperature ( $25\pm 2^\circ\text{C}$ ), constant pH solution in the range of 6.5-7.5, and electrolyte concentration of 0.001 M NaBr. The adsolubilization of organic solutes, styrene and phenylethanol, were conducted to evaluate the adsolubilization capacity of organic solutes with different degree of polarity in admicelles. Polymerization process provided by irradiates the adsorbed surfactant solution with UV light at a wavelength of 254 nm. Surface characterizations by AFM and contact angle measurement were used to evaluate the presence polymerized film within modified surfaces.

### 1.4 HYPOTHESES

Based on the effectiveness of gemini surfactants, we know that it is more surface active than other conventional surfactants. With the method of admicellar polymerization, we hypothesize that it can be used to fix the adsorbed surfactant film on the surface that possibly difficult to remove off of the surface. The specific hypotheses of this research by using polymerizable gemini surfactant are:

1. Enhance the property of solid oxide surface over the single head group conventional surfactant.

2. Minimize desorption of surfactant from the surface which will decrease surfactant losses from the surface and improve operating characteristics of the surfactant-modified medias.
3. Surface characteristic of adsorbed polymerized/non-polymerized surfactant aggregates or admicelles can be visualized by AFM technique.



ศูนย์วิทยทรัพยากร  
จุฬาลงกรณ์มหาวิทยาลัย

## CHAPTER II

### THEORETICAL BACKGROUNDS AND LITERATURE REVIEWS

#### 2.1 SURFACTANT PHENOMENA

Surfactants, or surface-active agents commonly known as soap or detergents, usually act to reduce the interfacial free energy and can enhance the pump and treat remediation technology. Surfactants have a characteristic amphiphilic molecular structure which consists of polar or hydrophilic group as head portions, with attraction for a polar solvent, and a non-polar or lipophilic group as tail portion, with little attraction for a polar solvent (Rosen, 1989). Depending on the nature of the hydrophilic group, surfactants are classified as: anionic or negative charged, cationic or positive charged, non-ionic or with no ionic charge, and zwitterionic which have both negative and positive charges. Surfactants are able to assemble in various form of aggregates with variation in surfactant concentration in aqueous solution. At low concentration, surfactant monomers act independently from each other. As the surfactants concentration increases until it goes beyond a certain level, the self assembly of monomers will occur and micelles are formed. The concentration where the first micelle is formed in aqueous solution is called the critical micelle concentration or CMC. With increasing surfactants above the CMC, additional micelles will form by the incremental of surfactants (West and Harwell, 1992). An example of micellization is shown in Figure 2-1. When a solid phase is added to the surfactant solution, the surfactants will aggregate at the solid-liquid interface where

the adsorption of surfactant molecules occurred. At low surfactant concentrations, micelle-like structures called hemimicelles and admicells are formed when surfactant molecules interact on the solid surface, depending on whether the aggregates have one or two surfactant layers. The amount of admicelles on the surface will not increase above the CMC level but enhance micelles form instead. Surfactant micelles composed of hydrophilic head groups or polar moieties at the exterior and hydrophobic tail groups or the non-polar moieties at the interior, exhibit unique properties. The polar exterior is able to dissolve in water, while the non-polar interior can effectively increase the solubility of organic compounds.

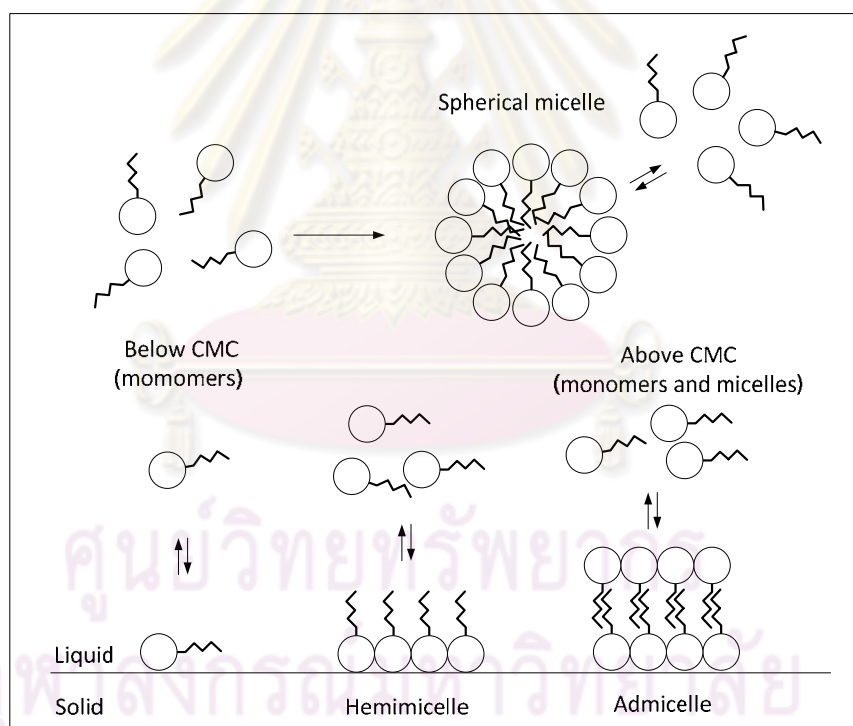


**Figure 2-1** Example of surfactant micellization

## 2.2 ADSORPTION OF IONIC SURFACTANTS ONTO METAL OXIDE SURFACES

### 2.2.1 Surfactant Adsorption Phenomena

Surfactant adsorption onto solid oxide surfaces such as silica is a complex process because it relates to different adsorption mechanisms, namely ion exchange, ion pairing, and hydrophobic bonding. Surfactant adsorption is considered when surfactant molecules in a bulk solution transfer to surface or interface (Paria and Khilar, 2004). To quantify the adsorption in order to determine the performance of surfactant, the adsorption isotherms, which correlate aqueous surfactant concentration and surfactant adsorption onto a solid surface at constant temperature, is used (Kittiyanan, et al., 1996).

To determine the equilibrium adsorption of the surfactant on the solid oxide surface, equation 1.1 can be used to calculate by assuming that the adsorption of water or salt and the adsorption of the surfactant have no effect on solution density and can be negligible (Lopata, 1988).

$$\Gamma_i = \frac{(C_{i,b} - C_{i,a})V}{W_g} \quad (1.1)$$

$\Gamma_i$  = Adsorption density of surfactant i (mole/g)

$C_{i,a}$  = Concentration of surfactant at equilibrium (mole/liter)

$C_{i,b}$  = Concentration of surfactant at initial (mole/liter)

$V$  = Volume of sample (liter)

$W_g$  = Weight of silica oxide (g)

The adsorption isotherm of ionic surfactants on oxide surfaces is typically an elongated 'S'-shaped curve that can be separated into four regions (Somasudaran and Fuerstenau, 1966; Scamehorn, et al., 1982). The four regions of surfactant isotherm shown in Figure 2-2 demonstrate the plot between the log of the adsorbed surfactant density versus the log of the equilibrium concentration of surfactant.

**Region I** is referred to as the Henry's law region because it corresponds to both very low concentration and thus low adsorption of surfactant. The interaction between molecules of surfactants is negligible because the surfactant monomers are dilute on the surface phase. Thus, adsorbed surfactants in this region are not forming aggregates.

**Region II** is identified by a sharply increased isotherm slope relative to the slope in region I. The increasing slope indicates the beginning of interactions between surfactant molecules, which results in aggregation and multilayer adsorption on the most energetic surface patches. The adsorbed surfactants are called admicelles or hemimicelles, depending upon whether the aggregates are viewed as one or two surfactant layers. Surfactant consists of a lower layer of head groups adsorbed on the substrate surface and an upper layer of head groups in contact with solution is called the admicelle bilayer structure. And the monolayer structure having the head group adsorbed on the solid phase and the tail group touching the aqueous phase is called hemimicelle. The critical admicelle concentration (CAC) or the hemimicelle concentration (HMC) is considered at the transition point from region I to region II, representing the first formation of adsorbed surfactant aggregates.

**Region III** represents the region that has the isotherm decreasing from the slope in Region II. This decrease in slope is caused by adsorption on lower energy



surface patches or the adsorption now must overcome electrostatic repulsion between closed ions and the similarly charged solid surface.

**Region IV** is the plateau region that has almost constant surfactant adsorption, while the surfactant concentration increases. The first formation of micelles corresponds to the critical micelle concentration (CMC) represented by the transition point from region III to region IV which occur after the interface is saturated by admicelles (Kitiyanan, et al., 1996).

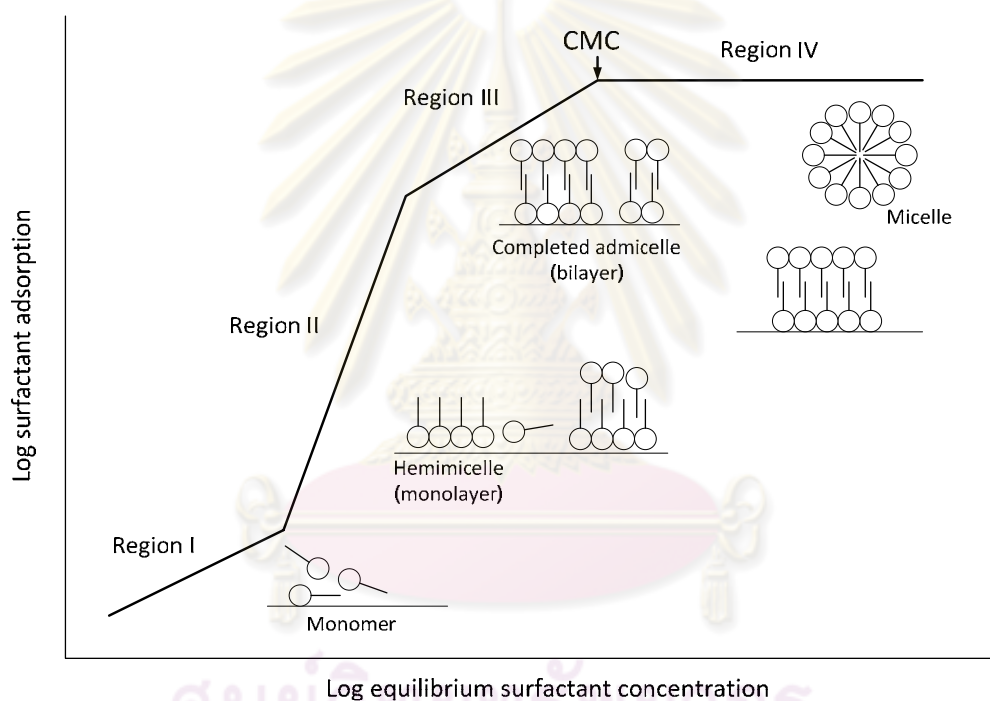


**Figure 2-2** Schematic presentation of typical surfactant adsorption isotherm

### 2.2.2 The adsorption of Silicon Oxide Surface and its Structure

Silica is one of the widely used adsorbents in chemical technology. The mechanism of adsorption on silica becomes importance through the study of surface chemistry (Davydov in Papiere (ed), 2000). Silica shows a very low pristine point of zero charge (PPZC) when compare to metal oxides. Most sources report PPZC of

silica is between pH 2 and 3. Thus, zeta potential of silica is negative over the usually studied pH range. In the other hand, silica is more acidic than most of metal oxides, as a result, surface hydroxyl groups are likely presence that behave as a weak acid (Kosmulski in Papirer (ed), 2000). Silica surface properties can be modified by adsorption of polymers and surfactants. When cationic surfactant adsorb readily on silica surface, the electrostatic interaction between silica and surfactant are accounted. As mentioned, the pH of most practical systems is above 2 that lead to the interactions between cationic reagent and negative charged silica. The adsorption of surfactants can alter the interfacial physiochemical properties of the silica, such as zeta potential and hydrophobicity that can be utilized in industrial applications, for example, flocculation/dispersion (Somasundaran and Zhang, 1989 in Papirer (ed), 2000).

### **2.2.3 Influence Parameters of Surfactant Adsorption**

The adsorption of surfactants at solid-liquid interfaces is strongly influenced by a number of parameters; 1) the nature of structural groups of the solid surface i.e., alumina, silica, and zeolite; 2) the molecular structure of surfactant being adsorbed; 3) the environment of aqueous solution i.e., solution pH, electrolyte concentration, and temperature. Together these parameters determined the mechanism, by which the adsorption occurs, and the efficiency and effectiveness of the surfactant adsorption (Rosen, 1989; Kitiyanan, et al., 1996).

#### **2.2.3.1 Influence of solution pH**

The adsorption of ionic surfactants onto solid surfaces may cause change in pH of solution. For example, when pH of aqueous phase is lowered, silica surface will become more positive or less negative due to the additional protons adsorbing from

the solution phase (Rosen, 1989). In the case of cationic surfactants, the adsorption capacity decreased by this pH changing. Therefore, the equilibrium pH is affected to the surfactant adsorption.

### ***2.2.3.2 Influence of Electrolyte Concentration***

The presence of electrolyte enhances the adsorption of cationic surfactant on a positively charge surface. Typically, the adsorbed amount of ionic surfactants apparently increases with increasing of ionic strength due to decreasing of electrostatic repulsion force between surfactant molecules. The report of electrolyte affect on adsorption of gemini surfactants with silica show that the adsorption of gemini surfactant on silica is enhanced by increasing NaBr concentration (Esumi, et al, 1996). Increasing of electrolyte concentration will affect to the decreasing of electrostatic repulsion in which impact to a high packing of gemini surfactant molecules in the adsorbed layer.

### ***2.2.3.3 Influence of Temperature***

Many studies observed that increasing temperature leads to decreasing the maximum adsorption of ionic surfactant. The rational are expected to the increasing of the kinetic energy of the species such as entropy of the system that results in a decrease of aggregate forming on the adsorbent surface (Pavan, et al., 1999; Paria and Khilar, 2004). Therefore, the effectiveness of adsorption surfactant modified material generally account on the temperature (Rosen, 1989; Saphanuchart et al., 2008). The effect of temperature is relatively small compared to that of solution pH. However, a rise in temperature usually results in an increase in the adsorption of non-ionic surfactants containing a polyelectrolyte chain as the hydrophobic group.

### 2.3 ADSOLUBILIZATION OF ORGANIC SOLUTES

Formally, adsolubilization is defined as the excess concentration of a species in the presence of an admicelle that would not exist in the absence of the admicelle. In other words, adsolubilization is the aggregation of surfactants which adsorbed at the solid-liquid interface and capable of acting as two-dimensional solvents for organic solutes, (Wu, et al, 1987). The admicelle structure is characterized into three-regions as shown in Figure 2-3. The outer region contains the most polar or ionic region because it is comprised of the surfactant head group. The inner region or the core region is non-polar due to the presence of the hydrocarbon chain or surfactant tail groups. The intermediate polarity region, or the so called the palisade region, is the place between surfactant head groups and the core region. Many researchers have been elucidated the locus of solubilization in the surfactant micelle and admicelle. The nonpolar organic solutes have been reported primarily partition into the core region, while the polar organic solutes partition into the palisade region of the admicelle (Nayyar, et al., 1994; Kitiyanan, et al., 1996; Dickson and O' Haver, 2002; Tan and O' Haver, 2004; Fuangswasdi, et al., 2006b; Saphanuchart, et al., 2008).

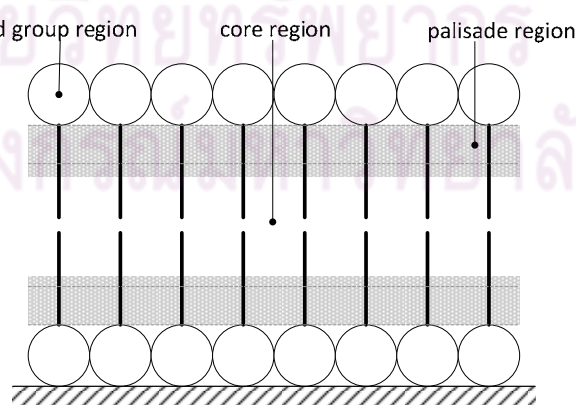


**Figure 2-3** The bilayer structure of surfactant admicelles at the solid-liquid interface

Adsolubilization may be described as the partitioning of non-surface-active molecules at a liquid-solid interface through the assistance of adsorbed surfactant molecules. The adsolubilization phenomena of organic solutes are illustrated in Figure 2-4. Generally, the amount of adsolubilization rises with increasing surfactant adsorption and with increasing concentration of organic solute in the supernatant. The saturation of adsolubilization process occurs when reach the limiting ratio of surfactant to organic solutes. The adsolubilization limit of saturated and aromatic hydrocarbons were tested and reported to be 2:1 (Harwell and O'Rear, 1989).

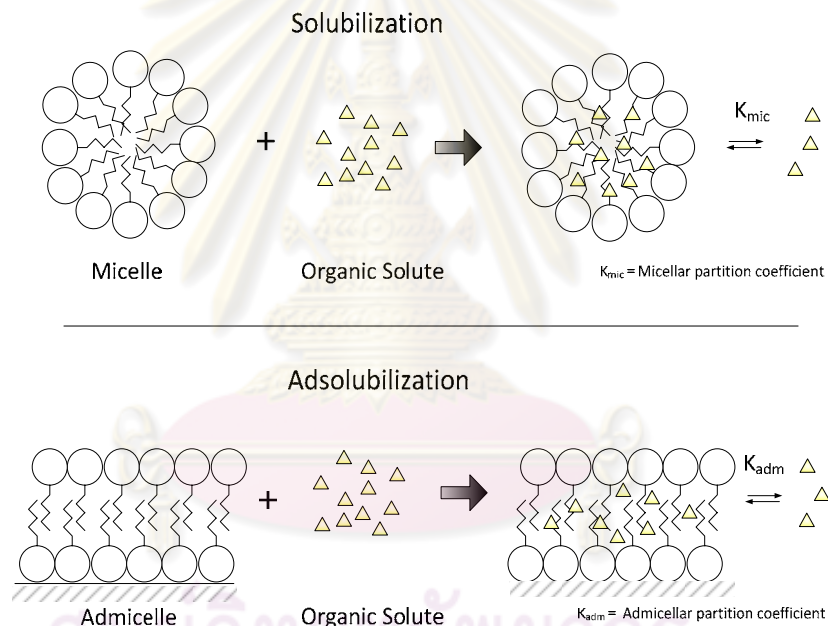


**Figure 2-4** Phenomena of solubilization and adsolubilization

## 2.4 GEMINI SURFACTANT AND POLYMERIZABLE SURFACTANTS

### 2.4.1 Gemini Surfactant

Gemini surfactants are sometimes called dimeric surfactants. They consist of three structural elements, a hydrophilic group, a hydrophobic group and a linkage or spacer that may vary to change the properties of the surfactant. Gemini surfactants are molecules possessing more than one hydrophobic tail and hydrophilic head group connected by a linkage close to hydrophilic groups, (Rosen, 1993). The longer in sequence of hydrocarbon chain, an ionic group, a spacer, a second ionic group and another hydrocarbon tail of gemini surfactant are considered more surface-active than the conventional surfactants which having single hydrophobic tail connected to an ionic or polar head group, (Hait and Moulik, 2002). Gemini surfactants with quaternary ammonium bromide head groups and linear alkyl tails have been the most studied. The general formula for these kind of surfactants is  $[C_mH_{2m+1}-N^+-(CH_3)_2-(CH_2)_s-(CH_3)_2-N^+C_mH_{2m+1}]2Br^-$ , and are referred to as m-s-m, 2 Br surfactants where m and s referred to the number of alkyl carbon atoms tails and spacer, respectively. Such molecules may be considered equivalent to the dimers of the mono-quaternary ammonium bromide surfactants  $C_mH_{2m+1}-(C_{s/2}H_{s+1})-N^+-(CH_3)_2Br^-$  (Zana, et al., 1980). These compounds have very much lower CMC value and much greater efficiency in reducing surface tension than expected (Abe, et. al., 2006). A schematic representation of a gemini surfactant is shown in Figure 2-5.



**Figure 2-5** A schematic represent of gemini surfactant

### 2.4.2 Polymerizable Surfactant

Polymerizable surfactants are classified as surface-active monomers which are molecules having a pair of hydrophobic and hydrophilic components together with a polymerizable group in their structure. Polymerizable surfactants can form micelles in water in a manner similar to conventional surfactants (Yutaka, 2000). The loss of surfactant due to such phenomena as precipitation, sorption, etc., affects the economics of surfactant-enhanced subsurface remediation (Rouse, et al., 1993). The other factors caused the surfactant loss are also the heating, varying of pH, and the dilution of the surfactant which make the equilibrium shift, then surfactant will desorb from the adsorbent surface (Esumi, et al., 1993). In a previous study, it was found that the loss of surfactant occurred when the solution pH contacting with admicelles changed in the column study (Sita Krajangpan, 2004). Polymerizable surfactant, the surfactant that can polymerize at the double bond in molecule, can enhance the dispersion stability of the alumina with the polymerized film and reduces desorption of the alumina surface (Esumi, et al., 1989; Esumi, et al., 1991).

### 2.4.3 Polymerizable gemini surfactant

Many polymerizable surfactants have been synthesized and studied having anionic, cationic, non-ionic or amphoteric groups. Recently, polymerizable gemini surfactant have been investigated as a novel pseudo-stationary phases in micellar electrokinetic chromatography (Akbay, et al., 2005). Sodium di(undecenyl) tartarate is one of those mentioned synthesis (Kunitake, et al., 1984). Polymerizable gemini surfactants is comprised of polymerizable group in the gemini surfactant structure. There were various studied about these polymerizable gemini surfactant such as the

designation nanostructures of lyotropic liquid-crystalline phase behavior of cross-linkable and polymerizable gemini surfactants, bis(alkyl-1,3-dine)-based phosphonium amphiphiles (Pindzola, et al., 2003), the synthesis of novel polymerizable cationic gemini surfactant with a polymerizable group at the terminal of each hydrophobic group to study their interfacial properties (Abe, et al., 2006).

## **2.5 DISPERSION STABILITY AND SURFACE MODIFICATION BY POLYMERIZABLE SURFACTANTS**

Solid dispersions can be stabilized by adsorption of surfactants onto solid particles such as silica, alumina. When ionic surfactants adsorb onto silica particles, the dispersion stability of the particles depend on the surfactant concentration. At the absence of surfactant concentration, high dispersion stability of silica particles is observed in the system. After additional a small amount of surfactant concentration, the stability of dispersed particle decreases. When increasing the surfactant concentration in the system, the stability of dispersed particle will enhance. This process is called “dispersion-flocculation-redispersion” which illustrates surface modification of particles by surfactants. As mentioned, a bilayer of surfactant is formed on the particles upon addition of surfactant concentration to the solid surface. In this bilayer, the interaction between the first and the second layer is the hydrophobic forces, so that the outer layer desorbs easily by dilution. Using of polymerizable surfactant is a possibility to fix the biliayer to the substrate. With the polymerization process, the stability of dispersed particles will enhance as a stabilization of the aggregate structure that the surfactants themselves form (Esumi, 1989; Esumi, 2001).



## 2.6 ADMICELLAR POLYMERIZATION AND ULTRATHIN POLYMER FILM

The film-forming process is based on the formation of admicelle at a solid-liquid interface. Admicellar polymerization is a process whereby in-situ monomer polymerization takes place inside of adsorbed surfactant bilayers on various substrates (Grady, et al., 1998). This method has potential for the formation of anticorrosion and lubricating coating. In addition, this technique can produce the composite materials that may be valuable for use as pigments, suspension aids, and chromatographic packings. Typically, admicellar polymerization consists of four steps. First, surfactant is adsorbed onto solid surfaces. In this step, aggregates of surfactant molecules are formed as an admicelles (or hemimicelles) under appropriate system conditions leading adsorption behavior to bring about bilayer coverage of the entire surface with surfactant. Second, polymerizable monomers are adsolubilized into admicelles. During this step, a polymerizable monomers with low water solubility is allowed to partition into admicelles. Third, polymerization of the monomers in the admicelles by chemical, thermal, or photochemical processes is initiated. Finally, the optional step to remove of accessible surfactant by washing in order to expose the polymerized monomer layer (Pongprayoon, et al, 2002; See and O'Haver, 2002; Wu, et al., 1987; O'Haver, et al., 1995; Nontasorn, et al., 2005).

In this study, polymerization was of the surfactant itself rather than an adsolubilized monomer. The schematic of surfactant polymerization is shown in Figure 2-6. In addition, the modified adsorbent will be ready for many applications, and it can be prepared in a large quantity for industrial scale application.

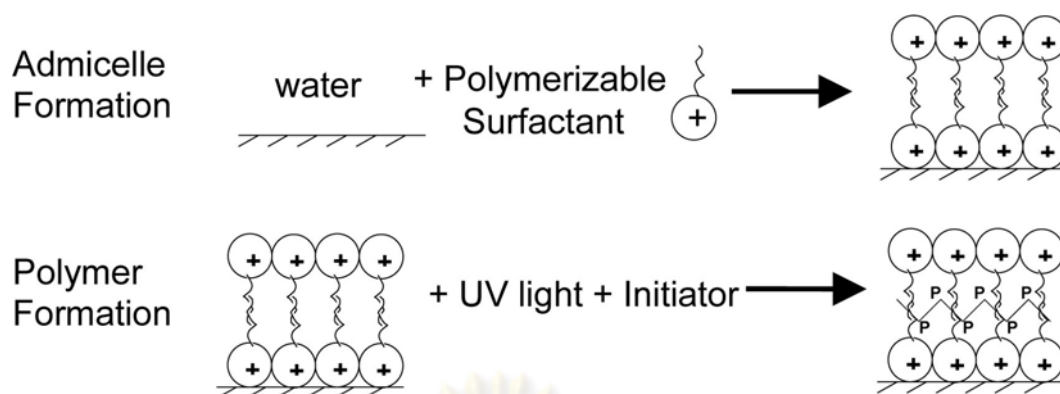


**Figure 2-6** Schematic of the polymerization process for this research

## 2.7 PARAMETERS EFFECT TO POLYMERIZATION OF SURFACTANTS

### 2.7.1 Dissolved Oxygen

The presence of dissolved oxygen will inhibit polymerization of surfactant. As reported by Esumi, et al., 1989, the system that eliminated dissolved oxygen rapidly enhances the polymerization of polymerizable surfactant coated on alumina, while the system with the presence of dissolved oxygen decreases the polarity in the polymerized bilayer resulted by slower rate of polymerization. Purging surfactant solution with nitrogen gas is the way to eliminate the presence of dissolved oxygen.

### 2.7.2 Position of polymerizable group in the surfactant structure

The position of a polymerizable group will affect the polymerization behavior. A polymerizable double bond located at the end of a lipophile (tail group) of the surfactant give a higher polymerization rate than the one located in the polar head group. In addition, the polymerizable double bond at the head group would exist in the surface of the micelle, while a polymerizable at the end of the tail group would exist in the interior of the micelle core (Yutaka, 2000).

## CHAPTER III

### RESEARCH METHODOLOGY

#### 3.1 MATERIALS

##### 3.1.1 Surfactants

Surfactants used in this study were divided into two types; polymerizable and non-polymerizable surfactants. For polymerizable surfactants, polymerizable cationic gemini surfactant (PG) and polymerizable monomeric surfactant (PM) were kindly supplied by Faculty of Science and Technology, and Institute of Colloid and Interface Science from Tokyo University of Science, Japan. For non-polymerizable surfactant, dodecyl trimethylammonium bromide (DTAB), was purchased from S.M. Chemical Supplies Co., Ltd., Thailand. The properties of these surfactants are shown in Table 3-1.

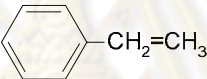
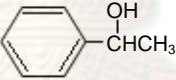
**Table 3-1.** The properties of surfactants used in this study

Surfactant	MW	% Active	Molecular structure
Polymerizable cationic gemini surfactant (PG)	690.8	97	$\begin{array}{c} \text{CH}_2=\text{C}(\text{CH}_3)\text{COO}(\text{CH}_2)_{11}\text{N}^+(\text{CH}_3)_2 \\   \\ \text{CH}_2 \\   \\ \text{CH}_2 \\   \\ \text{CH}_2=\text{C}(\text{CH}_3)\text{COO}(\text{CH}_2)_{11}\text{N}^+(\text{CH}_3)_2 \end{array} \cdot 2\text{Br}^-$
Polymerizable monomeric surfactant (PM)	346.4	95	$\text{CH}_2=\text{C}(\text{CH}_3)\text{COO}(\text{CH}_2)_{11}\text{N}^+(\text{CH}_3)_3 \cdot \text{Br}^-$
Dodecyl trimethylammonium Bromide (DTAB)	308.3	99	$\text{C}_{12}\text{H}_{25}\text{N}^+(\text{CH}_3)_3 \cdot \text{Br}^-$

### 3.1.2 Organic Solutes

For adsolubilization study, styrene and phenylethanol are selected to use. Styrene (99% purity, Aldrich) and 1-Phenylethanol (98% purity, Fluka) are represented as weak and strong polar organic solutes in this study, respectively. The properties of organic solutes are shown in Table 3-2.

**Table 3-2.** Properties of organic solutes

Organic solute	MW	Molecular formula		Solubility in water (Molar)	Density (g/mL) 25 °C	Dipole Moment
		formula	Structure			
Styrene	104.15	C <sub>8</sub> H <sub>8</sub>		0.0027	0.909	0.13
Phenyl ethanol	122.17	C <sub>8</sub> H <sub>10</sub> O		0.040	1.01	1.65

### 3.1.3 Adsorbent

Silica material (SiO<sub>2</sub>), 15 nm particle size, was purchased from S.M. Chemical Supplies Co., Ltd., Thailand, and was used as received. The specific surface area from manufacturer product is 140-180 m<sup>2</sup>/g.

The electrolyte concentration was controlled using 1 mM sodium bromide (NaBr). The solution pH was adjusted using NaOH and HCl. All chemicals were use as received and are ACS analytical reagent grade. Water used in this work was purified and has a resistance of 18.2 M Ω cm. Plastic and glassware were rinsed well with double-distilled water three times prior to use.

## 3.2 EXPERIMENTAL SECTION

### 3.2.1 CMC Measurement

The critical micelle concentrations (CMC) of the surfactant systems with an electrolyte concentration of 1 mM NaBr were determined by using a surface tensiometer (Kruss GmbH Hamburg Co.Ltd, Germany) with a platinum plate at room temperature ( $25\pm 2^\circ\text{C}$ ).

### 3.2.2 Surfactant adsorption study

The adsorption isotherms of all surfactant system onto negatively charge surface of silica ( $\text{SiO}_2$ ) were obtained using batch experiments. Different amounts of surfactant concentrations which covered the regions below and above CMC were added into several vials containing 0.01 g of silica. After that, all solutions were shaken at least 48 hours until they reached equilibrium. The pH of the solutions was periodically measured and adjusted using NaOH and/or HCl solution to  $7\pm 0.5$  after twelve hours of orbital shaking. This process was repeated, until the solution pH remained constant at the desired level. After being equilibrated, the solutions were centrifuged to remove the silica. The aqueous surfactant concentration was then analyzed.

$$\Gamma_i = \frac{(C_i - C_f)V}{W_g} \quad (3-1)$$

Where;

$\Gamma_i$  = Adsorption density of surfactant i (mole/g)

V = Volume of sample (liter)

$C_i$  = Concentration of surfactant at initial (mole/liter)

$C_f$  = Concentration of surfactant at equilibrium (mole/liter)

$W_g$  = Weight of silica oxide (g)

Equation 3-1 was used to calculate the adsorption of the surfactant on the mineral oxide surface. In this equation, the adsorption of water or salt is assumed to be negligible and the adsorption of the surfactant is assumed to have no effect on solution density (Lopata, 1988).

### **3.2.3 Surfactant polymerization study**

In this research, admicellar polymerization consisted of two steps; first, adsorption of surfactant onto silica surface, and second, polymerization of the admicelles by using UV light and initiator. The solutions contained 0.1 g of sodium persulfate after purging with nitrogen gas to remove dissolved oxygen. The surfactant polymerization was performed using irradiation with UV lamp at 254 nm wavelength with the average operating temperature at  $25\pm 2^\circ\text{C}$ . This lamp was allowed to place 10 cm. away from samples. During this time, surfactant suspensions were shaken at 150 rpm for 18 hours. Heat released during polymerization was observed by measuring the temperature before and after irradiation. To determine the extent of polymerization, the supernatant concentration of the polymerizable surfactants PG and PM are analyzed by UV-VIS spectroscopy at the wave length of 245 and 255 nm, respectively. The concentration of non-polymerizable surfactant, DTAB is determined by ion chromatography with ECD detector. Zeta potential measurements were also evaluated after polymerization at various time based on UV-VIS spectroscopy results.

### **3.2.4 Adsolubilization study**

The adsorption isotherms were used for determining the appropriate concentration in which the maximum surfactant coverage on the solid surface occurs without the presence of micelles in the bulk solution which is slightly below the CMC

of the surfactants. In this study, surfactant concentrations at 80% of CMC were selected for the next adsolubilization experiment.

An adsolubilization studies were performed after polymerization by varying organic solute concentration. Vials contained adsolubilized solution were shaken for 48 hours and then centrifuged to remove silica. The surfactant concentration and the organic solute concentration in aqueous solution were kept further for analyzed by Ion Chromatography and HPLC, respectively.

### **3.2.5 Surfactant desorption study**

Surfactant suspensions before and after polymerization were allowed to settle for one day before removing the supernatant from the solution. Silica media was allowed to drying in the desiccator for several days to ensure that it was completely dried. After that, silica was transferred to the new test tube and rinsed three to five times to remove excess surfactant. Then, DI water was added to in the new test tube as a blank solution for silica before shaking at 150 rpm for 48 hours for washing (desorption) study. Finally, the clear liquid was kept for further analyzed.

### **3.2.6 Surfactant Surface Characterization Study**

To identify the polymerized feature of solid oxide particles, the studies of surface characterization were carried out after polymerization of surfactants by analyzed with Atomic Force Microscopy (AFM) and contact angle measurement were used to evaluate the presence of polymerized film fixed on the adsorbed aggregates of surfactant.

### 3.3 ANALYTICAL METHOD

Cationic surfactants in the adsorption studies were analyzed by Ion Chromatography (ICS-2500, Dionex) using a coupling agent, Methanesulfonic acid (MSA). The natural complex was separated with reverse phase column (NS1, Dionex) and the acetonitrile-water mobile phase, the complex was eluted from the column and de-coupled by ionic suppression (CSRS ultra-cationic suppressor, Dionex). UV detector and electrical conductivity detector (ECD) were used to detect polymerizable surfactants and conventional cationic surfactant (DTAB), respectively.

In adsolubilization experiment, surfactant concentrations and organic solute concentrations (styrene and phenylethanol) were analyzed by HPLC (Agilent) equipped with acclaim surfactant column and detected with ELSD and UV detector at 247 nm, respectively. Mobile phase of the system were prepared by using 0.1 M of ammonium acetate ( $C_2H_3O_2NH_4$ ) at pH 5.4 and acetonitrile ( $C_2H_3N$ ) with the ratio of  $C_2H_3O_2NH_4$  to  $C_2H_3N$  equal 60:40.

Polymerized surfaces obtained by polymerization of surfactant were observed by Atomic force microscopy (AFM). In addition, contact angle measurement also conducted to evaluate the nature of the modified surfactant surface.



## CHAPTER IV

### EFFECT OF IONIC HEAD GROUP ON ADMICELLE FORMATION BY POLYMERIZABLE SURFACTANTS

#### 4.1 ABSTRACT\*

One of the problems of using surfactant-modified adsorbents in a surfactant-based adsorption process is the loss of surfactant due to desorption. Recently, polymerizable surfactants have been used to minimize surfactant losses through polymerization of the surfactant admicellar structure to help secure it to the solid oxide surface. For this study, the adsorption of polymerizable cationic gemini surfactant is used to form polymerized bilayers on silica oxide. UV light is used to irradiate and initiate the polymerization process. Surfactant adsorption and desorption are evaluated to compare the efficiency of polymerized and non-polymerized surfactants using gemini and conventional surfactants, respectively. Results demonstrate that the increased stability of the polymerized surfactant-modified surface can reduce the desorption of surfactant from the surface, thereby improving operating characteristics of the surfactant-modified media (e.g, maintain adsolubilization potential, dispersion stability, etc.).

#### 4.2 INTRODUCTION

Surfactant-modified adsorbents have been investigated for a number of applications. Various surfactant systems have been evaluated for surface modification including mixed anionic and cationic surfactants (Fuangwasadi, et al., 2006a;

---

\*Asnachinda, E., Khaodhiar, S. and Sabatini, D. A. Effect of Ionic Head Group on Admicelle Formation by Polymerizable Surfactants. *J Surfactants Deterg* (2009): Available from [http://www.springerlink.com/content/8710056235202v\\_30/fulltext.pdf](http://www.springerlink.com/content/8710056235202v_30/fulltext.pdf).

Fuangwasasdi, et al., 2006b; Fuangwasasdi, et al., 2007), and linker-based and extended surfactants (Charoenseang, et al., 2008). Surfactant losses from the surface because of desorption negatively affects the stability of surfactant-modified surfaces (Rouse, et al., 1993; Sita Krajangpan, 2004). The hypothesis of this research is that fixing an admicellar structure to the surface by polymerization will reduce surfactant losses.

Gemini surfactants have received increased attention in recent years. Bis(quaternary ammonium) is a gemini surfactant containing two quaternary ammonium moieties which has been evaluated (Oda, et al., 1997). Gemini surfactants have very low CMC values compared with the corresponding monomeric and conventional surfactant, thereby requiring less raw materials for upscale production (Hait and Moulik, 2002). Previous studies have reported on the fact that gemini surfactants can assemble into various phases depending on their structure when dissolved in water (Oda, et al., 1997). The desirable properties of gemini surfactants can be modified by changing their alkyl tail length and their spacer length and flexibility (Zana, 2002). Based on the effectiveness of gemini surfactants, cationic polymerizable gemini surfactants are expected to be strongly adsorbed on the silica surface with minimal desorption of surfactant from the surface, thereby improving the operating characteristics of the surfactant-modified media.

## **4.3 BACKGROUND**

### **4.3.1 Polymerizable Surfactants**

Polymerization of amphiphile molecules has been evaluated for a variety of purposes. For example, polymerizable amphiphiles with fluorocarbon chains were

studied as early as 1984 (Elbert, et al., 1984), with hydrocarbon and fluorocarbon amphiphiles evaluated in Langmuir Blodgett multilayers (Laschewsky, et al., 1985). Two years later, the monolayer microstructure of amphiphilic copolymers consisting of two-chain surfactant was also investigated (Frey, et al., 1987). Polymerization of admicelles is a process whereby adsorbed surfactant bilayers are polymerized after admicelle formation (Grady, et al., 1989). In 1989, Esumi, et al. studied the polymerization of the surfactant bilayer of sodium 10-undecenoate on alumina surface using UV irradiation. Further, research demonstrated that the dispersion stability of alumina with a polystyrene layer was increased with UV irradiation time and somewhat enhanced compared with that of alumina without the polystyrene layer, probably because of the increased electric repulsion force between alumina particles (Esumi, et al., 1991; Esumi, et al., 1993).

#### **4.3.2 Gemini and Polymerizable Gemini Surfactant**

Gemini surfactants contain two hydrophobic tails and hydrophilic heads. Such molecules may be regarded as equivalent to the dimers of the mono-quaternary ammonium bromide surfactants  $C_mH_{2m+1}-(C_{S/2}H_{S+1})-N^+-(CH_3)_2Br^-$  (Zana, et al., 1980). These compounds have much lower CMC values and much higher surface activity (produces lower surface tension) than the corresponding monomeric surfactant. Adsorption of the gemini surfactant 12-2-12, was found to increase as the size of spacer group increased, resulting in a decrease of the maximum surface excess of surfactant (Abe, et al., 2006). The tighter packing of the hydrophilic groups of gemini surfactants results in a more cohesive and stable interfacial film, and double-tailed and doubly charged gemini surfactants interact more prominently with neutral and oppositely charged surfactants (Hait and Moulik, 2002). Once the gemini

surfactant is adsorbed at the surface, the second charged head-group is brought into close proximity with the surface, an effect which becomes more pronounced as the spacer length is reduced (Atkin, et al., 2003).

Polymerizable gemini surfactants have also been investigated as novel pseudo-stationary phases in micellar electrokinetic chromatography (Alami, et al., 1993) one such example is sodium di(undecenyl) tartrate (Kunitake, et al., 1984). Various properties of these polymerizable gemini surfactants have been reported, for example designation of the nanostructures of the lyotropic liquid crystalline phase behavior of the cross-linkable and polymerizable gemini surfactants, bis(alkyl-1,3-diene)-based phosphonium amphiphiles (Pindzola, et al., 2003). Synthesis of a polymerizable cationic gemini surfactant with a polymerizable group at the terminus of each hydrophobic group was achieved by Abe et al, to investigate its basic interfacial properties in water and in the presence of 0.05 M NaBr (Abe, et al., 2006). For comparison, the properties of the corresponding monomeric surfactant were also studied. In this research, we hypothesized that by using polymerizable surfactants, we could stabilize the surfactant-modified silica and reduce surfactant desorption from the silica surface (Esumi, et al., 1989; Esumi, et al., 1991; Esumi, et al., 1993).

#### **4.4 HYPOTHESES**

The major objective of this research was to demonstrate that polymerizable gemini surfactants lead to desirable stability of surfactant-modified silica surfaces (reduced decomposition) compared with single-head-group polymerizable and non-polymerized surfactants. It was hypothesized that strong interaction of dimeric surfactant head groups with the solid oxide surface would increase adsorption and that the crosslinking of adsorbed surfactant after polymerization would minimize

desorption of surfactant from the surface, thereby reducing surfactant losses from the surface and improving the operating characteristics of the surfactant-modified media.

## 4.5 MATERIALS AND ANALYTICAL SECTION

### 4.5.1 Materials

Surfactants used in this study were divided into two types: polymerizable and non-polymerizable. For polymerizable surfactants, polymerizable cationic gemini surfactant (PG) and polymerizable monomeric surfactant (PM) were kindly supplied by the Faculty of Science and Technology, and the Institute of Colloid and Interface Science, Tokyo University of Science, Japan. For non-polymerizable surfactant, dodecyl trimethylammonium bromide (DTAB) was purchased from S.M. Chemical Supplies, Thailand. The properties of these surfactants and their surface properties are shown in Table 4-1. The CMC of the gemini surfactant (PG) is reported as  $5 \times 10^{-4}$  M and PM and DTAB have reported CMC values of  $1.8 \times 10^{-2}$  M and  $1.6 \times 10^{-2}$  M, respectively. Furthermore, the PG surfactant has been reported to produce lower surface tension values than PM and DTAB ( $\gamma_{\text{cmc}}$  for PG, PM and, DTAB are 32.1, 42.1 and, 39 mN/m, respectively) (Hait and Moulik, 2002; Zana, 2002; Abe, et al., 2006; Rosen, et al., 1999).

Silica ( $\text{SiO}_2$ ), 15-nm particle size, was purchased from S.M. Chemical Supplies, and was used as received. The specific surface area reported by the manufacturer product is  $160 \text{ m}^2/\text{g}$ . The electrolyte concentration was controlled by use of 1 mM sodium bromide (NaBr). Solution pH was adjusted by use of NaOH and HCl. All chemicals were used as received and are ACS analytical reagent grade.

Water used in this work was purified and had a resistance of 18.2 MΩ cm. Plastic and glassware were rinsed well with double-distilled water three times prior to use.

**Table 4-1** The properties of surfactants used in this study

Surfactant	MW	% Active	Molecular structure
Polymerizable cationic gemini surfactant (PG)	690.8	97	$\begin{array}{c} \text{CH}_2=\text{C}(\text{CH}_3)\text{COO}(\text{CH}_2)_{11}\text{N}^+(\text{CH}_3)_2 \\   \\ \text{CH}_2 \\   \\ \text{CH}_2 \\   \\ \text{CH}_2=\text{C}(\text{CH}_3)\text{COO}(\text{CH}_2)_{11}\text{N}^+(\text{CH}_3)_2 \end{array} \cdot 2\text{Br}^-$
Polymerizable monomeric surfactant (PM)	346.4	95	$\text{CH}_2=\text{C}(\text{CH}_3)\text{COO}(\text{CH}_2)_{11}\text{N}^+(\text{CH}_3)_3 \cdot \text{Br}^-$
Dodecyl trimethylammonium Bromide (DTAB)	308.3	99	$\text{C}_{12}\text{H}_{25}\text{N}^+(\text{CH}_3)_3 \cdot \text{Br}^-$

#### 4.5.2 Analytical Method

Surfactant concentrations were analyzed by ion chromatography (Agilent) and UV-vis spectrophotometer (Shimadzu UV 1601). In addition, the zeta potentials of surfactant suspensions were measured by means of an electrophoretic apparatus (Zeta-Meter System 3.0) to examine the effect of polymerization on the dispersion stability of silica and also to confirm the presence of a surfactant bilayer before and after desorption studies. The UV lamp used as the source (initiator) in the polymerization process was purchased from Cole Parmer, USA.

#### 4.5.3 Determination of the Adsorption Isotherm

The adsorption isotherms of all surfactant system were obtained by use of batch experiments. Different concentrations of surfactant covering the regions below and above the CMC were added into several vials containing 0.01 g silica. All

solutions were then shaken for at least 48 h until they reached equilibrium. The pH of the solutions was periodically measured and adjusted to  $7\pm 0.5$ . After being equilibrated, the solutions were centrifuged to remove the silica. The concentrations of DTAB and polymerizable surfactants in the supernatants were then determined by ion chromatography (ECD) and UV-visible spectrophotometry at the wavelengths 245 and 255 nm for PG and PM, respectively.

#### **4.5.4 Determination of the Surfactant Polymerization**

In this research, admicellar polymerization consisted of two steps; first, adsorption of surfactant on to the silica surface, and, second, polymerization of the admicelles by use of UV light and initiator. The solutions contained 0.1 g sodium persulfate after purging with nitrogen gas to remove dissolved oxygen. Polymerization of the surfactant was performed by irradiation with the UV lamp (30 W power supply) at 254 nm wavelength with the average operating temperature  $25 \pm 2^\circ\text{C}$ . The lamp was placed 10 cm from samples. During this time, surfactant suspensions were shaken at 150 rpm for 18 h. Heat released during polymerization was observed by measuring the temperature before and after irradiation. To determine the extent of polymerization, the supernatant concentrations of the polymerizable surfactants PG and PM were analyzed by UV-visible spectroscopy at the wavelengths of 245 and 255 nm, respectively. The concentration of non-polymerizable surfactant, DTAB was determined by ion chromatography with ECD detector. Zeta potential measurements were also evaluated after polymerization at various times on the basis of UV-visible spectroscopy results.

#### **4.5.5 Determination of the Effect of Polymerization on the Dispersion Stability of Silica**

Surfactant concentrations were varied to represent surfactant formation from monolayer through bilayer above the CMC concentration. After the adsorbed surfactant suspension samples were equilibrated/washed, the surface chemistry was characterized before and after polymerization/desorption by using zeta potential measurement. Each surfactant sample was placed into an electrophoretic cell before applying 50-75 mV to the apparatus. Zeta potential values were read and recorded for the silica particles in the electric field. The measurement was repeated ten times per sample, with the average value reported as the zeta potential for each condition.

#### **4.5.6 Determination of the Surfactant Desorption**

Surfactant suspensions before and after polymerization were allowed to settle for one day before removal of the supernatant from the solution. Silica media were allowed to dry in the desiccator for several days to ensure that they were completely dry. The silica was then transferred to a new test tube and rinsed three to five times to remove excess surfactant. DI water was then added to in the new test tube as a blank solution for silica before shaking at 150 rpm for 48 hours for the washing (desorption) study. Finally, the clear liquid was kept for further analysis.

### **4.6 RESULT**

#### **4.6.1 Adsorption Studies**

The adsorption isotherms were obtained by analysis of aqueous surfactant before and after adsorption on silica surface and then plotted in terms of surfactant adsorption (mM/g) versus equilibrium surfactant concentration (mM). Figure 4-1



shows the adsorption isotherm of polymerizable cationic gemini surfactant (PG), the corresponding monomeric polymerizable surfactant (PM), and the conventional cationic surfactant (DTAB) on silica. For all systems, the amount of surfactant adsorbed increased with increasing equilibrium surfactant concentration prior to plateau adsorption. The plateau adsorption levels, which are related to CMC values, are higher for the polymerizable monomer and gemini surfactants than for DTAB (see Fig 4-1; Table 4-2). To confirm the absence of micelles below the plateau adsorption transition point, pinacyanol chloride was added into each vial of surfactant as an indicator. At concentrations slightly below the CMC and when the transition point (plateau adsorption) was reached and exceeded, the solutions were red and blue, respectively, indicating absence and presence of micelles, respectively (Pongprayoon, et al., 2002).

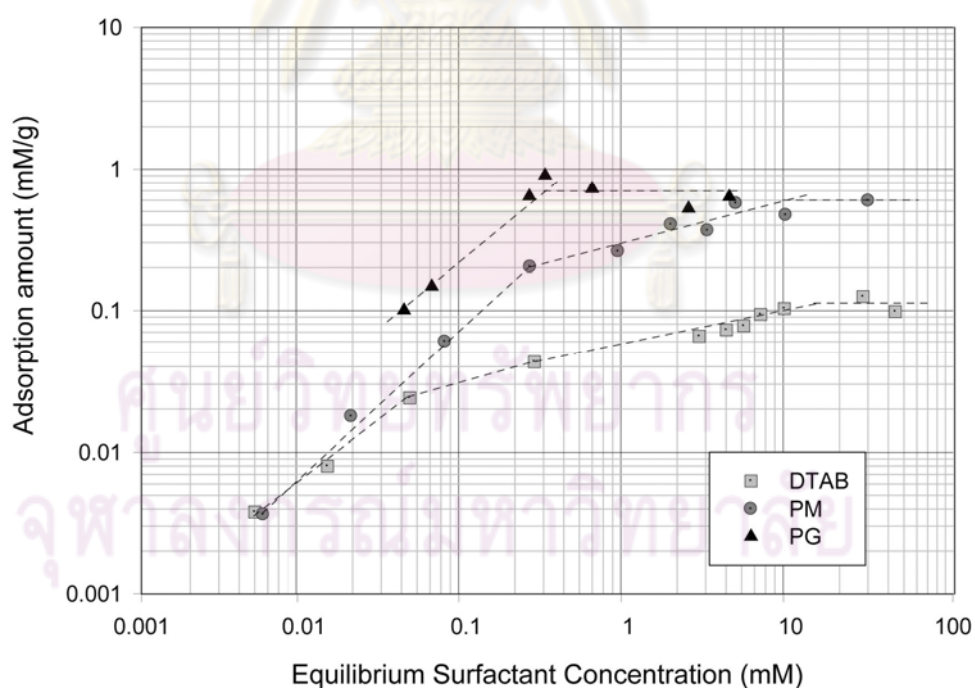


**Figure 4-1** The adsorption isotherm of PG, PM, and DTAB onto silica at electrolyte concentration of 1 mM NaBr, equilibrium pH of 6.5-7.5 and temperature of  $25 \pm 2^\circ\text{C}$

**Table 4-2** Experimentally determined maximum adsorption, molecule per area, and CMCs from adsorption isotherm for PG, PM and DTAB.

Type of Surfactants	Transition Point <sup>a</sup> (mM)	Maximum adsorption (q <sub>Max</sub> )	
		mmole/gram	molecule/nm <sup>2</sup>
<i>Polymerizable Surfactants</i>			
Polymerizable cationic gemini (PG)	0.31	0.70	2.6
Polymerizable monomeric (PM)	10	0.53	2.0
<i>Conventional Surfactant</i>			
DTAB	12	0.11	0.41

#### 4.6.2 Polymerization of Surfactants

Zeta potential measurement and UV irradiation of 80% CMC for polymerizable gemini surfactant were carried out as a function of polymerization time, as shown in Fig 4-2. The absorbance results indicate that complete polymerization is achieved when the samples have been irradiated for 12 h. In addition, polymerized silica coated with surfactant retained a positively charged surface, albeit reduced in charge after irradiation with UV light. System temperature was measured during polymerization in order to examine the heat released by UV irradiation. It was found that temperature rose by 3°C during the 18 h polymerization time (pre and post- polymer temperatures were 24°C and 27°C, respectively). This finding shows there is no a significant heat effect (temperature change) during irradiation by the UV lamp in this study.

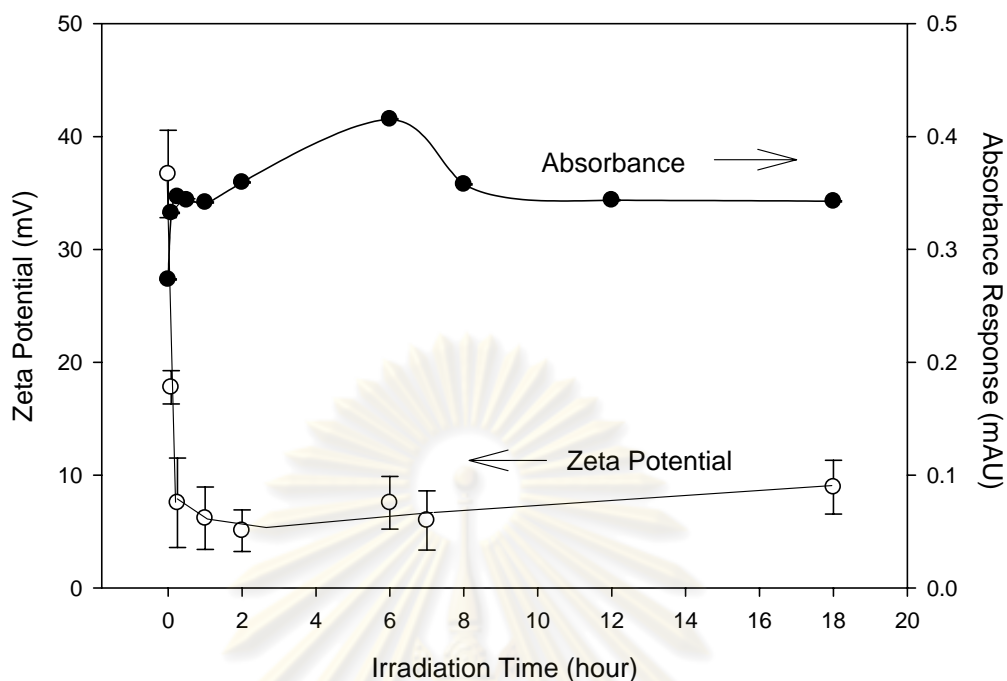


**Figure 4-2** Zeta potential (o) and absorbance response (●) at the concentration of 80% CMC for polymerizable gemini surfactant in a function of UV irradiation time

#### 4.6.3 Effect of Polymerization on the Dispersion Stability of Silica

In order to determine the silica surface charge as a function of surfactant coverage and polymerization, the zeta potential of silica dispersed in water was measured at different pH. It was found that the zeta potential of unmodified silica was negative (of the order of -40 mV) in the pH ranges studied (6.5-7.5), which is consistent with the point of zero charge (pzc) of silica (pH 2-3) (Kosmulski, 2000). At low surfactant loading, the surfactant-modified silica is expected to remain negative; however, bilayer sorption of surfactant is expected to result in positively charged surface because of the head of the cationic surfactant extending into the solution.

Before polymerization, comparison of zeta potential after adsorption for PG, PM, and DTAB are shown in Fig 4-3. As can be seen, the zeta potential of surfactant-

modified silica increases from negative to positive consistent with increased adsorption of the three surfactants studied, going from -40 mV to +40 mV.

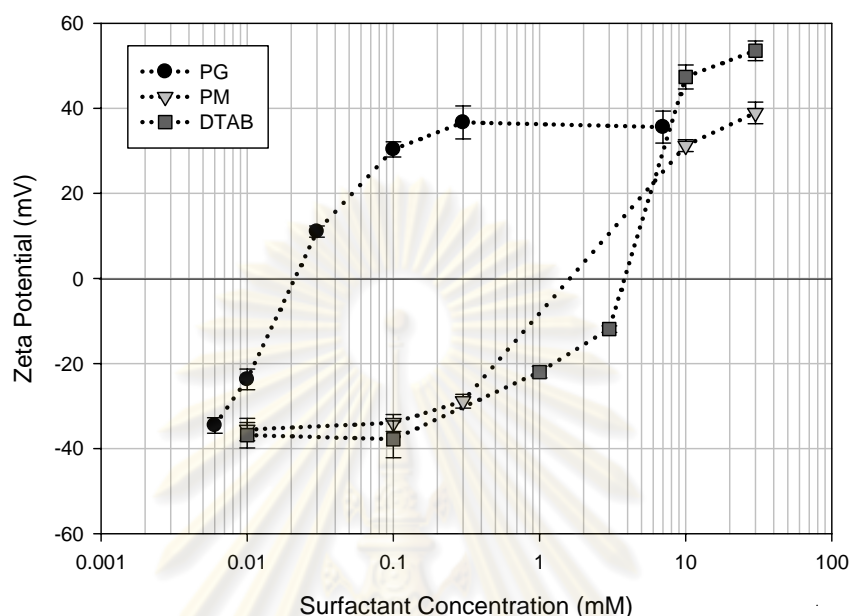


**Figure 4-3** Zeta potential of surfactant-modified silica; before polymerization of PG, PM and, DTAB. Electrolyte concentration; 1 mM of NaBr

Figure 4-4 shows the comparison of zeta potential with adsorption for PG, PM, and DTAB after polymerization. The results demonstrate that, as before, with increasing surfactant concentrations the zeta potential increases from negative to positive as the surfactant concentration approaches and exceeds the transition point/plateau adsorption. It is apparent that polymerization alters the zeta potential profile and that the zeta potential approaches a maximum of +20 mV after polymerization, compared with +40 mV before polymerization (Fig 4-3). Thus, while charge reversal is still achieved, the polymerized admicelle surface is less positive than before, suggesting alteration of the nature of the surface aggregates.

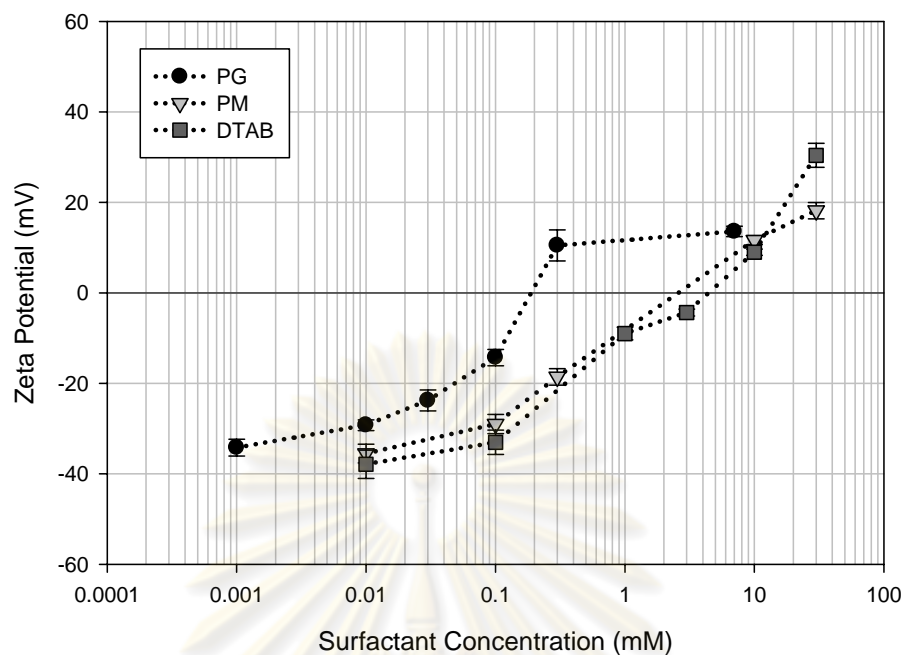


**Figure 4-4** Zeta potential of surfactant-modified silica; after polymerization of PG, PM and, DTAB. Electrolyte concentration; 1 mM of NaBr

#### 4.6.4 Surfactant Desorption Studies

Indirect evaluation of the performance of polymerization for fixing the bilayer on to the silica surface was achieved by zeta potential measurement before and after desorption studies. The objective was to evaluate whether admicelle polymerization would reduce surfactant losses after desorption, compared with systems without polymerization, indicating the presence of a more fixed bilayer. If this is true, then the zeta potential values should indicate retention of more of its positive charge after washing (desorption) of the admicellar system. As discussed in the section “Determination of Surfactant Desorption” the systems were washed (desorbed) by decanting the aqueous phase and replacing with surfactant-free deionized water and allowing to equilibrate (desorb) for 48 h.

Results from zeta potential measurement in desorption studies without polymerization of surfactant PG, PM, and DTAB are shown in Fig 4-5. After washing, the zeta potentials of PG, PM, and DTAB decreased, with the most dramatic decrease for the higher surfactant concentration (compare with Fig 4-3). For most of the higher surfactant concentration, the zeta potential of the non-polymerized system changed from positive to negative which indicates significant desorption. For the highest surfactant concentrations, the zeta potential decreased from  $> 40$  mV for all systems (Fig 4-3) to 20 mV for PG,  $< 10$  mV for PM and -40 mV for DTAB (Fig 4-5). With additional washing steps it is expected that PG and PM would likewise become negatively charged, because the admicelles have not been polymerized and fixed to the surface.

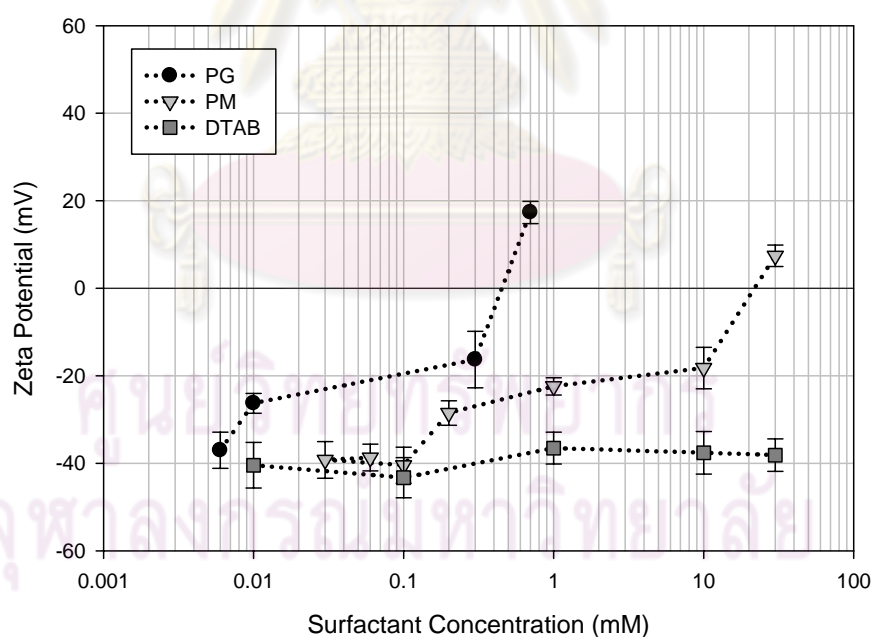


**Figure 4-5** Zeta potential of surfactant-modified silica; before polymerization and after washing of PG, PM and, DTAB. Electrolyte concentration; 1 mM of NaBr

After polymerization, surfactant desorption results for PG, PM, and DTAB are shown in Fig 4-6. Comparing Fig 4-5 and 4-6, we see that the polymerizable

surfactants (PG and PM) retain their cationic zeta potential after washing much better after polymerization (Fig 4-6) than prior to polymerization (Fig 4-5). For PG and PM, zeta potentials remained positive, demonstrating that surfactant bilayers still exist on the surface, although the reduced charge suggests some reconfiguration in the nature of the surface aggregates (Fig 4-6). In contrast, after desorption, the DTAB, surfactant bilayer was not observed, because the surface charge returned to the negative zeta potential value of the original silica, indicating that the DTAB had been “washed off” (desorbed from) the surface. Thus, the result in Fig 4-6 demonstrates the improved stability of the adsorbed surfactant bilayer when the surfactant admicelles are capable of polymerization and have been polymerized.

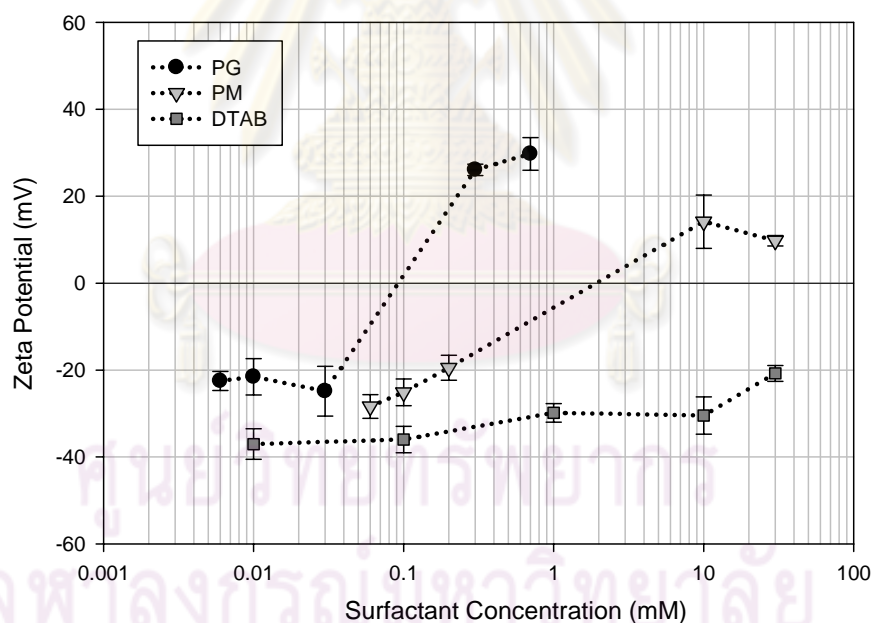


**Figure 4-6** Zeta potential of surfactant-modified silica; after polymerization and after washing of PG, PM and, DTAB. Electrolyte concentration; 1 mM of NaBr

The final results for percentage desorption, surfactant retention, and zeta potential values for each surfactant system before and after polymerization at bilayer concentrations is shown in Table 4-3. The percentage desorption is quantified by mass

balance of surfactant in decanted water in the washing (desorption) study. The results in Table 4-3 show a similar trend to the zeta potential measurements above and are consistent with the polymerizable surfactants reported by previous study (Chodchanok Attaphong, 2006).

**Table 4-3** Experimentally determined for desorption studies at plateau surfactant concentration for PG, PM and DTAB before and after polymerization.

Surfactant Types	% Desorption		% Retained		Zeta Potential (mV)		
	Before Polymerized	After Polymerized	Before Polymerized	After Polymerized	Before Polymerized	Before Polymerized (after washing)	After Polymerized (after washing)
PG	6.96	0.813	93.0	99.3	+36.7	-16.3	+26.1
PM	10.3	4.62	89.7	95.4	+31.2	-18.9	+14.1
DTAB*	61.6	63.7	38.4	36.3	+47.4	-37.0	-30.7

\*Not polymerizable

#### 4.7 DISCUSSION

It is interesting to note that the surface charge goes from -40 mV at very low surfactant coverage to + 40 mV at plateau adsorption indicating complete charge reversal of the surfactant admicelles (i.e., cationic head groups facing out into solution causing a net cationic surface charge). Granted, at intermediate surfactant coverage it is likely that patchy “islands” of bilayer coverage occur, without necessarily yet having complete monolayer coverage as reported by others (Rosen, et al., 1999; Paria and Khilar, 2004; Schemehorn, et al., 1982). The zeta potential values are slightly lower after polymerization, indicating that the adsorbed surfactant is altered somewhat during polymerization. Nonetheless, the zeta potential is still sufficient to maintain the electrostatic nature of the modified silica (i.e., stable dispersion), which is important for numerous applications. In addition, consistent with the main objective of this work, the polymerization process reduced desorption of the surfactant from the surface during washing, as demonstrated both by surfactant in the decanted water and



the zeta potential of the washed surfaces. These results thus support the lower desorption of gemini over non-gemini surfactant, and the increased stability of polymerized admicelles (gemini or not) as reflected by their resistance to desorption. For the conventional surfactant, DTAB, it was apparent that the surfactant bilayer readily desorbs during washing, further demonstrating the improved stability and performance of the adsorbed polymerizable gemini surfactant in the surface modification.



ศูนย์วิทยทรัพยากร  
จุฬาลงกรณ์มหาวิทยาลัย

## CHAPTER V

### ATOMIC FORCE MICROSCOPY AND CONTACT ANGLE MEASUREMENT STUDIES OF POLYMERIZABLE SURFACTANT ADMICELLE ON MICA

#### 5.1 ABSTRACT\*

Atomic force microscopy was used to directly observe and characterize a polymer modified mica surface prepared using a polymerizable gemini surfactant. Normal tapping mode and contact mode AFM were used to image the treated mica surface morphologies in air and liquid environments, respectively. The root mean square roughness of mica surfaces before and after surface modification and polymerization was analyzed from these scans. To determine the effect of styrene adsorption on the surfactant-modified mica, AFM measurements of the modified mica were made at various styrene concentrations. Contact angle measurements were also made to further characterize the nature of the surfactant-modified mica surface. The surface morphology and surface hydrophilicity were observed to be different for the modified mica after polymerization. In addition, the polymerized surface maintained its morphology after washing/desorption studies demonstrating the stability of the polymerized surfactant film.

#### 5.2 INTRODUCTION

Surfactant-modified adsorbents have been extensively investigated for a number of solid surfaces, including alumina (Lopata, 1988; Nayyar, et al., 1994; Charoensaeng, et al., 2008), silica (Sita Krajangpan, 2004; Fuangsawasdi, et al., 2006a; Fuangsawasdi, et al., 2006b), titanium dioxide (Esumi, 2001), and zeolite

---

\*Asnachinda, E., O'Haver, J. H., Sabatini, D. A., and Khoadhiar, S. "Atomic Force Microscopy and Contact Angle Measurement Studied of Polymerizable Gemini Surfactant Admicelle on Mica" Accepted (July, 2009) at Journal of Applied Polymer Science.

(Hayakawa, et al., 1997; Li and Bowman, 1998). Surfactant adsorption and adsolubilization behavior is important in a number of applications such as surface modification, detergency, lubrication, corrosion inhibition, and mineral flotation (Johansson, et al., 2000; Wang, et al., 2004; Qiu, et al., 2007; Zhang and Somasundaran, 2006; Paria, 2007; Serreau, et al., 2008).

Adsolubilization results from aggregation of surfactants at the solid-liquid interface which act as a two-dimensional solvent for organic solutes (Wu, et al., 1987). The inner or core region of the bilayer structure is a non-polar region that can facilitate the solubilization of non-polar solute molecules. The intermediate polarity region, or so-called palisade region, is the region between the surfactant head groups and the core region that is characterized by the penetration of water molecules (Nayyar, et al., 1994). This area has the potential to adsolubilize both polar and non-polar organic solutes.

Surfactant-modified surfaces face the challenge of substantial losses due to desorption and due to decreases in aqueous surfactant concentration or changes in system pH (Rouse et al., 1993). A previous study showed the loss of adsorbed SDS (sodium dodecyl sulfate) and PADD (pentamethylolelyl alkyl-1, 3-propane diammonium dichloride) when the solution pH changed in a column study (Krajangpan, 2004). To reduce the amount of surfactant desorbed from the surface, polymerization of the admicelle (adsorbed surfactant aggregate/layer) has been proposed to create a fixed surfactant film (Esumi, et al., 1989; Esumi, et al., 1991; Esumi, et al., 1993).

Gemini surfactants have been reported to be more surface-active than conventional surfactants (Kunitake, et al., 1984; Hait and Moulik, 2002; Akbey, et al.,

2005; Abe, et al., 2006). To minimize surfactant desorption, polymerization of an adsorbed polymerizable gemini surfactant was carried out in this work. The process is similar to the formation of a polymeric thin film by admicellar polymerization which has been used to modify substrate surface properties in other works such as Kittiyanan, et al., 1996, Pongprayoon, et al., 2002. Admicellar polymerization is a process whereby in-situ monomer polymerization takes place inside of adsorbed surfactant bilayers on various substrates (Grady, et al., 1989).

Classically, the four steps in admicellar polymerization consist of: surfactant adsorption onto solid surfaces, adsolubilization of polymerizable monomers into admicelles, polymerization of the monomers in the admicelles, and removal of accessible surfactant by washing in order to expose the polymerized monomer layer (Pongprayoon, et al., 2002; See and O'Haver, 2003a). In this work, polymerization was of the surfactant itself rather than an adsolubilized monomer. The schematic of surfactant polymerization is shown in Figure 5-1. To verify the presence of the polymer thin film, indirect analytical techniques such as FTIR UV-visible spectroscopy have been conducted (Esumi, et al., 1989; Esumi, et al., 1991; Esumi, et al., 1993). More recently, the examination of polymer formation via admicellar polymerization has been studied using atomic force microscopy (AFM) which allows the film to be studied at the nanometer scale (See and O'Haver, 2003a; See and O'Haver, 2003b; See and O'Haver, 2004). AFM has been used to probe the nature of surfactant-modified mica surface morphologies (Phillips, 1994; See and O'Haver, 2004; Li, et al., 2008). The AFM tip can interact with the sample surface at the atomic level. Software is used to interpret the interactions between tip and sample that are sensed as the tip scans across surface to form images of the surface (Eastman and Zhu, 1996). Imaging in aqueous solution has become popular because it has less

impact on the samples prior to imaging and is more representative of surface morphology in an aqueous environment (Senden, 1995). The objectives of this research are to directly observe and characterize the presence of a polymer thin film prepared from polymerizable gemini surfactant using atomic force microscopy, to evaluate the stability of this film when subjected to desorption (washing), and to examine the effect of adsolubilization on the nature of this film. Along with the AFM examination, contact angle measurements of the admicellar-modified mica surface have been made to help examine these objectives.

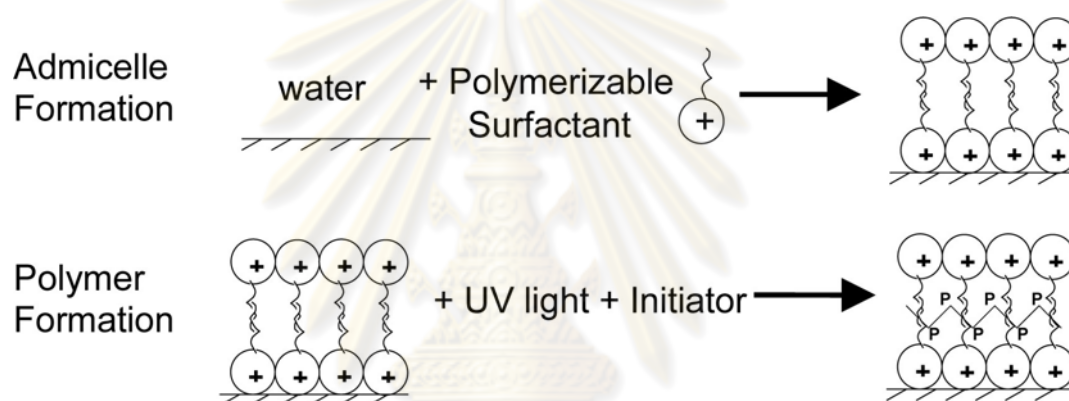


**Figure 5-1** Schematic of the polymerization process for this research

## 5.3 EXPERIMENTAL SECTION

### 5.3.1 Materials

The polymerizable cationic gemini surfactant (PG) used in this study was supplied by the Faculty of Science and Technology, and Institute of Colloid and Interface Science from Tokyo University of Science, Japan (Abe, et al., 2006). Table 5-1 provides a summary of pertinent surfactant properties for this surfactant. For AFM studies, 9 mm mica discs and 12 mm AFM specimen discs were obtained from Ted Pella Inc. (Reddings, CA). The electrolyte concentration was controlled using 1 mM sodium bromide (NaBr). Water used in this work was purified with a resistance

of 18.2 MΩ cm. All experiments were conducted in ambient air at approximately 25±1°C.

**Table 5-1** Polymerizable surfactant properties used in this research

Surfactant	MW	% Active	CMC (mM)	Molecular structure
Polymerizable cationic gemini surfactant (PG)	690.8	97	0.5	$\begin{array}{c} \text{CH}_2=\text{C}(\text{CH}_3)\text{COO}(\text{CH}_2)_{11}\text{N}^+(\text{CH}_3)_2 \\   \\ \text{CH}_2 \\   \\ \text{CH}_2 \\   \\ \text{CH}_2=\text{C}(\text{CH}_3)\text{COO}(\text{CH}_2)_{11}\text{N}^+(\text{CH}_3)_2 \end{array} \cdot 2\text{Br}^-$

### 5.3.2 Atomic Force Microscopy

The multimode Nanoscope V AFM used was from Veeco/Digital Instruments, Inc. (Santa Barbara, CA). Both contact mode AFM and tapping mode AFM were used to evaluate the samples in this study. In contact mode, topographic and deflection images of liquid samples were captured in a standard fluid cell. The fluid cell was initially cleaned by boiling in an 80/20 volume mixture of deionized water and methanol. Scan rate and set point were changed as needed to prevent applying too much force to the sample surface and thus intrude inside the adsorbed structure.

Silicon nitride tips (0.32 N/m) obtained from Veeco/Digital Instruments, Inc. were used for the liquid imaging. In tapping mode, topography and phase images of dry modified surfaces were captured using standard 42 N/m silicon probes (Veeco/Digital Instrument, Inc.).

### **5.3.2.1 AFM Force Measurement**

Force measurements were made by recording the deflection of the free end of the AFM cantilever as the fixed end of the cantilever is extended towards and retracted from the sample. The AFM was set to image the cantilever deflection with a scan rate of 1  $\mu\text{m}/\text{min}$ . The force sensed by the AFM probe is calculated by multiplying the deflection of the cantilever with a spring constant. In this work, the spring constant is 0.0678 N/m. After the tip engaged, the tracking force was adjusted by changing the set point deflection. Force curve analysis allows graphic determination of force exerted by a given deflection set point. Force curve analysis was conducted according to the method of Senden, 2001, which determines the force versus separation curve based on the force versus distance data.

## **5.4 CONTACT ANGLE MEASUREMENT**

Contact angles were measured to observe the hydrophobicity/hydrophilicity of the surfactant modified-mica surfaces using the static sessile drop method with a contact angle goniometer (IT Concepts). A 3  $\mu\text{L}$  drop of double-distilled water was produced manually by a 1 mL syringe and placed on the freshly cleaved and surfactant-modified mica surfaces to test the initial condition of clean mica and surfactant-modified mica surfaces, respectively. Furthermore, examination of changes in surface hydrophobicity was carried out for specific samples by placing a drop of styrene on the same modified-mica surface after measuring water contact angle. All contact angle values are reported as an average of three measurements per sample.

## 5.5 SAMPLE PREPARATION

### 5.5.1 Characterization of Modified-mica Surface

Surfactant solutions were made at 20% (0.1 mM) and 80% of the CMC (0.4 mM) with 1 mM added NaBr in glass vials both without (NP) and with (P) polymerization (experimental sets 1 (NP) and 2 (P), respectively, in Table 5-2). Mica discs were placed into each surfactant system and allowed to equilibrate for 2 days. Samples were then removed from the vials for imaging. An initiator (0.05 g of sodium persulfate) was added to the samples in the second set and they were then placed at a distance of 10 cm from a 30 watt UV lamp for 18 hours to achieve polymerization.

The mica discs were mounted on 12 mm AFM specimen discs using polymer adhesive with no adhesive exposed on the edges. Contact mode fluid-cell samples were prepared by carefully placing a drop of solution onto freshly cleaved mica. The AFM fluid tip holder was then carefully placed into the fluid cell. Additional solution was gently injected into the fluid cell to achieve a total volume of approximately 0.05 mL. After imaging, the fluid cell and tip were rinsed by methanol followed with deionized water. Dried samples were used for the tapping-mode analysis.

### 5.5.2 Characterization of Styrene Adsolubilized in PG Aggregates Adsorbed on Modified-polymerize Mica Discs

Varying amounts of pure styrene were added to the glass vials containing polymerized surfactant-modified mica discs in the presence of 80% CMC of PG solution. Two sets of samples were prepared and analyzed as initial state and equilibrium state corresponding to the time of styrene addition (experimental sets 3 (SI) and 4 (SE), respectively, in Table 5-2). For the initial state, samples were



captured immediately after styrene addition while equilibrium samples were analyzed after 4 days of equilibration.

### 5.5.3 Determination of Surfactant Desorption

Both polymerized and un-polymerized samples were washed/desorbed by decanting the surfactant solution and replacing it with (25 ml) deionized water (experimental sets 5 (NPW) and 6 (PW), respectively, in Table 5-2). This process was repeated five times. The final wash water was allowed to equilibrate for two days before the samples were removed for imaging.

**Table 5-2** Summary of experimental set carried out in this research

Mica disc samples	PG (mM)	Percent of surfactant concentration	Styrene (mg/l)	Ratio of styrene feed conc. to surfactant
<b>Experiment set 1</b> NP1 NP2	0.1 0.4	20% CMC 80% CMC	n/a n/a	n/a n/a
<b>Experiment set 2</b> P1 P2	0.1 0.4	20% CMC 80% CMC	n/a n/a	n/a n/a
<b>Experiment set 3</b> SI1 SI2	0.4 0.4	80% CMC 80% CMC	72.5 109	1:0.57 1:0.40
<b>Experiment set 4</b> SE1 SE2	0.4 0.4	80% CMC 80% CMC	72.5 109	1:0.57 1:0.40
<b>Experiment set 5</b> NPW1 NPW2	0.1 0.4	20% CMC 80% CMC	n/a n/a	n/a n/a
<b>Experiment set 6</b> PW1 PW2	0.1 0.4	20% CMC 80% CMC	n/a n/a	n/a n/a

NP = Non-polymerize; P = Polymerize; NPW = Non-polymerize with washing; PW = Polymerize with washing; SI = Styrene addition at initial state; SE = Styrene addition at equilibrium state; 1-20% of CMC; 2- 80% of CMC; n/a = not available

## 5.6 RESULT AND DISCUSSION

### 5.6.1 Unmodified-mica

A topography image of an unmodified mica disc is shown in Figure 5-2a. The aggregate free surface had a root mean square roughness (RMS) of 0.068 nm as comparable to the literature (Deacon, et al., 2000), which provides a baseline for evaluating morphology changes for subsequent surfactant-modified surfaces. All the RMS values reported in this work are obtained from the average of the different AFM images. They were captured from the different positions on the sample. To determine the hydrophobicity of the surfaces, contact angle measurements were conducted as a measure of surface wettability. The results show that the unmodified mica is hydrophilic (water-wet) with an average initial contact angle of  $12^\circ$  (Table 5-3).



**Figure 5-2** Topography images of mica surfaces for unmodified mica (a), and images of PG adsorbed on mica before polymerization at NP1, 20% CMC (b), NP2, 80% CMC (c) with the presence of 1 mM NaBr electrolyte.

**Table 5-3** Summary of contact angle measurements

Sample Condition	Average Contact Angle (degree)			
<b><i>Effect of Concentration</i></b>				
Clean mica	Low Feed Concentration		High Feed Concentration	
12 <sup>b</sup>	57± 3.7 (NP1)		61± 1.5 (NP2)	
<b><i>Effect of Polymerization</i></b>				
Sample condition	Before polymerization		After polymerization	
Low feed Concentration (20% CMC)	57± 3.7 (NP1)		53± 2.2 (P1)	
High Feed Concentration (80% CMC)	61± 1.5 (NP2)		47± 4.1 (P2)	
<b><i>Effect of Desorption</i></b>				
Sample condition	Before polymerization		After polymerization	
	Before Desorption	After Desorption (washing)	Before Desorption	After Desorption (washing)
Low feed concentration (20% CMC)	57± 3.7(NP1)	58± 3.1 (NPW1)	53± 2.2 (P1)	53± 3.1 (PW1)
High Feed Concentration (80% CMC)	61± 1.5 (NP2)	48± 3.6 (NPW2)	47± 4.1 (P2)	41± 3.6 (PW2)
<b><i>Effect of organic solute on admicellar polymerization formation (styrene addition)</i></b>				
Sample condition	Initial State		Equilibrium State	
Low feed concentration	52± 2.9 (SI1)		53± 5.2 (SE1)	
High Feed Concentration	53± 1.1 (SI2)		54± 2.9 (SE2)	

NP = Non-polymerize; P = Polymerize; NPW = Non-polymerize with washing; PW = Polymerize with washing; SI = Styrene addition at initial state; SE = Styrene addition at equilibrium state; 1-20% of CMC; 2- 80% of CMC; n/a = not available

<sup>b</sup>Value is initial contact angle; at five minutes completely water wet (contact angle = 0)

### 5.6.2 Adsorption of PG on Mica

The first set of surfactant-modified mica disc samples investigates the adsorbed structure of non-polymerized PG. The bulk PG concentrations of 0.1 and, 0.4 mM added are approximately 20% and 80% of the CMC value (0.5 mM), respectively. These values are below but approach the CMC to avoid aqueous micelle surface admicelle interaction which would occur above the CMC. Contact mode AFM was used to examine the topographic images for adsorbed surfactant on the mica surface in water. Figure 5-2b, and 5-2c show deflection images of the adsorbed PG for sample NP1 (20% CMC) and NP2 (80% CMC) (see Table 2) with the presence of 1 mM NaBr electrolyte, respectively. The results demonstrate that at low surfactant concentrations (Figure 5-2b) little visible change is observed relative to the mica surface without surfactant (Figure 5-2a) even though low levels of surfactant adsorption exist in Figure 5-2b, while at 80% CMC surfactant loading (Figure 5-2c), patchy aggregates or 'islands' of adsorbed surfactant can be seen on the surface.

As mentioned by Song, et al., 2006, contact angle measurements can provide useful information on the nature of surfactant aggregates on the surface. Contact angle measurements in Table 5-3 indicate that the surface hydrophobicity (contact angle) increases with surfactant adsorption on the mica even at the low surfactant concentration. Increasing of surface contact angles were observed in every condition when compared with the clear blank mica. This agrees with results of Song, et al., 2006, who reported that contact angles increased with surfactant adsorption due to organic nature of the adsorbed surfactant bilayer.

### 5.6.3 Polymerization of PG on Mica

The second set of modified mica surfaces was established by applying UV irradiation to polymerize the surfactant-modified surfaces. The average surface roughness of sample P2 (80% CMC), is 249 nm which is much higher than the samples without polymerization, (e.g., 70 nm. for sample NP2) and for the virgin mica surface (0.068 nm). The huge difference in these values indicates the major change in the surface of the modified mica. The lack of long-range or repeatable structure in the aggregates demonstrates the heterogeneity of the modified surface.

The contact angles for samples P1 and NP1 are quite similar ( $53 \pm 2.2$  and  $57 \pm 3.7$ , respectively), while the P2 contact angle ( $47^\circ$ ) is much lower (more hydrophilic) than NP2 ( $61^\circ$ , see Table 5-3). Thus, a more hydrophilic surface is obtained after polymerization, although still not as hydrophilic as the mica surface. The reason that polymerization creates a more hydrophilic surface at high surfactant loading (80% CMC), while not doing so at lower surfactant concentration (20% CMC), is unclear and should be further evaluated in future research.

### 5.6.4 Adsolubilization of Styrene onto Polymerized-surfactant-modified Mica Surfaces

Experimental sets three and four investigate the impact of styrene addition on the polymerized-surfactant-modified mica surface at the initial state (SI) and at the equilibrium state (SE), respectively. Initial state samples (SI1 and SI2) refer to polymerized surfactant mica surfaces that were imaged immediately after styrene addition. Polymerized samples evaluated four days after styrene addition are referred to as the equilibrium state samples (SE1 and SE2). The topographic and phase images of sample SE2 are shown in Figure 5-3. These results demonstrate that the surface

morphology changes after styrene addition and equilibration. At the initial state, few aggregates are observed with the average surface roughness equal to 132 nm. (as compared to 252 nm before styrene addition). As equilibrium is approached, the surface roughness increased to 268 nm and the aggregates become smaller and more numerous. This is in agreement with the literature (See and O'Haver, 2004), where changes in surface morphology were observed during the equilibration of the adsorbed aggregates with styrene. The topography images were especially interesting, as they showed the surface going from a relatively flat layer with droplets of styrene present, to what appears to be a surface aggregate composed of connected emulsion-like droplets with an average diameter of  $755 \pm 132$  nm (Figure 5-3a). The phase images in Figure 5-3b emphasize the change to be more discrete, interconnected aggregates. This change was unexpected, and points to future research areas examining the extent of cross-linking/network formation during polymerization and the ability of this polymerized layer to undergo radical phase changes.

The force-distance curve measurements at liquid environment for treated styrene adsorbilize surfaces are shown in Figure 5-4. The results show that with increasing surfactant admicelles and thus adsorbilization (SE1 versus SE2, respectively), stronger adhesive forces were observed between the tip and the surface. These findings indicate that the tip required more force to get free from the surface while it was retracted with higher surfactant and styrene loading. The non-flat baseline is due to the presence of Coulombic forces encountered near the surface of the aggregate which has adsorbed counterions. This has been observed, and also explained by DLVO theory (McBride and Baveye, 2002). Though these samples were examined in water, the presence of the surfactant layer, and of a surfactant layer which contains a core which is either very rich in styrene, or nearly pure styrene,

allows for capillary forces to occur. This was previously observed during examinations of similar systems (See and O'Haver, 2004). While sample SE1 had adhesion forces of 2.7 nN, the SE2 adhesion force is about 6.6 nN which is two times larger than samples with low styrene loading. Thus, the presence of a larger amount of adsolubilized styrene either increased the bilayer viscosity, or the presence of a styrene zone in the surfactant layer allowed true capillary forces to increase the adhesive forces between the tip and the bilayer. Collectively these results demonstrate that adsolubilization does in fact impact the properties of the surfactant-modified surface.

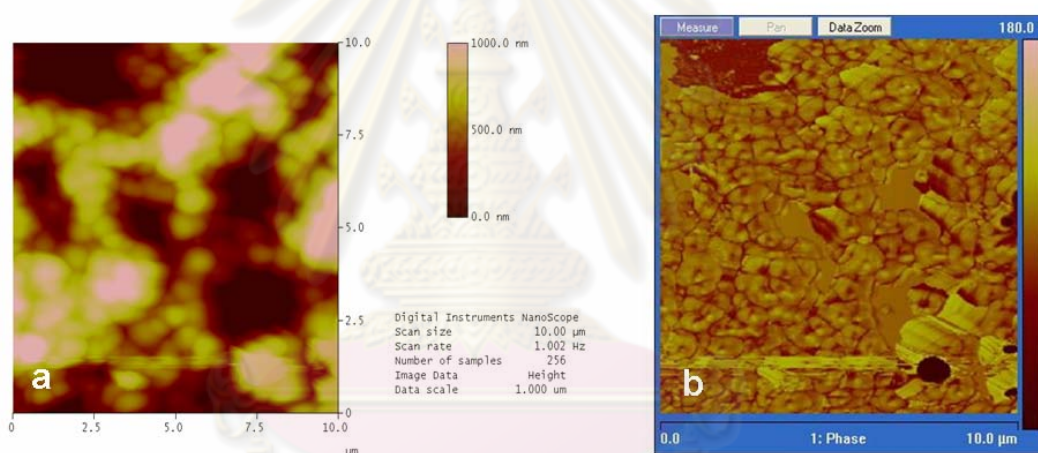


**Figure 5-3** Topography (a) and phase (b) images of styrene adsolubilized into polymerized PG mica surface at the 80% CMC of PG concentration with the presence of 1 mM NaBr electrolyte for equilibrium state, SE2.

จุฬาลงกรณ์มหาวิทยาลัย

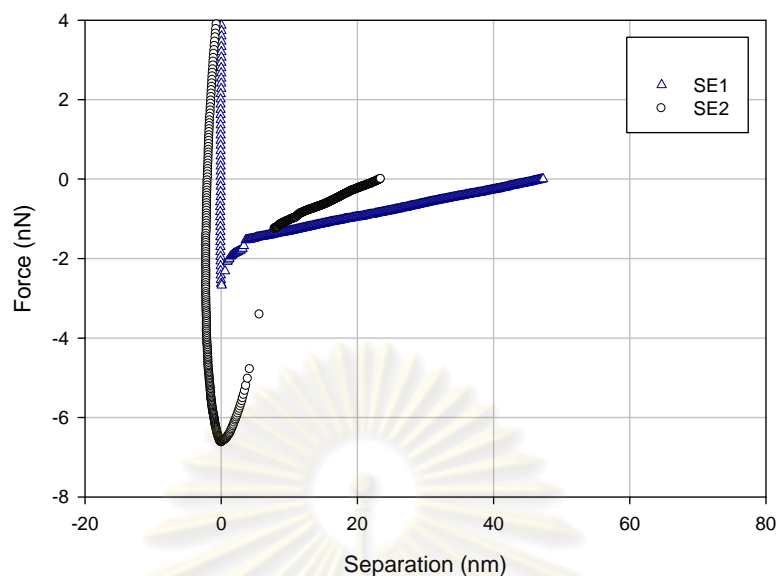


**Figure 5-4** Typical interaction forces between the tip and mica surface as a function of tip-surface separation for sample SE1 and SE2.

### 5.6.5 Desorption of PG on Mica

Experimental sets five and six examined the impact of washing/desorption of the surfactant from non-polymerized and polymerized surfaces, respectively. Results from surface roughness measurements and visual observation demonstrate increasing surface roughness with increased surfactant loading. Figure 5-5 shows the topographic images comparison of PG adsorbed on mica before and after washing at different surfactant loading and both with and without polymerization (sample NP2, NPW2, P2 and PW2). The result from non-polymerized samples (Figure 5a, and 5b) show a different morphology of modified-mica surface obtained after washing. Surprisingly, the surface roughness increases and more visible surface aggregates are present when non-polymerized samples are washed. However, at 80% of CMC washed surfaces have a lower contact angle with water ( $48^\circ$ ), indicating a decrease in hydrophobicity, when compared with the un-washed samples (contact angle =  $61^\circ$ ).



For the polymerized samples, the visual results in Figures 5-5c and 5-5d demonstrate that the surface topography is similar after washing (desorption) and before; this is corroborated by contact angle measurements which are statistically the same before and after washing (contact angles of  $47\pm 4.1$  before washing and  $41\pm 3.6$  after washing – see Table 5-3). These findings demonstrate that the polymerized surfactant film is extremely stable on the mica surface.

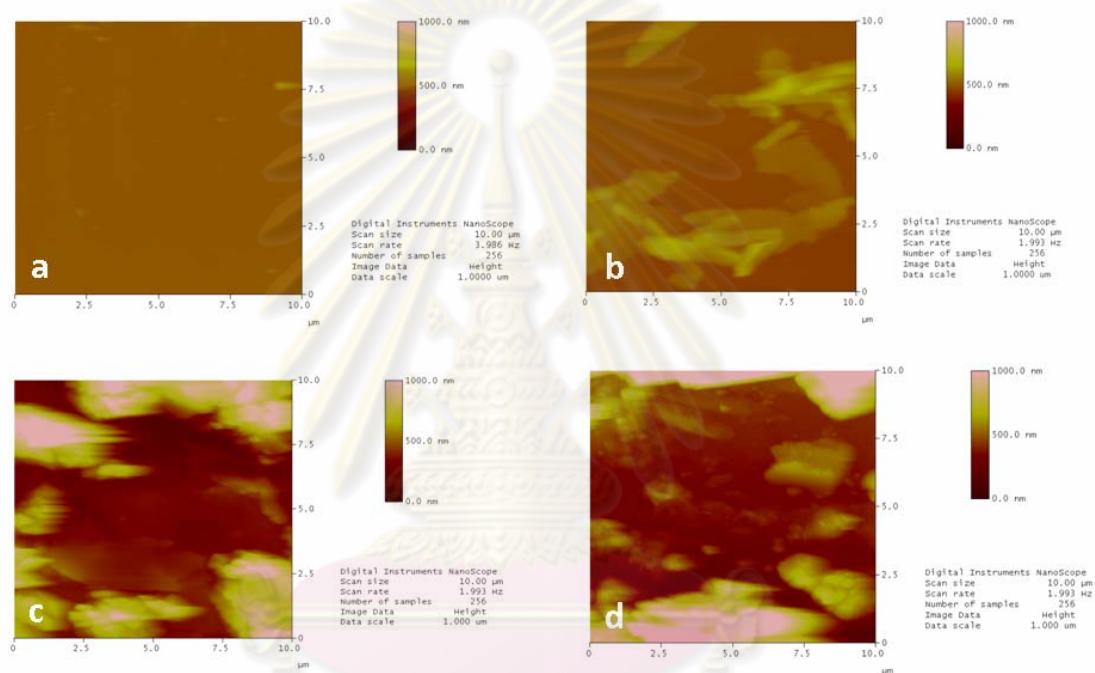


**Figure 5-5** Topographic images comparison of PG adsorbed on mica; a) NP2, before washing of non-polymerized surface at 80% CMC b) NP2W, after washing of non-polymerized surface at 80% CMC; Polymerized system; c) P2, before washing of polymerized surface at 80% CMC d) PW2, after washing of polymerized surface at 80% CMC with the presence of 1 mM NaBr electrolyte

## 5.7 CONCLUSIONS

Contact mode and tapping mode AFM were used to examine the presence of a polymer thin film formed from the polymerization of a gemini surfactant on mica. Contact angle measurements were also used to evaluate the hydrophobicity of treated surfaces. Polymerized PG at a concentration slightly below CMC (80%CMC) show the obvious surface morphology changes over the non-polymerized surfaces. The surfaces demonstrate decreasing contact angle (increasing hydrophilicity) when modified by the polymerized surfactant. Surface aggregate morphology changes dramatically with the addition of adsolubilized styrene, and the styrene core in the adsorbed layer shows tip-surface adhesion which increased with increasing of styrene loading. The polymerized layers remained essentially unchanged after washing, demonstrating the robust nature of the polymerized layer.



ศูนย์วิทยทรัพยากร  
จุฬาลงกรณ์มหาวิทยาลัย

## CHAPTER VI

### STYRENE AND PHENYLETHANOL ADSOLUBILIZATION OF POLYMERIZABLE GEMINI SURFACTANT

#### 6.1 ABSTRACT\*

A polymerizable gemini surfactant was used to adsolubilize styrene and phenylethanol, representing weak and strong polar organic solutes, respectively, in order to evaluate the impact of admicellar polymerization on the adsolubilization process. Adsolubilization was also evaluated using a polymerizable monomeric surfactant (PM) and conventional surfactant (DTAB) for comparison purposes. The main results were that:

(1) Polymerized and unpolymerized admicelles showed similar adsolubilization potential - validating the use of polymerized admicelles without sacrificing adsolubilization.

(2) Gemini surfactants showed equal to slightly higher adsolubilization than conventional surfactants.

#### 6.2 INTRODUCTION

Surfactant adsorption and adsolubilization is important to many industrial and environmental applications (Paria and Khilar, 2004; Karapanagioti, et al., 2005; Fuangswasdi, et al., 2006a; Fuangswasdi, et al., 2006b; Fuangswasdi, et al., 2007; Charoengseang, et al., 2008). However, a critical problem facing surfactant-modified materials is the loss of surfactant due to desorption (Rouse, et al., 1993; Sita Krajangphan, 2004; Chodchanok Attapong, 2006). Polymerization of polymerizable

---

\*Asnachinda, E., Khaodhiar, S., and Sabatini, D. A. "Styrene and Phenylethanol Adsolubilization of Polymerizable Gemini Surfactant" Submitted at Journal of Surfactants and Detergents (July, 2009).

surfactant admicelles shows potential for reducing these losses. Gemini surfactants have been reported to be more surface active and have very low cmc values compared to the corresponding monomeric and conventional surfactant, thus the less raw materials for upscale production are required (Kunitake, et al., 1984; Oda, et al., 1997; Zana, et al., 2002; Hait and Moulik, 2002; Akbey, et al., 2005; Abe, et al., 2006). Recently, polymerizable cationic gemini surfactant which having structure based on bis(quaternary ammonium) gemini surfactant has been synthesized and studied (Abe, et al., 2006). With the effectiveness of gemini surfactants, cationic polymerizable gemini surfactants are expected to exhibit strong adsorption on the silica surface while minimizing desorption of surfactant from the surface, thereby improving operating characteristics of the surfactant-modified media.

## **6.3 BACKGROUND**

### **6.3.1 Adsolubilization of Surfactant onto Solid Oxide Surface**

Adsorbed surfactants (admicelles) act as a two-dimensional solvent that promotes organic solute partitioning into the admicelles, a process known as adsolubilization (Wu, et al., 1987; Tan and O'Haver, 2004). The admicelle bilayer structure can be divided into three regions similar to a micelle. The outer region contains the most polar or ionic region because it is comprised of the surfactant head group. The inner region or the core region is non-polar and comprised of the hydrocarbon surfactant tail groups. The intermediate polarity region, or the so-called palisade region, is the place between surfactant head groups and the core region (Nayyar, 1994). The number of surfactant chains can affect the adsolubilization capacity (Esumi et al., 1997; Esumi et al., 2000; Dickson and O'Haver, 2002).

### 6.3.2 Polymerization of Surfactant

Polymerizable gemini surfactants have various been reported to possess unique properties such as better solubilization, lower Krafft temperatures, lower critical micelle concentration (CMC), greater efficiency in lowering the surface tension, and foaming properties than the conventional monomeric surfactants (Hait and Moulik, 2002; Akbey, et al., 2005). Polymerization of admicelles is a process whereby adsorbed surfactant bilayers are polymerized after admicelle formation (Grady, et al, 1989). After admicelle formation, the double bonds in the surfactant are polymerized and bond together, with the desired goal of mitigating the potential for surfactant desorption. In this study, a polymerizable cationic gemini surfactant (Abe, et al., 2006) was used to evaluate its adsolubilization capacity for organic solutes. Previous research has reported on the adsorption and desorption properties of these surfactants on silica (Asnachinda, et al., 2009).

Main purpose of this study is to determine the adsolubilization capacity of the polymerizable gemini admicelles, with and without polymerization, and to compare with conventional surfactant. The secondary purpose of this work is to determine the effect of organic solute polarity on adsolubilization by a polymerizable surfactant. It is hypothesized that the polymerized admicelles will retain their adsolubilization potential and that the two head/ two tail gemini surfactant will demonstrate similar or higher adsolubilization capacity. This work will extend previous research demonstrating high adsorption and lower desorption of these same surfactants (Asnachinda, et al., 2009) by assessing the adsolubilization potential of these admicelles.

## 6.4 EXPERIMENTAL SECTION

### 6.4.1 Materials

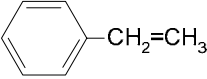
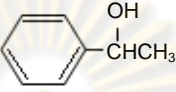
Surfactants used in this study were divided into two types; polymerizable and non polymerizable surfactants. Polymerizable cationic gemini surfactant (PG) and polymerizable monomeric surfactant (PM) were kindly supplied by Faculty of Science and Technology, and Institute of Colloid and Interface Science from Tokyo University of Science, Japan. Non-polymerizable surfactant, dodecyl trimethylammonium bromide (DTAB), was purchased from S.M. Chemical Supplies Co., Ltd., Thailand. The properties of these surfactants and their surface properties are shown in **Table 6-1**.

**Table 6-1** The properties of surfactants used in this study

Surfactant	MW	% Active	Molecular structure
Polymerizable cationic gemini surfactant (PG)	690.8	97	$\begin{array}{c} \text{CH}_2=\text{C}(\text{CH}_3)\text{COO}(\text{CH}_2)_{11}\text{N}^+(\text{CH}_3)_2 \\   \\ \text{CH}_2 \\   \\ \text{CH}_2 \\   \\ \text{CH}_2=\text{C}(\text{CH}_3)\text{COO}(\text{CH}_2)_{11}\text{N}^+(\text{CH}_3)_2 \end{array} \cdot 2\text{Br}^-$
Polymerizable monomeric surfactant (PM)	346.4	95	$\text{CH}_2=\text{C}(\text{CH}_3)\text{COO}(\text{CH}_2)_{11}\text{N}^+(\text{CH}_3)_3 \cdot \text{Br}^-$
Dodecyl trimethylammonium bromide (DTAB)	308.3	99	$\text{C}_{12}\text{H}_{25}\text{N}^+(\text{CH}_3)_3 \cdot \text{Br}^-$

Styrene (99% purity, Aldrich) and 1-phenylethanol (98% purity, Fluka) were selected as weak and strong polar organic solutes in this study, respectively. Properties of these organic solutes are shown in **Table 6-2**.

**Table 6-2** Properties of organic solutes

Organic Solutes	MW	Molecular formula		Solubility in water (Molar)	Density (g/mL) 25 °C	Dipole Moment
		formula	Structure			
Styrene	104.15	C <sub>8</sub> H <sub>8</sub>		0.0027	0.909	0.13
Phenyl ethanol	122.17	C <sub>8</sub> H <sub>10</sub> O		0.040	1.01	1.65

Silica material (SiO<sub>2</sub>) was selected as an adsorbent with 15 nm particle size. It was purchased from S.M. Chemical Supplies Co., Ltd., Thailand, and was used as received. The specific surface area from manufacturer product is 140-180 m<sup>2</sup>/g. The electrolyte concentration was controlled using 1 mM sodium bromide (NaBr). The solution pH was adjusted using NaOH and HCl. All chemicals were use as received and are ACS analytical reagent grade. Water used in this work was purified and has a resistance of 18.2 MΩ cm. Plastic and glassware were rinsed well with double-distilled water three times prior to use.

ศูนย์วิทยทรัพยากร  
จุฬาลงกรณ์มหาวิทยาลัย

## 6.4.2 Methods

### 6.4.2.1 Surfactant Adsolubilization

Adsolubilization studies were designed based on previous adsorption isotherms (Asnachinda, et al., 2009) which allowed determination of the appropriate concentration where maximum surfactant coverage occurred without the presence of micelles in the bulk solution; i.e., a point just below the CMC to avoid the complications of having micelles in solution.

Adsolubilization experiments were performed by varying the organic solute concentration (individual batches for styrene and phenylethanol each) in a surfactant suspension which had been pre-equilibrated with surfactant adsorption. The solution was shaken for 48 hours and then centrifuged. To compare the adsolubilization capacity between polymerized and non-polymerized systems, additional batches of styrene and phenylethanol adsolubilization were carried out after polymerization of surfactant admicelles. Polymerization experiments were conducted by the radiation of UV light with the help of initiator (sodium persulfate) (Esumi, et al., 1989; Esumi, et al., 1991; Esumi, et al., 1993). The suspension at equilibrium condition was added by initiator for polymerization reaction. Then, the suspension was irradiated with a 30 W, UV lamp and shaking for 18 hours.

### 6.4.2.2 Measurements

Surfactant concentrations and organic solute concentrations (styrene and phenylethanol) were analyzed by HPLC (Agilent) equipped with Acclaim surfactant column and detected with ELSD and UV detector at 247 nm, respectively. Mobile phase of the system were prepared by using 0.1 M of ammonium acetate ( $C_2H_3O_2NH_4$ ) at pH 5.4 and acetonitrile ( $C_2H_3N$ ) with the ratio of  $C_2H_3O_2NH_4$  to



C<sub>2</sub>H<sub>3</sub>N equal 60:40. A Cole-Parmer UV lamp was used as the initiator in the polymerization process. All measurement were carried out at 25±2°C

## 6.5 RESULTS

### 6.5.1 Styrene Adsolubilization

The adsolubilization isotherms of styrene with the four surfactant admicellar systems are shown in Figure 6-1. From Figure 6-1, it is seen that as the equilibrium concentration of styrene increased, the adsolubilization per gram of silica increased for all surfactant systems. These results demonstrate that increasing adsolubilization occurs with increasing aqueous solute concentrations as expected for a partitioning process. This process can be described by the partitioning coefficient  $K_{adm} = X_{adm} / X_{aq}$  where  $X_{adm}$  = the molar ratio of solute in the admicellar phase and  $X_{aq}$  = the molar ratio of solute in the aqueous phase (Tan and O'Haver, 2004; Chareonseang, et al., 2008; Chareonseang, et al., 2009).

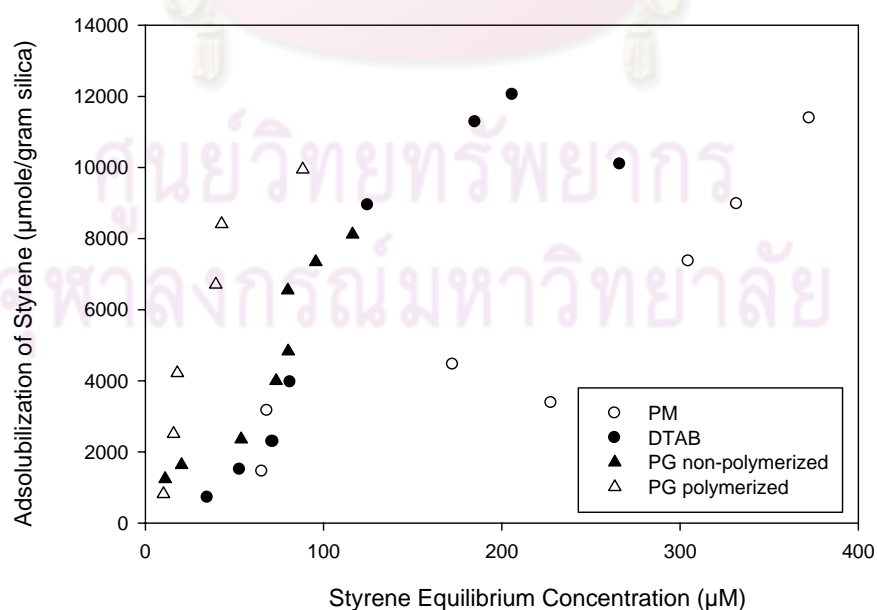


**Figure 6-1** Adsolubilization isotherms of styrene by PG, PM and DTAB

Figure 6-2 shows the admicellar partition coefficient of styrene,  $K_{adm}$ , as a function of the styrene aqueous mole fraction in DTAB, PM, PG and PG-polymerized. Decreasing values of  $K_{adm}$  with increasing  $X_{aq}$  suggests palisade layer adsolubilization; with increased loading the  $K_{adm}$  decreases as adsolubilization sites fill and become saturated (Fuangswasdi, et al., 2006b; Rouse, et al., 1995; Charoenseang, et al., 2009; Dickson and O'Haver, 2002). Polymerized and non-polymerized PG admicelles show virtually the same styrene adsolubilization illustrating that polymerization did not decrease the adsolubilization potential. This is a very important finding relative to the utility of polymerized admicelles; as shown in previous work, polymerization has the positive effect of decreasing surfactant desorption from the admicelles (Asnachinda, et al., 2009), and here we demonstrate that no loss in adsolubilization potential occurs. Polymerized and non-polymerized PG admicelles show similar  $K_{adm}$  trends with PM and DTAB, albeit with higher  $K_{adm}$  suggesting twin tail groups in PG molecule can facilitate larger amounts of polar solute in the admicellar core region, again demonstrating a desirable characteristic of the polymerizable gemini surfactant.

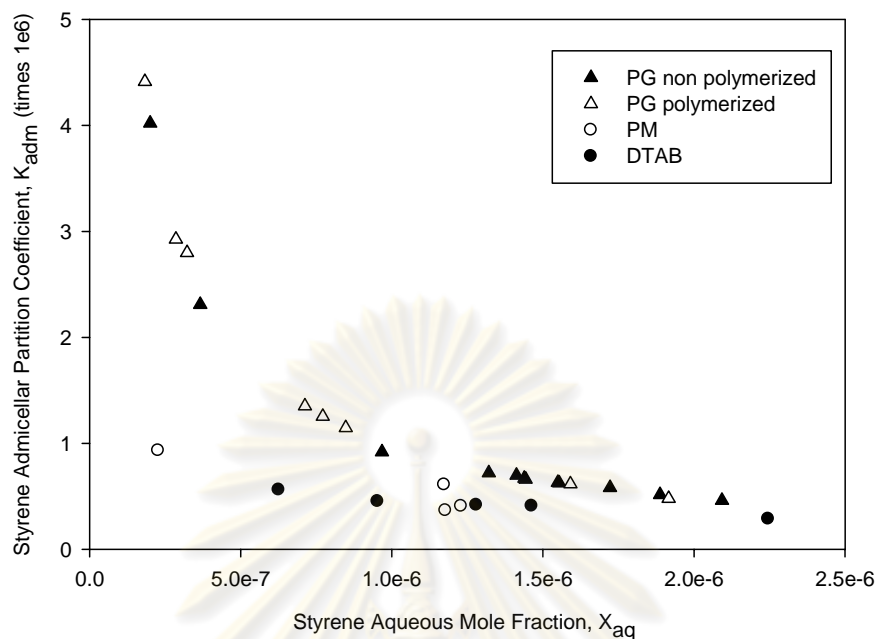


**Figure 6-2** The styrene admicellar partition coefficient ( $K_{adm}$ ) as a function of the styrene aqueous mole fraction ( $X_{aq}$ ) in DTAB, PM and PG.

Table 6-3 summarizes the adsolubilization coefficients ( $K_{adm}$ ) for the solutes used in this work by tabulating  $K_{adm}$  values at the highest levels of  $X_{aq}$  (i.e., closet to maximum additivity or water solubility).  $\log K_{adm}$  values show similar value for unpolymerized and polymerized PG ( $\log K_{adm} = 5.66$  and  $5.68$ , respectively). From Figure 2 it is observed that as  $X_{aq}$  approaches to water solubility,  $K_{adm}$  values of PG adsolubilization systems approach (decrease) towards values observed for PM and DTAB ( $\log K_{adm} = 5.61$  and  $5.46$ , respectively), although non-polymerized and polymerized PG still adsolubilize more styrene than PM and DTAB. However, the greater adsolubilization potential of PG and PM is even more obvious at lower values of  $X_{aq}$  (see Figure 6-2).

**Table 6-3** Summary of adsolubilization capacities of the surfactants used in this study

Surfactant (1 mM NaBr)	Maximum adsorption ( $q_{Max}$ ) (mmole/gram)	Styrene Adsolubilization		Phenylethanol Adsolubilization	
		$K_{adm}^a$	$\log K_{adm}^a$	$K_{adm}^a$	$\log K_{adm}^a$
<b>Non polymerized system</b>					
PG	0.70	461,422	5.66	1,120	3.05
PM	0.53	407,296	5.61	N/M	
DTAB	0.11	286,818	5.46	779.6	2.89
<b>Polymerized system</b>					
PG	N/A	479,406	5.68	1,100	3.04

<sup>a</sup>Based on high  $X_{aq}$  values (mole fraction of organic solute in the aqueous phase)

<sup>b</sup>N/M not measured

### 6.5.2 PHNYLETHANOL ADSOLUBILIZATION

The adsolubilization capacities of phenylethanol with PG (polymerized and unpolymerized) and DTAB are shown in Figure 6-3. The results show that as  $X_{aq}$  values increase and approaches water solubility,  $\log K_{adm}$  values decrease for all surfactant systems, again due to the palisade effect. Both the unpolymerized and polymerized PG admicelles show very similar levels of adsolubilization ( $\log K_{adm} = 3.04$  compared to  $\log K_{adm} = 3.05$ , respectively, see Table 6-3). This finding suggests that polymerization process does not affect the phenylethanol adsolubilization capacity by PG. This is again important to the potential use of polymerized surfactant which decreases surfactants desorption from the admicelles (Asnachinda, et al., 2009).

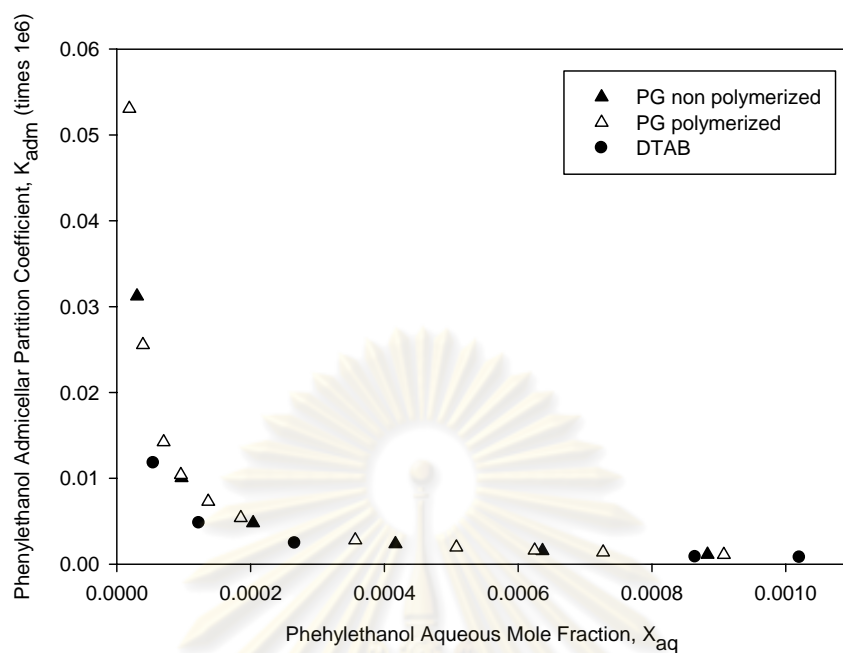


**Figure 6-3** The phenylethanol admicellar partition coefficient ( $K_{adm}$ ) as a function of the phenylethanol aqueous mole fraction ( $X_{aq}$ ) in DTAB and PG.

## 6.6 SUMMARY

This research thus demonstrates that gemini admicelles retain their adsolubilization capacity upon polymerization. This combined with the previously reported lower desorption of the polymerized gemini surfactants (Asnachinda, et al., 2009), demonstrate the desirable characteristics of these surfactant systems for surface modification and adsolubilization. The adsolubilization isotherms indicated palisade layer partitioning for both polar solutes studied. The gemini admicelles showed similar to higher adsolubilization as compared to other surfactant systems while requiring less surfactant to achieve bilayer coverage due to the lower CMC of the gemini surfactants.

# CHAPTER VII

## SUMMARIES, CONCLUSIONS AND ENGINEERING SIGNIFICANCE

### 7.1 SUMMARIES

Surfactant adsorption and desolubilization is important to many industrial and environmental applications. However, the crucial problem of using surfactant-modified materials is the loss of surfactant (desorption). So far, gemini surfactants have been reported to be more surface active and have very low CMC values compared to the corresponding monomeric and conventional surfactant, thus the less raw materials for upscale production are required. In this study, surfactant polymerization by using polymerizable gemini surfactant (PG) as well as its monomeric (PM) counterpart and conventional surfactant (DTAB) were used to evaluate in order to reduce these substantial losses. Laboratory scale batch experiments were conducted to study the surfactant adsorption, desolubilization of organic solutes by polymerizable surfactants. In addition, surfactant-modified surfaces were characterized by Atomic Force Microscopy (AFM) and contact angle measurement. The major goal of this research is to demonstrate that the polymerizable gemini surfactants show desirable stability of surfactant-modified silica surfaces versus using single head group polymerizable and non-polymerized surfactants.

The critical micelle concentrations (CMC) of the surfactant systems with an electrolyte concentration of 1 mM NaBr were examined through measurement of

surface tension of the surfactant at liquid-air interface by a surface tensiometer with a platinum plate at room temperature (25°C). CMC values of polymerizable gemini surfactant (PG) was two order of magnitude lower than CMC values of its monomeric (PM) and conventional surfactant (DTAB).

Surfactant adsorption studies were conducted to evaluate the impact of various surfactant systems on admicelle formation. Polymerizable gemini surfactant showed the higher surfactant adsorption than the monomeric and conventional surfactants. The polymerizable gemini surfactant also reached its maximum adsorption capacity at a lower aqueous surfactant concentration.

The attempt to reduce surfactant desorption was evaluated through the polymerization process. Polymerization of surfactant is accomplished by UV irradiation to surfactant solution. The polymerization reached its equilibration after 12 hours without showing a significant heat effect (temperature change) during irradiation by the UV lamp in this study.

The evidence of admicelle formation and surfactant desorption were determined indirectly by zeta potential measurement through the silica surface charge as a function of surfactant coverage and polymerization. Results show lower desorption of gemini over non-gemini surfactant, and the increased stability of polymerized admicelles (gemini or not) as reflected by their resistance to desorption. For the conventional surfactant, DTAB, it was apparent that the surfactant bilayer readily desorbs during washing.

To examine the presence of a polymer thin film formed from the polymerization of a gemini surfactant on mica. Contact mode and tapping mode AFM were used. Contact angle measurements were also implemented to determine the

hydrophobicity of treated surfaces. Polymerized of polymerizable gemini surfactant at a concentration slightly below CMC show the obvious surface morphology changes over the non-polymerized surfaces. In addition, surfaces hydrophilicity increase when modified by the polymerized surfactant.

In general, AFM study is particular difficult to qualitatively evaluate results for evaluation. Thus, the replication of sample imaging is needed to be precise in order to obtain a statistically characterized in each single sample. In this work, the idea of surface properties before and after polymerization, desorption has been proposed. However, specific details of surface characterization such as the extent of network formation, surface force has not been made because it might distracting of research objectives. Thus, future research are suggested to fulfill the questions of surface characterization at the end of this chapter.

The adsolubilization of polymerizable gemini surfactant when subject to different polarity of organic solutes were evaluated. Adsolubilization reaches its maximum when surfactant adsorbed onto the solid-liquid interface with the complete bilayer formation and/or maximum adsorption.

The effect of styrene adsolubilize into surfactant admicelle was found through the surface aggregate morphology changes of adsolubilized styrene. The styrene core in the adsorbed layer shows tip-surface adhesion increased with increasing of styrene loading.



## 7.2 CONCLUSIONS

The specific conclusions are made based on the results of this research:

1. The CMCs values are similar between DTAB and PM while the CMC of PG was over an order of magnitude lower.
2. For all systems, the amount of adsorbed surfactant was enhanced with increased equilibrium surfactant concentration prior to plateau adsorption. The maximum adsorption of PG and PM are comparable and are higher than conventional surfactant, DTAB. However, PG require smaller amount of surfactant concentration to reach its maximum adsorption capacity than PM and DTAB.
3. Zeta potential of non-modified silica was negative (on the order of -40 mV) in the studied pH ranges (6.5-7.5). Before polymerization, the comparison of zeta potential after adsorption for PG, PM and, DTAB increased from negative to positive consistent with increased surfactant, indicating complete charge reversal reflective of the bilayer surfactant coverage. However, the zeta potential values are slightly lower after polymerization but still sufficient to maintain the electrostatic nature of the modified silica (i.e., stable dispersion).
4. The polymerized bilayer of polymerizable surfactant PM and PG were more strongly fixed at silica surface and more resistant to desorption after washing; in contrast non polymerizable, DTAB, was not able to maintain its bilayer upon washing.
5. The polymerization process has been observed to have only slight or no impact on the adsolubilization capacity of styrene and phenylethanol.

6. Styrene increases its adsorption capacity to the core where it can expand to facilitate more solute molecules. On the other hand, phenylethanol adsorption was preferential related to the palisade region of admicelle structure due to its strong polarity and partitions well into the polar area.
7. Polymerized PG at a concentration slightly below CMC (80%CMC) shows the obvious surface morphology changes over the non-polymerized surfaces. The surfaces demonstrate decreasing contact angle (increasing hydrophilicity) when modified by the polymerized surfactant.
8. Surface aggregate morphology changes dramatically with the addition of adsorbed styrene, and the styrene core in the adsorbed layer shows tip-surface adhesion which increased with increasing of styrene loading.
9. The polymerized layers remained essentially unchanged after washing, demonstrating the robust nature of the layer.

### 7.3 ENGINEERING SIGNIFICANCE

Polymerizable surfactant-modified adsorbents appear promising based on decreases in surfactant loss/desorption during application. As a result, the lower surfactant requirements in terms of raw material will be required in the treatment of groundwater and wastewater contaminated with organic solutes. In addition, the unique characteristic of polymerizable gemini surfactant including the polymerizable group, the two hydrophilic and hydrophobic groups and organic solutes properties including structure, degree of polarity; all of the factors impact the efficiency of admicelle formation and adsolubilization enhancement. Polymerizable gemini surfactant also demonstrate none or slightly impact to the adsolubilization. However, selecting of the appropriate surfactant for specific solute is crucial for enhancing the efficiency of adsolubilization process.

A number of applications are possible such as surface modification, detergency, lubrication, corrosion inhibition, and mineral flotation are based on surfactant adsorption and adsolubilization. In field of surfactant modification, organic solute removal for both of filter and packed-bed reactor could be implementing. For in-situ application, passive permeable barrier by surfactant-modified adsorbent could be applied for mitigate groundwater contamination.

## 7.4 RECOMMENDATIONS AND FUTURE WORKS

Polymerization of surfactant demonstrates the promising reduces in surfactant loss/desorbed during application as well as the AFM studies that illustrate an effective way to characterize the polymerized film by polymerizable surfactant-modified surface. However, there are some specific issues of surface characterization that could be considered in order to help comprehension of surface properties. The recommendations are listed as the follow;

### **Effect of condition parameters**

1. Determine the effect of pH to understand more about interaction between oxide surface and its layer surfactant.
2. Using different kind of surfactants to elaborate more adsorption mechanism.

### **Surface characterization**

1. Surface analysis experiment to determine the internal surface characteristic.
2. The extent of cross-linking/network formation during polymerization and the ability of this polymerized layer to undergo radical phase changes.
3. The observation of surface force measurement in order to determine surface thickness before and after polymerization.

## REFERENCES

- Abe, M., Tsubone, K., Koike, T., Tsuchiya, K., Ohkubo, T. and Sakai, H. Polymerizable Cationic Gemini Surfactant. Langmuir 22 (2006):8923.
- Akbey, C., Gill, N., Powe, A., Warner, I. M. Monomeric and polymeric anionic gemini surfactants and mixed surfactant systems in micellar electrokinetic chromatography, Part I: Characterization and application as novel pseudostationary phases. Electrophoresis 26 (2005):415.
- Alami, E., Beinert, G., Marie, P. and Zana, R. Alkanediyl- $\alpha,\omega$ bis(dimethylalkylammoniumbromide) surfactants. 3. behavior at the air-water interface. Langmuir 9 (1993):1465.
- Asnachinda, E., Khaodhiar, S. and Sabatini, D. A. Effect of Ionic Head Group on Admicelle Formation by Polymerizable Surfactants. J Surfactants Deterg (2009):Published Online. (<http://www.springerlink.com/content/8710056235202v30/fulltext.pdf>).
- Atkin, R., Craig, VS. J., Wanless, E. J. and Biggs, S. Mechanism of cationic surfactant adsorption at the solid-aqueous interface. J Colloid and Interf Sci 103 (2003):219.
- Attaphong, C. Adsorption and Adsolubilization of Polymerizable Surfactant onto Aluminum Oxide Surface. Master Thesis, Graduate School, Chulalongkorn University, 2006.
- Charoensaeng, A. Admicelle and Adsolubilization Using Linker Molecules and Extended Surfactants onto Aluminum Oxide Surface. Ph.D. Thesis, Graduate School, Chulalongkorn University, 2008.
- Charoensaeng, A., Khaodhiar, S. and Sabatini, D. A.. Styrene Solubilization and Adsolubilization on an Aluminum Oxide Surface Using Linker Molecules and Extended Surfactants. J. Surfactants Deterg. 11 (2008) 61
- Charoensaeng A, Sabatini DA, Khaodhiar S. Solubilization and Adsolubilization of Polar and Nonpolar Organic Solutes by Linker Molecules and Extended Surfactants. J Surfactants Deterg. 12 (2009):209
- Davydov, V. Y. Adsorption on Silica Surfaces. In Papirer E, Adsorption on silica surfaces. New York : Marcel Dekker, 2000.
- Deacon, M. P., McGurk, S., Roberts, C. J., Williams, P. M., Tender, S. J. B., Davies, M. C., Davis, S. S. (Bob) and Harding, S., Biochem J 348 (2000):557.
- Dickson, J. and O' Haver, J. Adsolubilization of Naphthalene and  $\alpha$  - Naphthol in  $C_n$ TAB Admicelles. Langmuir 18 (2002):1917.
- Eastman, T. and Zhu, D. M. Adhesion Forces between Surface-Modified AFM Tips and a Mica Surface. Langmuir 12 (1996):2859.

- Elbert, R., Folda, T. and Ringsdorf, H. Saturated and polymerizable amphiphiles with fluorocarbon chains. Investigation in monolayers and liposomes. J Am. Chem. Soc., 106 (1984):7687.
- Esumi, K., Watanabe, N. and Meguro, K. Polymerization of surfactant bilayer on alumina using a polymerizable surfactant. Langmuir 5(1989):1420.
- Esumi, K., Watanabe, N. and Meguro, K. Polymerization of styrene adsolubilized in polymerizable surfactant bilayer on alumina. Langmuir 7(1991):1775.
- Esumi, K., Nakao, T. and Ito, S. Fixation of polymerizable surfactant on alumina by uv irradiation. J Colloid and Interf Sci 156(1993):256.
- Esumi, K., Goino, M. and Koide, Y. The effect of added salt on adsorption and adsolubilization by a gemini surfactant on silica. J Colloid and Interface Sci 118 (1996):161
- Esumi, K., Takeda, Y., Goino, M., Ishiduki, K., Koide, Y. Adsorption and adsolubilization by cationic surfactants on laponite clay. Langmuir 13(1997):2585.
- Esumi, K., Maedomari, N., Torigoe, K. Mixed surfactant adsolubilization of 2-naphthol on alumina. Langmuir 16(2000):9217.
- Esumi, K. Interactions between Surfactants and Particles: Dispersion, Surface Modification, and Adsolubilization. J. Colloid Interface Sci, 241(2001):1.
- Frey, W., Schneider, J., Ringsdorf, H. and Sackmann, E. Preparation, microstructure, and thermodynamic properties of homogeneous compound monolayers of polymerized and monomeric surfactants on the air/water interface and on solid substrates. Macromolecules 20(1987):1312.
- Fuangswasdi, A., Charoensaeng, A., Sabatini, D. A., Scamehorn, J. F., Acosta, J. E., Osathaphan, K. and Khaodhiar, S. Mixtures of Anionic and Cationic Surfactants with Single and Twin Head Groups: Adsorption and Precipitation Studies. J. Surfactants Deterg, 9(2006a):21.
- Fuangswasdi, A., Charoensaeng, A., Sabatini, D. A., Scamehorn, J. F., Acosta, J. E., Osathaphan, K. and Khaodhiar, S. Mixtures of Anionic and Cationic Surfactants with Single and Twin Head Groups: Solubilization and Adsolubilization of Styrene and Ethylcyclohexane. J. Surfactants Deterg 9(2006b):29.
- Fuangswasdi, A., Krajangpan, S., Sabatini, D.A., Acosta J.E., Osathaphan, K. and Tongcumpou, C. Effect of Admicellar Properties on Adsolubilization: Column Studies and Solute Transport. Water Res, 41(2007):1343.
- Grady, B.P., O'Rear, E.A., Penn, L.S. and Pedicini, A. Polymerization of styrene-isoprene on glass cloth for use in composite manufacture. Polym composites 19(1989):597.
- Hait, S.K, Moulik, S.P. Gemini surfactants: a distinct class of self-assembling molecules. Current Sci, 82(2002):1101.

- Harwell, J. H. and O'Rear, E. A. Adsorbed Surfactant Bilayers as Two-Dimensional Solvents: Admicellar-Enhanced Chromatography, In Scamehorn, J. F. and Harwell, J. H. 155, New York: Marcel Dekker, 1989.
- Hayakawa, K., Dobashi, A., Miyamoto, Y. and Satake, I. Adsolubilization equilibrium of rhodamine B by zeolite/surfactant complexes. Zeolite and Microporous Materials 105(1997):2115.
- Johansson, B., Pugh, R. J. and Alexandrova, L. Flotation de-inking studies using model hydrophobic particles and non-ionic dispersants. Colloids Surf. A, 170(2000):217.
- Karapanagioti, HK., Sabatini, DA. and Bowman, RS. Partitioning of Hydrophobic Organic Chemicals (HOC) into Anionic and Cationic Surfactant-Modified Sorbents. Water Research 39(2005):699.
- Kitiyanan, B., O'Haver, J. H., Harwell, J. H. and Osuwan, S. Adsolubilization of Styrene and Isoprene in Cetyltrimethylammonium Bromide Admicelle on Precipitated Silica. Langmuir 12(1996):2162.
- Krajangpan, S. Enhanced Adsolubilization in Silica-Packed Column by Mixture of Cationic and Anionic Surfactants. Master Thesis, Graduate School, Chulalongkorn University, 2004.
- Kosmulski, M. Surface charge and zeta potential of silica in mixtures of organic solvents and water. In Papirer E, Adsorption on silica surfaces. New York:Marcel Dekker, 2000.
- Kunitake, T., Nagai, M., Yanagi, H., Takarabe, K. and Nakashima, N. Bilayer formation by aggregate of polymeric amphiphiles. Macromol Sci Chem A 21(1984):1237.
- Laschewsky, A., Ringsdorf, H. and Schmidt, G. Polymerization of hydrocarbon and fluorocarbon amphiphiles in Langmuir-blodgett multilayers. Thin solid film, 134(1985):153.
- Li, R., Chen, Q., Zhang, D., Liu, H., Hu, Y. Mixed monolayers of gemini surfactants and stearic acid at the air/water interface. J Colloid and Interf Sci 327(2008):162.
- Li, Z. and Bowman, R.S. Sorption of Perchloroethylene by Surfactant-Modified Zeolite as Controlled by Surfactant Loading. Sci Technol 32(1998):2278.
- Lopata, J. J. A Study of the Adsorption of Binary Anionic Surfactant Mixtures on Alpha Alumina Oxide. Master Thesis, Department of Chemical Engineering, University of Oklahoma, 1988.
- McBride, M. B. and Baveye, P. Division S-2-Particle Interactions in Colloidal Systems. Soil Sci Soc Am J 66(2002):1207.
- Nayyar, S. P., Sabatini, D. A., and Harwell, J. H. Surfactant Adsolubilization and Modified Admicellar Sorption of Nonpolar, Polar, and Ionizable Organic Contaminants. Environ. Sci. Technol 28(1994):1874.
- Nontasorn, P., Chavadej, S., Rangsunvijit, P., O'Haver, J. H., Chaisirimahamorakot, S. and Na-Ranong, N. Admicellar polymerization modified silica via a continuous

- stirred-tank reactor system: Comparative properties of rubber compounding. Chemical Engr J 108(2005):213.
- Oda, R., Huc, I. and Candan, S.J. Gemini surfactants, the effect of hydrophobic chain length and dissymmetry. Chem. Commun (1997):2105
- O'Haver, J. H., Lobban, L. L., Harwell, J. H. and O'Rear, E. A. Adsolubilization and Solubilization in Surfactant Aggregates, In Christian, S. D. and Scamehorn, J. F., Marcel Dekker, New York, Chapter 8(1995):277.
- Paria, S., Khilar, K. C.. A review on Experimental Studies of Surfactant Adsorption at the Hydrophilic Solid-water Interface. Adv Colloid Interface Sci 110 (2004):75.
- Paria, S. Surfactant-enhanced Remediation of Organic Contaminated Soil and Water. Adv Colloid Interface Sci 138(2007):24.
- Pavan, P. C., Crepaldi, E. L., Gomes, G. A. And Valim, J. B. Adsorption of sodium dodecylsulfate on a hydrotalcite-like compound. Effect of temperature, pH and ionic strength. Colloids Surf. A 154(1999):399.
- Phillips, R.W. Atomic force microscopy for thin film analysis. Surface and coating tech 68-69(1994):770.
- Pindzola, B.A., Jin, J. and Gin, D. Cross-linked normal hexagonal and bicontinuous cubic assemblies via polymerizable gemini amphiphiles. J Am Chem Soc 125(2003):2940.
- Pongprayoon, T., Yanumet, N., O'Rear, E.A. Admicellar polymerization of styrene on cotton. J Colloid and Interf Sci 249(2002):227.
- Qiu, L. G., Wu, Y., Wang, Y. M. and Jiang, X. Synergistic Effect between Cationic Gemini Surfactant and Chloride Ion for the Corrosion Inhibition of Steel in Sulfuric Acid. Corrosion Sci 50(2007):576.
- Rosen, M. J. Surfactants and Interfacial Phenomena. New York:Wiley, 1989.
- Rosen, M. J. Geminis: A New Generation of Surfactants: These Materials have Better Properties than Conventional Ionic Surfactants as well as Positive Synergistic Effects with Non-ionic. Chemtech 23(1993):30.
- Rosen, M. J., Mathias J. H. and Davenport, L. Aberrant aggregation behavior in cationic Gemini surfactants investigated by surface tension, interfacial tension, and fluorescence methods. Langmuir 15(1999):7340.
- Rouse, J. D., Sabatini, D. A. and Harwell, J. H. Minimizing Surfactant Losses Using Twin-Head Anionic Surfactants in Subsurface Remediation. Environ. Sci. Technol 27(1993):2072.
- Rouse, J. D., Sabatini, D. A., Deeds, N.E. and Brown, R. E. Micellar Solubilization of Unsaturated Hydrocarbon Concentrations As Evaluated by Semiequilibrium Dialysis. Environ Sci Technol 29(1995):2484.
- Saphanuchart, W., Saiwan, C. and O'Haver, J. H. Temperature Effects on Adsolubilization of Aromatic Solutes Partitioning To Different Regions in Cationic Admicelles, Colloids Surf. A 317(2008):303.



- Scamehorn, J. F., Schechter, R. S. and Wade, W. H. Adsorption of Surfactants on Mineral Oxide Surfaces from Aqueous Solutions: I: Isomerically Pure Anionic Surfactants. J. Colloid Interface Sci 85 (1982): 463.
- Serreau, L. Beauvais, M. Heitz, C. and Barthel, E. Adsorption and Onset of Lubrication by a Double-chained Cationic Surfactant on Silica Surfaces. J Colloid Interface Sci 332(2008):382.
- See, C. H., O'Haver, J. H. Atomic force microscopy studies of admicellar polymerization polystyrene-modifies amorphous silica. J Applied polymer Sci 87(2003a):290.
- See, C. H., O'Haver, J. H. Atomic force microscopy characterization of ultrathin polystyrene films formed by admicellar polymerization on silica disks. J Applied polymer Sci 89(2003b):36
- See, C. H., O'Haver, J. H. Two-dimensional phase transition of styrene adsolubilized in cetyltrimethylammonium bromide admicelles on mica. J Colloid and Surf 243(2004):169.
- Senden T. J., Drummond C. J.. Surface chemistry and tip-sample interactions in atomic force microscopy. J Colloid and Interf Sci 94(1995):29
- Somasundaran, P. and Fuerstrnsu, D. W. Mechanism of Alkyl Sulfonate Adsorption at the Alumina-Water Interface. J. Phys. Chem 70 (1966):90.
- Somasundaran, P. and Zhang, L. Modification of Silica-Water Interfacial Behavior by Adsorption of Surfactants, Polymers, and Their Mixtures. In Papirer E, Adsorption on silica surfaces. New York : Marcel Dekker, 2000.
- Tan, Y. and O'Haver, J. H. Lipophilic Linker Impact on Adsorption of and Styrene Adsolubilization in Polyethoxylated Octylphenols. Colloid Surf. A 232(2004):101.
- Wang, W., Zhou, Z., Nandakumar, K., Xu, Z., and Masliyah, J. H. J Colloid Interface Sci 274(2004):625.
- Wang, Y., Han, Y., Huang, X., Cao, M. and Wang, Y. Aggregation behaviors of a series of anionic sulfonate gemini surfactant and their corresponding monomeric surfactant. Colloid and Interface Science 319(2007):534.
- West, C. C., and Harwell, J. H. Surfactants and Subsurface Remediation. Environ Sci Technol 26(1992):2324.
- Wu, J., Harwell J. H. and O'Rear, E. A. Two-Dimensional Reaction Solvents: Surfactant Bilayers in gemini surfactant on Silica. Colloid Surf A 118 (1987):161.
- Yutaka, Y. Polymerizable Surfactants: spontaneous polymerization in organized micellar media. In Karsa, D. R. Design and Selection of Performance Surfactant. Sheffield, UK:2000.
- Zana, R., Yiv, S., Kale, K. M. Chemical relaxation and equilibrium studies of association in aqueous solutions of bolaform detergents. 3. docosane-1, 22 bis(trimethylammonium bromide). J Colloid and Interf Sci 77(1980):456.

Zana, R. Dimeric and oligomeric surfactants behavior at interfaces and in aqueous solution: a review. J Colloid and Interf Sci 97(2002):205.

Zhang, R. and Somasundaran, P. Advances in Adsorption of Surfactant and their Mixtures at Solid/Solution Interfaces. Adv Colloid Interface Sci 123-126(2006):213.



ศูนย์วิทยทรัพยากร  
จุฬาลงกรณ์มหาวิทยาลัย



**APPENDICES**

ศูนย์วิทยทรัพยากร  
จุฬาลงกรณ์มหาวิทยาลัย

## APPENDIX A

### CMC MEASUREMENTS

Critical micelle concentration (CMC) values were determined from the point of inflection in the plots of surface tension versus log of surfactant concentration. Figure A-1 shows the plot between surface tension and surfactant concentration in the presence of 1 mM NaBr electrolyte concentration.

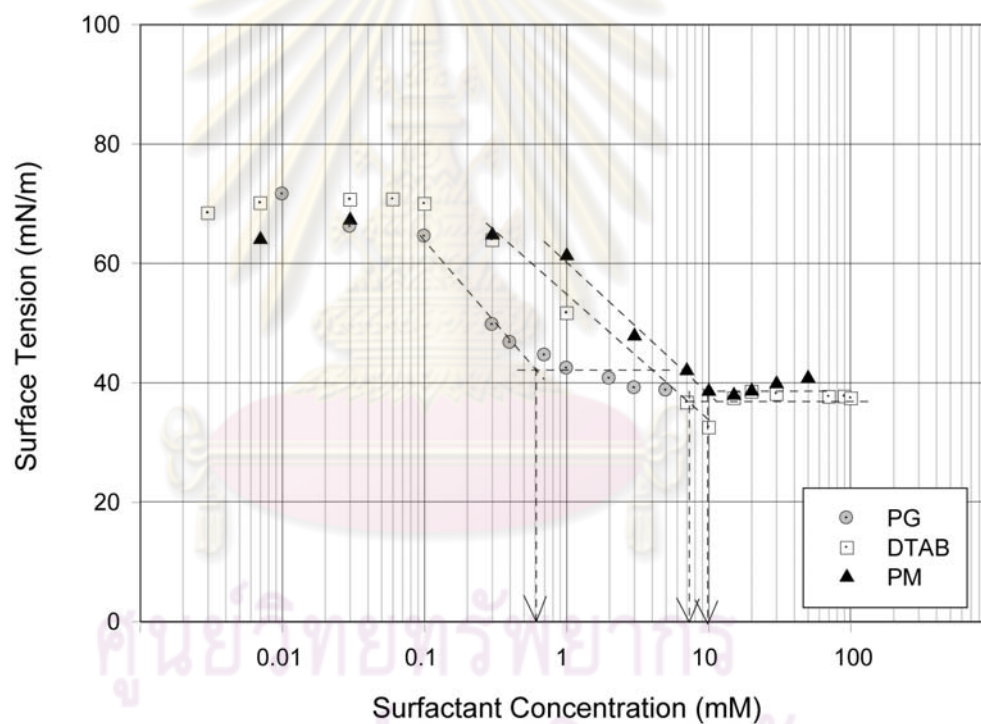


**Figure A-1** Interfacial surface tension of PG, PM, and DTAB at electrolyte concentration at 1 mM NaBr, equilibrium pH of 6.5-7.5 and temperature of  $\pm 25\text{ C}^\circ$

Table A-1 shows the experimentally determined CMCs from surface tension and the minimum surface tension for polymerizable cationic surfactant (PG), polymerizable monomeric surfactant (PM), and conventional cationic surfactant

(DTAB). While the CMC values are similar between DTAB and PM, the CMC of PG was over an order of magnitude lower. This is in agreement with literatures results (Kunitake, et al., 1984; Wang, et al., 2007) which show that two heads groups in gemini surfactant have lower CMC values than conventional surfactants. Gemini surfactants have a stronger aggregation ability and are packed more closely than the single-chain surfactant because of two hydrophobic chains in their molecule are connected at the level of the head groups which enhanced the hydrophobic interaction among the hydrocarbon chain and reduced the electrostatic among the hydrophilic head group.

**Table A-1** Experimentally determined CMCs from surface tension, the minimum surface tension, and surfactant adsorption for PG, PM and DTAB

Type of Surfactants	CMC (mM)	Min. Surface Tension (mN/m)
<i>Polymerizable Surfactants</i>		
Polymerizable cationic gemini (PG)	0.60	38.7
Polymerizable monomeric (PM)	10	37.9
<i>Conventional Surfactant</i>		
DTAB	8.0	37.8

**Calculation: Effective area per head surfactant (Rosen, et al., 1989)**

Salt : swamping amount of electrolyte (high salt concentration)

$$\Gamma = -\frac{1}{2.303RT} \left( \frac{\partial \gamma}{\partial \log C_1} \right)_T$$

No Salt : absence of any other solute

$$\Gamma = -\frac{1}{4.606 RT} \left( \frac{\partial \gamma}{\partial \log C_1} \right)_T$$

where

$g$	=	Interfacial tension (N/m)
$R$	=	8.314 J mol <sup>-1</sup> K <sup>-1</sup>
$G$	=	in unit mol/1000m <sup>2</sup>
<u>K@25</u>	=	298 K

**The area per molecule at the interface**

$$a_1^s = \frac{10^{-16}}{NT_1}$$

$N$  = Avogadro's number (= 6.023 x 10<sup>23</sup>)

$\gamma$  = in unit mol/cm<sup>2</sup>

$\Gamma$  = Interfacial tension (N/m)

When  $G$  is in mol/1000m<sup>2</sup>, in square angstroms, equals 10<sup>23</sup>/NT

$\gamma$  = N/m then

$\Gamma$  = mol/1000m<sup>2</sup>

## APPENDIX B

### SURFACE CHARACTERIZATION

#### 1) Surface Characterization by FTIR

Polymerization of surfactant was verified by the absence of FTIR spectra. Figure A-2 shows the FTIR spectra of surfactant adsorbed on silica before and after various periods of admicelle polymerization. The polymerizable surfactant PG and PM included characteristic peaks from the C=C aliphatic bond at around  $1,640\text{ cm}^{-1}$ , N-H Amine at  $3,300\text{-}3,500\text{ cm}^{-1}$  and C-H alkanes and C-H alkenes at  $2,850 - 2,960$  and  $3,020 - 3,080\text{ cm}^{-1}$  respectively. Our main interest is in the C=C around  $1640\text{ cm}^{-1}$  as we would expect this peak to disappear if polymerization has occurred. According to the results, it was difficult to conclude that C=C bands were present before polymerization reaction and were absent after polymerization because the unclear spectra were observed. Thus, the validation of polymerized surfactant film by FTIR technique was not appropriated in this study.

ศูนย์วิจัยทรัพยากร  
จุฬาลงกรณ์มหาวิทยาลัย

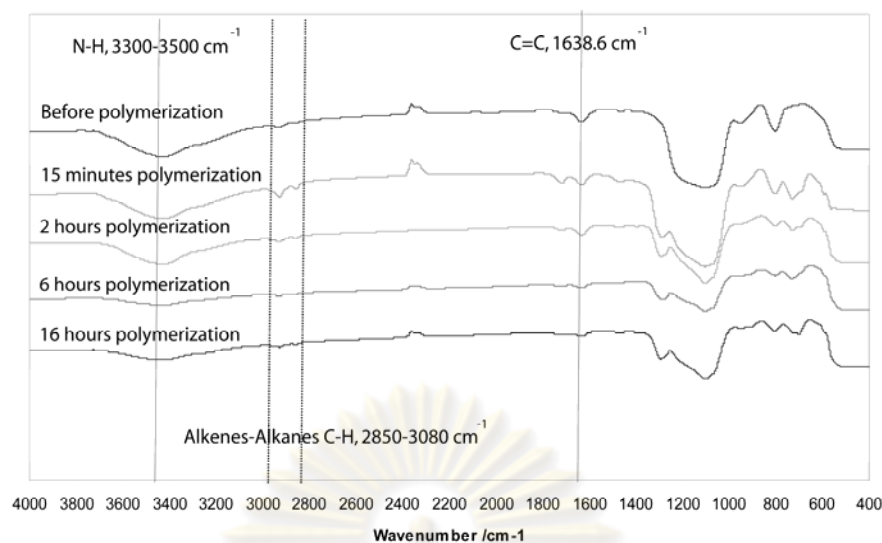


**Figure A-2** FTIR spectra of polymerizable gemini surfactant as a function of polymerization time

## 2. Atomic Force Microscopy

Atomic force microscopy (AFM) is the promising technique to use as surface characterization. To determination of AFM topography images in this study, section analysis and surface roughness were analyzed by the accompany software.

The example of section and surface roughness analysis shown as follows;

### a) Section Analysis

Ball part sizing of sample SE2 was determined by section analysis mode as shown in Figure A-3 and Table A-2.

ศูนย์วิจัยทรัพยากร  
จุฬาลงกรณ์มหาวิทยาลัย



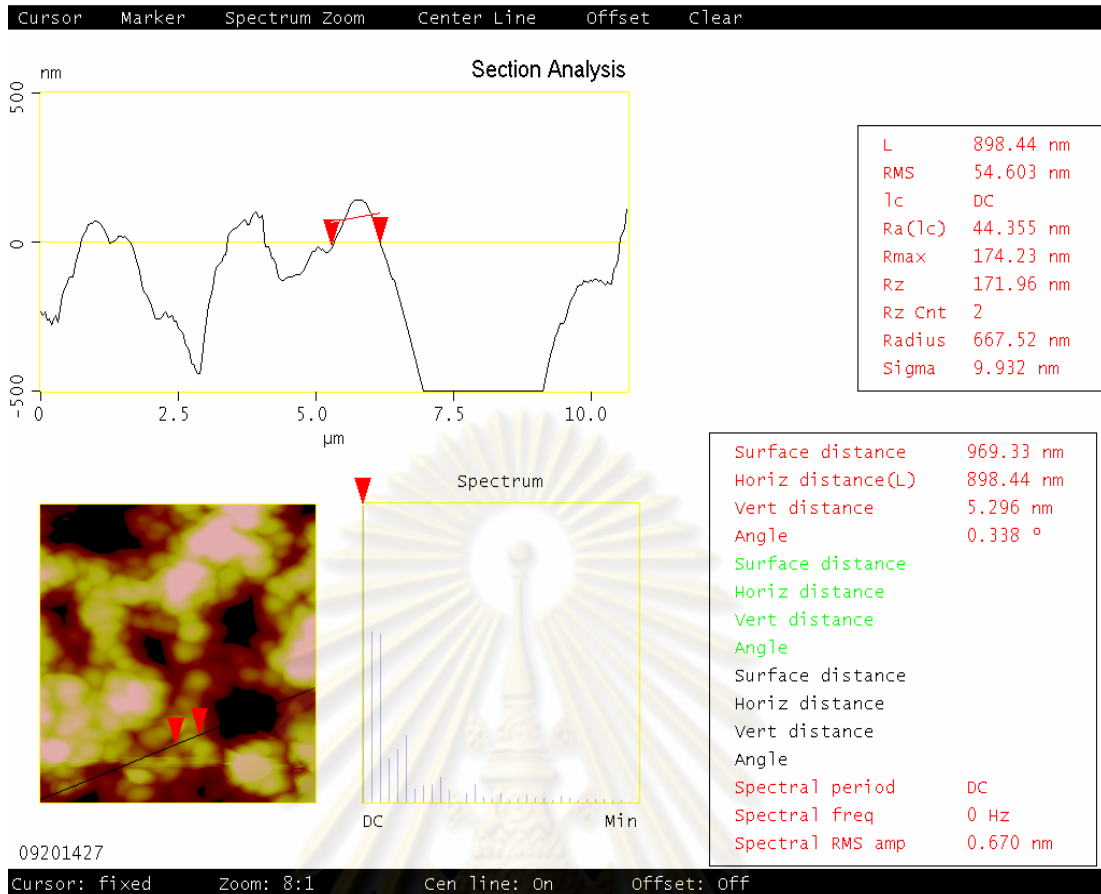


**Figure A-3** Example of section analysis

**Table A-2** Ball part sizing of sample SE2

No. of measurement	Radius (nm)	Ball part dia. (nm)
1	1037	2074
2	790.64	1581.28
3	653.95	1307.9
4	911.85	1823.7
5	783.95	1567.9
6	753.16	1506.32
7	672.14	1344.28
8	624.46	1248.92
9	660.09	1320.18
10	667.52	1335.04
<b>Average</b>	<b>724.195556</b>	<b>1510.952</b>
<b>SD</b>	<b>132.083133</b>	<b>264.1663</b>
<b>% error</b>	<b>5.48287687</b>	<b>5.719701</b>

## b) Roughness Analysis

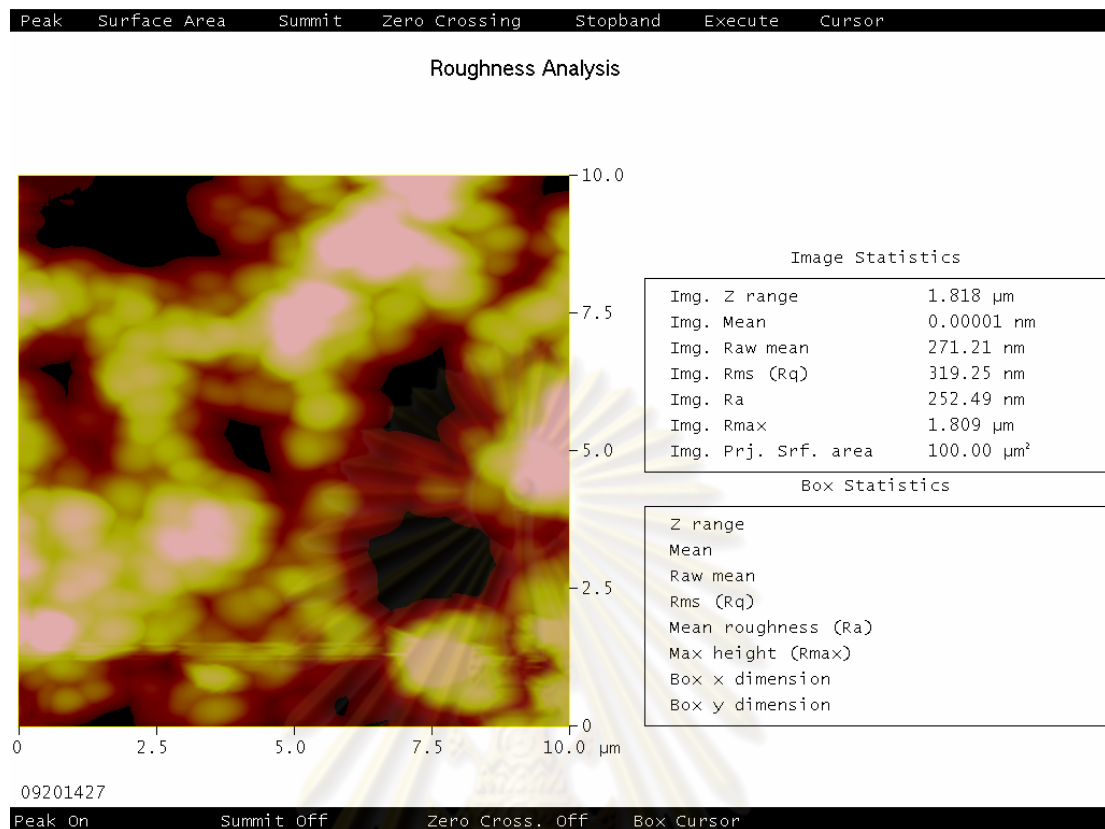


**Figure A-4** Example of roughness analysis

Where;

- Rq (RMS):** Root mean square average of height deviations taken from the mean image data plane.
- Ra:** Arithmetic average of the absolute values of the surface height deviations measured from the mean plane.
- Rmax:** Maximum vertical distance between the highest and lowest data points in the image following the planefit.
- Rz:** The avg. difference in height between the five highest peaks and five lowest valleys relative to the Mean Plane.
- Surface area:** The three-dimensional area of the entire image calculated from the sum of the area of all the triangles formed by three adjacent points.

## 2. Calculation: AFM Force Measurement (Senden, 2001)

Force  $F = kx$  where  $k =$  spring constant  
(in this work = 0.06780 N/m)

Deflection (V)  $X = \frac{(\text{deflection} - z)}{\Omega}$  where  $z =$  separation at zero force

Separation ( $\mu\text{m}$ )  $d = \frac{(Z - c)}{x}$  where  $c =$  constant position =  $X_0$

Compliance  $\Omega = \frac{dy}{dx}$   $dy =$  div deflection  
 $dx =$  div Z

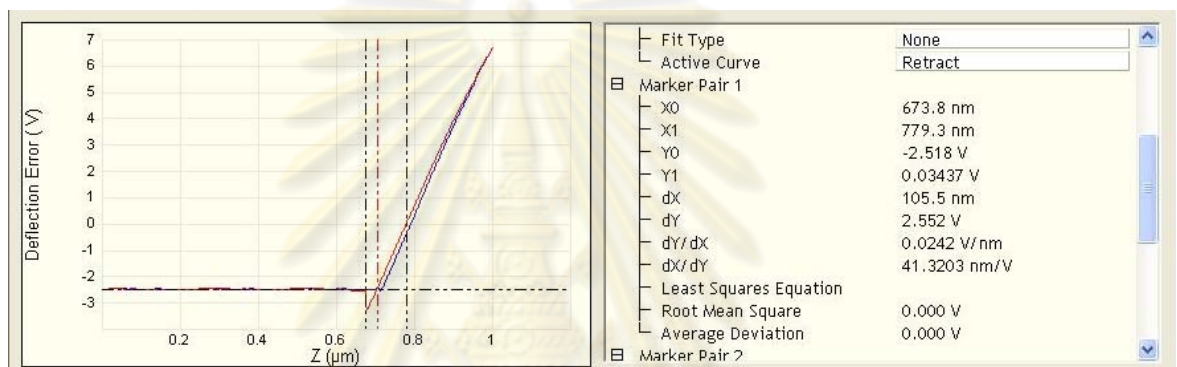
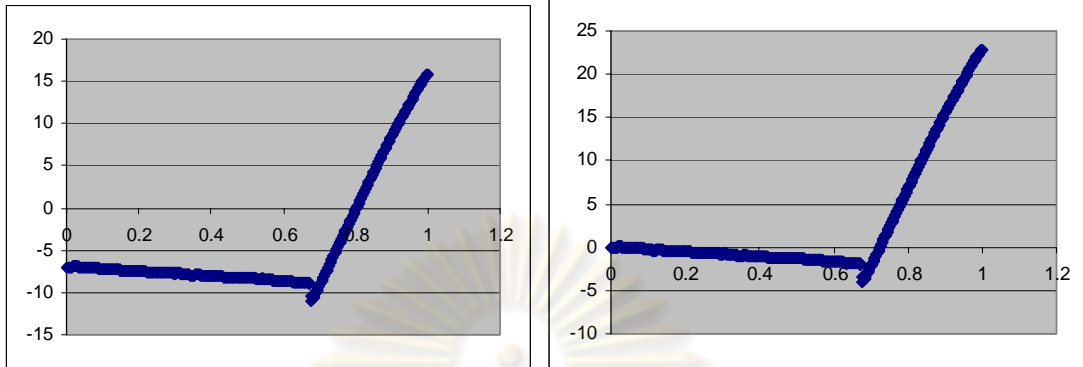


**Figure A-5** Given data from the Nanoscope V software determination of force curve using contact or tapping imaging mode

ศูนย์วิทยทรัพยากร  
จุฬาลงกรณ์มหาวิทยาลัย

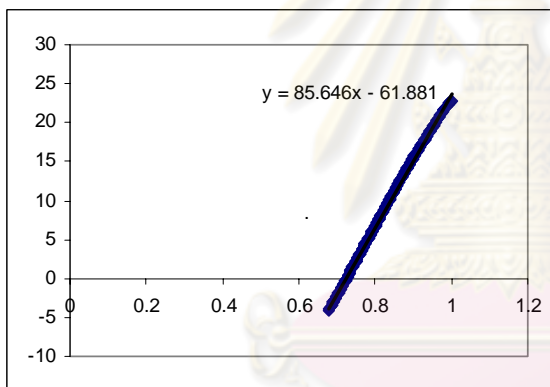
### 3. Force Curve Plotting

**STEP 1:** Offset the force. Take Force at infinity (distance = 0) and minus all the force value with Force at  $Z = 0 \mu\text{m}$

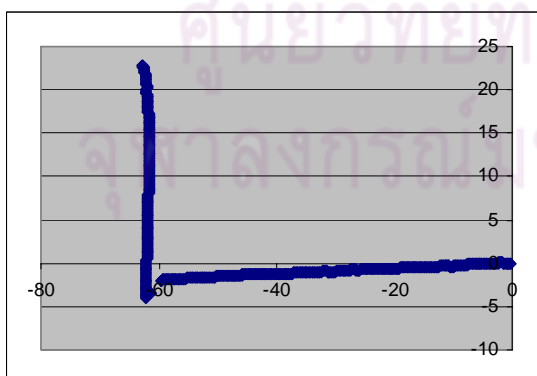


**STEP 2:** Find the minimum force value

**STEP 3:** Find the slope of the deflection region by the linear regression till  $z=0.678 \mu\text{m}$



**STEP 4:** plot  $Y = [\text{Force after offsetted}]$  vs  $X = [\text{Force after offsetted} - (\text{Slope} \times Z)]$



Note; All plots refer to Z (displacement in  $\mu\text{m}$ ) and deflection in Volt for x and y axis, respectively.

## APPENDIX C

### EXPERIMENTAL RAW DATA

**Table A - 3** Surface tension measurement for polymerizable gemini surfactant (PG)

<b>Tube PG</b>	<b>Conc. (M)</b>	<b>Surface Tension mN/m</b>
1	1.0E-5	68.8
2	3.0E-5	66.1
3	1.0E-4	51.0
4	3.0E-4	49.5
5	4.0E-4	46.7
6	5.0E-4	46.5
7	7.0E-4	43.2
8	9.0E-4	43.0
9	1.0E-3	42.7
10	2.0E-3	42.0
11	3.0E-3	39.1
12	5.0E-3	38.7

Note water surface tension = 71.4 mN/m

**Table A - 4** Surface tension measurement for polymerizable monomeric surfactant (PM)

<b>Tube PM</b>	<b>Conc. (M)</b>	<b>Surface Tension mN/m</b>
1	7.0E-6	64.0
2	3.0E-5	67.2
3	3.0E-4	64.8
4	1.0E-3	61.2
5	3.0E-3	47.8
6	7.0E-3	42.0
7	1.0E-2	38.6
8	1.5E-2	37.9
9	2.0E-2	38.6
10	3.0E-2	39.8
11	5.0E-2	40.8

Note water surface tension = 71.3 mN/m

**Table A – 5** Surface tension measurement for dodecyltrimethyl ammoniumbromide (DTAB)

<b>Tube DTAB</b>	<b>Conc. (M)</b>	<b>Surface Tension mN/m</b>
1	3.0E-6	68.4
2	7.0E-6	70.1
3	3.0E-5	70.7
4	6.0E-5	70.7
5	1.0E-4	69.9
6	3.0E-4	63.9
7	4.0E-4	58.0
8	7.0E-4	53.0
9	1.0E-3	51.7
10	7.0E-3	38.7
11	1.0E-2	37.5
12	1.5E-2	37.4
13	3.0E-2	37.1
14	7.0E-2	37.6
15	9.0E-2	37.7
16	1.0E-1	37.4

Note water surface tension = 71.3 mN/m

ศูนย์วิทยทรัพยากร  
จุฬาลงกรณ์มหาวิทยาลัย

**Table A – 6** Adsorption of PG at 0.001 M NaBr, pH 7.0 ± 0.5 and temperature 25±2 °C

Sample PG	PG (M)	Solution (ml)	PG_ini		PG_eq		Cs (M)	Silica (g)	q mole/g	pH final
			Absorbance (mAu)	(M)	Absorbance (mAu)	(M)				
1	3.00E-05	40	0.239	2.00E-05	0.237	9.74E-06	1.03E-05	0.0105	3.91E-05	6.78
1	3.00E-05	40	0.238	1.49E-05	0.236	4.61E-06	1.03E-05	0.0105	3.92E-05	6.78
1	3.00E-05	40	0.239	2.00E-05	0.236	4.61E-06	1.54E-05	0.0105	5.86E-05	6.78
2	1.00E-04	40	0.256	1.07E-04	0.240	2.51E-05	8.19E-05	0.0105	3.12E-04	6.60
2	1.00E-04	40	0.255	1.02E-04	0.236	4.62E-06	9.74E-05	0.0105	3.71E-04	6.60
2	1.00E-04	40	0.253	9.18E-05	0.236	4.62E-06	8.72E-05	0.0105	3.32E-04	6.60
3	4.00E-04	40	0.306	3.64E-04	0.282	2.41E-04	1.23E-05	0.0101	4.87E-04	6.81
3	4.00E-04	40	0.308	3.73E-04	0.283	2.46E-04	1.27E-04	0.0101	5.03E-04	6.81
3	4.00E-04	40	0.309	3.79E-04	0.284	2.51E-04	1.28E-04	0.0101	5.07E-04	6.81
4	5.00E-04	40	0.340	5.35E-04	0.294	3.02E-4	2.33E-04	0.0101	9.23E-04	6.59
4	5.00E-04	40	0.342	5.48E-04	0.295	3.07E-04	2.41E-04	0.0101	9.54E-04	6.59
4	5.00E-04	40	0.347	5.74E-04	0.296	3.12E-04	2.62E-04	0.0101	1.04E-03	6.59
5	7.00E-04	40	0.390	7.94E-04	0.351	5.94E-04	2.00E-04	0.0097	8.25E-04	6.94
5	7.00E-04	40	0.391	7.99E-04	0.352	6.00E-04	1.99E-04	0.0097	8.21E-04	6.94
5	7.00E-04	40	0.392	8.04E-04	0.353	6.05E-04	1.99E-04	0.0097	8.21E-04	6.94
6	3.00E-03	40	0.817	2.98E-03	0.691	2.34E-03	6.40E-04	0.0500	5.12E-04	6.77
6	3.00E-03	40	0.823	3.01E-03	0.694	2.35E-03	6.60E-04	0.0500	5.28E-04	6.77
6	3.00E-03	40	0.824	3.02E-03	0.696	2.36E-03	6.60E-04	0.0500	5.28E-04	6.77
7	5.00E-03	40	1.203	4.96E-03	1.050	4.18E-03	7.80E-04	0.0503	6.20E-04	6.65
7	5.00E-03	40	1.209	4.99E-03	1.053	4.19E-03	8.00E-04	0.0503	6.36E-04	6.65
7	5.00E-03	40	1.212	5.01E-03	1.055	4.20E-03	8.10E-04	0.0503	6.44E-04	6.65

**Table A – 7** Summarizes: adsorption of PG with standard deviation

Sample PG	Cini (M)	Ceq	q mole/g	q stDEV	molecule	[q] molecule/nm <sup>2</sup>	[q] stDEV
1	1.49E-05	4.61E-06	3.92E-05	1.372E-05	2.36E+19	0.147187	1.59E+00
1	2.00E-05	4.61E-06	5.86E-05	1.372E-05	3.53E+19	0.147564	2.60E+00
2	1.07E-04	2.51E-05	3.12E-04	3.001E-05	1.88E+20	0.220592	9.58E-02
2	1.02E-04	4.62E-06	3.71E-04	3.001E-05	2.23E+20	1.174485	5.95E-02
2	9.18E-05	4.62E-06	3.32E-04	3.001E-05	2.00E+20	1.396583	1.80E-01
3	3.64E-04	2.41E-04	4.87E-04	1.058E-05	2.93E+20	1.249773	1.23E-02
3	3.73E-04	2.46E-04	5.03E-04	1.058E-05	3.03E+20	1.833251	2.95E-03
3	3.79E-04	2.51E-04	5.07E-04	1.058E-05	3.05E+20	1.893481	1.67E-01
4	5.35E-04	3.02E-04	9.23E-04	6.062E-05	5.56E+20	1.908538	6.62E-03
4	5.48E-04	3.07E-04	9.54E-04	6.062E-05	5.74E+20	3.474518	1.63E-02
4	5.74E-04	3.12E-04	1.04E-03	6.062E-05	6.26E+20	3.591214	4.71E-02
5	7.94E-04	5.94E-04	8.25E-04	2.309E-06	4.97E+20	3.91495	1.11E-03
5	7.99E-04	6.00E-04	8.21E-04	2.309E-06	4.94E+20	3.105609	0.00E+00
5	8.04E-04	6.05E-04	8.21E-04	2.309E-06	4.94E+20	3.090552	1.38E-01
6	2.98E-03	2.34E-03	5.12E-04	9.238E-06	3.08E+20	3.090552	1.11E-02
6	3.01E-03	2.35E-03	5.28E-04	9.238E-06	3.18E+20	1.92736	0.00E+00
6	3.02E-03	2.36E-03	5.28E-04	9.238E-06	3.18E+20	1.98759	5.28E-02
7	4.96E-03	4.18E-03	6.20E-04	1.222E-05	3.73E+20	1.98759	7.63E-03
7	4.99E-03	4.19E-03	6.36E-04	1.222E-05	3.83E+20	2.333913	3.67E-03
7	5.01E-03	4.20E-03	6.44E-04	1.222E-05	3.88E+20	2.394143	3.67E-03



**Table A – 8** Adsorption of PM at 0.001 M NaBrI, pH 7.0 ± 0.5 and temperature 25±2 °C

Sample PM	PM (M)	Soluti on (ml)	PM_ini		PM eq		Cs (M)	Silica (g)	q mole/g	pH final
			Area (us*min)	(M)	Area (us*min)	(M)				
1	3.0E-06	40	0.0388	N.A.	0.0090	1.0E-06		0.0107		6.58
2	1.0E-05	40	0.1523	6.54E-06	0.0247	6.0E-06	9.15E-07	0.0100	3.66E-06	6.56
3	3.0E-05	40	0.5639	2.42E-05	0.1310	2.0E-05	4.58E-06	0.0103	1.78E-05	6.77
4	1.0E-04	40	2.0837	8.95E-05	0.4574	7.4E-05	1.53E-05	0.0102	6.00E-05	6.89
5	3.0E-04	40	6.9933	3.00E-04	1.7277	2.48E-04	5.20E-05	0.0103	2.02E-04	6.85
6	1.0E-03	40	23.3066	9.35E-04	5.7823	9.17E-04	6.87E-05	0.0106	2.59E-04	6.64
7	2.0E-03	40	18.5485	1.94E-03	17.5669	1.84E-03	1.03E-04	0.0102	4.02E-04	6.94
8	3.0E-03	40	28.0750	3.18E-03	27.2452	2.85E-03	9.67E-05	0.0106	3.65E-04	7.05
9	4.0E-03	40	37.3286	4.75E-03	36.7098	3.88E-03	1.44E-04	0.0101	5.68E-04	6.51
10	5.0E-03	40	48.2513	9.46E-03	43.7509	4.57E-03	1.23E-04	0.0105	4.69E-04	6.76
11	8.0E-03	40	76.7519	3.03E-02	71.9024	7.51E-03	1.45E-04	0.0098	5.93E-04	6.65

ศูนย์วิทยทรัพยากร  
จุฬาลงกรณ์มหาวิทยาลัย

**Table A – 9** Summarizes: adsorption of PM

Sample	Cini	Ceq	q		[q]
PM	(M)	(M)	mole/g	molecule	molecule/nm <sup>2</sup>
1	N.A.	1.00E-06			
2	7.00E-06	6.00E-06	3.66E-06	2.20E+18	0.01
3	2.40E-05	2.00E-05	1.78E-05	1.07E+19	0.07
4	9.00E-05	7.40E-05	6.00E-05	3.61E+19	0.23
5	3.00E-04	2.48E-04	2.02E-04	1.22E+20	0.76
7	1.00E-03	9.17E-04	2.59E-04	1.91E+20	0.98
8	1.94E-03	1.84E-03	4.02E-04	2.42E+20	1.51
8	2.93E-03	2.85E-03	3.65E-04	1.97E+20	1.37
9	3.95E-03	3.88E-03	5.68E-04	1.57E+20	2.14
10	5.04E-03	4.57E-03	4.69E-04	1.08E+21	1.77
11	8.02E-03	7.51E-03	5.93E-04	1.25E+21	2.23

**Table A – 10** Adsorption of DTAB at 0.001 M NaBr, pH 7.0 ± 0.5 and temperature 25±2 °C

Sample DTAB	DTAB (M)	Solution (ml)	DTAB_ini		DTAB_eq	Cs	Silica (g)	q mole/g	pH final
			Area (us*min)	(M)	(M)	(M)			
1	1.00E-05	40	0.1611	6.00E-06	5.00E-06	1.00E-06	0.0105	3.81E-06	6.61
2	2.00E-05	40	0.4116	1.60E-05	1.40E-05	2.00E-06	0.0100	8.00E-06	6.52
3	6.00E-05	40	1.2812	5.10E-05	4.50E-05	6.00E-06	0.0100	2.40E-05	6.45
4	1.00E-04	40	2.1829	8.70E-05	7.60E-05	1.10E-05	0.0100	4.40E-05	6.77
5	3.00E-04	40	6.8879	2.75E-04	2.64E-04	1.10E-05	0.0102	4.31E-05	6.62
6	1.00E-03	40	23.5461	9.72E-04	9.45E-04	2.70E-05	0.0100	1.08E-04	6.63
7	3.00E-03	40	49.2763	2.76E-03	2.74E-03	1.74E-05	0.0106	6.57E-05	6.64
8	4.00E-03	40	75.1217	4.07E-03	4.03E-03	4.00E-05	0.0101	1.58E-04	7.01
9	7.00E-03	40	78.0113	6.56E-03	6.54E-03	2.35E-05	0.0100	9.38E-05	7.20
10	1.00E-02	40	102.0883	9.18E-03	9.16E-03	2.69E-05	0.0104	1.03E-04	6.61
11	3.00E-02	40	205.8721	2.80E-02	2.80E-02	3.17E-05	0.0101	1.26E-04	6.64
12	5.00E-02	40	269.6940	4.43E-02	4.42E-02	1.23E-04	0.0500	9.82E-05	6.53

จุฬาลงกรณ์มหาวิทยาลัย

**Table A – 11** Summarizes: adsorption of DTAB

<b>Sample</b>	<b>Cini</b>	<b>Ceq</b>	<b>q</b>		<b>[q]</b>
<b>DTAB</b>	(M)	(M)	mole/g	molecule	molecule/nm <sup>2</sup>
1	6.00E-06	5.00E-06	3.81E-06	2.29E+18	0.01
2	1.60E-05	1.40E-05	8.00E-06	4.82E+18	0.03
3	5.10E-05	4.50E-05	2.40E-05	1.44E+19	0.09
4	8.70E-05	7.60E-05	4.40E-05	2.65E+19	0.16
5	2.75E-04	2.64E-04	4.31E-05	2.60E+19	0.25
6	9.72E-04	9.45E-04	1.08E-04	6.50E+19	0.27
7	2.76E-03	2.74E-03	6.57E-05	3.95E+19	0.29
8	4.07E-03	4.03E-03	1.58E-04	9.54E+19	0.35
9	6.56E-03	6.54E-03	9.38E-05	5.65E+19	0.39
10	9.18E-03	9.16E-03	1.03E-04	6.22E+19	0.47
11	2.80E-02	2.80E-02	1.26E-04	7.57E+19	0.37
12	4.43E-02	4.42E-02	9.82E-05	5.91E+19	0.01

**Table A-12** Styrene adsolubilization of DTAB at 0.001 M NaBr, pH 7.0±0.5 and temperature 25±2 °C

Sample	Cs	Silica	q	[q]	Sty(in-f)	Sty(in-f)	Adsolubilized	Degree of adsl	X <sub>adm</sub>	X <sub>aq</sub>	X <sub>aq</sub> × 10 <sup>6</sup>	K <sub>adm</sub>
DTAB	(M)	(g)	mole/g	molecule/nm <sup>2</sup>	(mg/l)	Molar	μmole/g(silica)					
1	3.32E-04	0.0100	1.33E-03	5.72	18.79	1.80E-04	719.30	0.84	0.35	6.26E-07	0.63	5.61E+06
2	4.98E-04	0.0100	1.99E-03	8.57	39.32	3.76E-04	1504.96	0.88	0.43	9.53E-07	0.95	4.52E+06
3	4.98E-04	0.0100	1.99E-03	8.57	59.84	5.73E-04	2290.62	0.89	0.53	1.28E-07	1.28	4.18E+06
4	6.64E-04	0.0100	2.66E-03	11.43	103.63	9.92E-04	3966.56	0.92	0.60	1.46E-07	1.46	4.09E+06
5	1.24E-03	0.0101	4.94E-03	11.43	233.62	2.24E-03	8942.57	0.95	0.64	2.25E-07	2.25	2.87E+06
6	1.11E-03	0.0102	4.44E-03	21.27	263.69	2.52E-03	10093.44	0.90	0.69	4.79E-07	4.79	1.45E+06
7	1.11E-03	0.0100	4.44E-03	23.52	294.59	2.82E-03	11276.29	0.94	0.72	3.33E-07	3.33	2.15E+06
8	1.11E-03	0.0100	4.43E-03	19.08	314.84	3.01E-03	12051.30	0.94	0.73	3.71E-07	3.71	1.97E+06

**Table A-13** Styrene adsolubilization of PG at 0.001 M NaBr, pH 7.0±0.5 and temperature 25±2 °C

Sample	Cs	Silica	q	[q]	Sty(in-f)	Sty(in-f)	Adsolubilized	Degree of adsl	X <sub>adm</sub>	X <sub>aq</sub>	X <sub>aq</sub> × 10 <sup>6</sup>	K <sub>adm</sub>
PG	(M)	(g)	mole/g	molecule/nm <sup>2</sup>	(mg/l)	Molar	μmole/g(silica)					
1	7.46E-05	0.0100	2.99E-04	1.12	61.65	5.90E-04	2359.88	0.92	0.89	9.68E-07	0.97	9.17E+04
2	2.32E-05	0.0100	9.29E-04	0.35	80.67	7.72E-04	3087.90	0.90	0.97	1.55E-06	1.55	6.25E+04
3	5.01E-05	0.0100	2.00E-04	0.75	104.45	1.00E-03	3998.05	0.93	0.95	1.32E-06	1.32	7.21E+04
4	5.80E-05	0.0100	2.32E-04	0.87	126.16	1.21E-03	4829.24	0.94	0.95	1.44E-06	1.44	6.61E+04
5	6.28E-05	0.0101	2.51E-04	0.95	171.04	1.64E-03	6546.84	0.95	0.96	1.44E-06	1.44	6.69E+04
6	7.23E-05	0.0100	2.89E-04	1.09	212.09	2.03E-03	8118.60	0.95	0.97	2.09E-06	2.09	4.61E+04
7	7.23E-05	0.0100	2.89E-04	1.09	258.12	2.47E-03	9880.32	0.96	0.97	1.89E-06	1.89	5.15E+04
8	7.23E-05	0.0100	2.89E-04	1.09	304.93	2.92E-03	11672.03	0.97	0.98	1.55E-06	1.55	6.30E+04
9	4.82E-05	0.0100	1.93E-04	0.73	328.15	3.14E-03	12560.86	0.98	0.98	1.41E-06	1.41	6.97E+04

**Table A-14** Styrene adsolubilization of PM at 0.001 M NaBr, pH 7.0±0.5 and temperature 25±2 °C

Sample PG	Cs (M)	Silica (g)	q mole/g	[q] molecule/nm <sup>2</sup>	Sty(in-f) (mg/l)	Sty(in-f) Molar	Adsolubilized μmole/g(silica)	Degree of adsl	X <sub>adm</sub>	X <sub>aq</sub>	X <sub>aq</sub> x 10 <sup>6</sup>	K <sub>adm</sub>
1	4.78E-04	0.0100	1.91E-03	7.20	38.01	3.64E-04	1455.07	0.85	0.43	1.18E-06	1.18	3.67E+04
2	2.31E-04	0.0100	9.23E-04	3.47	59.78	5.72E-04	2288.20	0.89	0.71	1.29E-06	1.29	5.52E+04
3	7.88E-04	0.0100	3.15E-03	11.86	82.56	7.90E-04	3160.07	0.92	0.50	1.23E-06	1.23	4.07E+04
4	5.75E-04	0.0100	2.30E-03	8.67	88.33	8.45E-04	3380.95	0.79	0.59	4.10E-06	4.10	1.45E+04
5	5.93E-04	0.0101	2.37E-03	8.93	116.5	1.12E-03	4460.14	0.87	0.65	3.10E-06	3.10	2.10E+04
6	8.14E-04	0.0100	3.26E-03	12.26	124.7	1.19E-03	4774.2	0.79	0.59	5.55E-06	5.55	1.07E+04
7	1.39E-03	0.0100	5.55E-03	20.91	192.4	1.84E-03	7364.47	0.86	0.57	5.48E-06	5.48	1.04E+04
8	1.44E-03	0.0100	5.77E-03	21.71	234.4	2.24E-03	8972.60	0.87	0.61	5.97E-06	5.97	1.02E+04
9	1.44E-03	0.0100	5.77E-03	21.71	297.4	2.85E-03	11384.79	0.88	0.66	6.71E-06	6.71	9.89E+03

**Table A-15** Styrene adsolubilization of PG after polymerization at 0.001 M NaBr, pH 7.0±0.5 and temperature 25±2 °C

Sample PG	Cs (M)	Silica (g)	q mole/g	[q] molecule/nm <sup>2</sup>	Sty(in-f) (mg/l)	Sty(in-f) Molar	Adsolubilized μmole/g(silica)	Degree of adsl	X <sub>adm</sub>	X <sub>aq</sub>	X <sub>aq</sub> x 10 <sup>6</sup>	K <sub>adm</sub>
1	4.85E-05	0.0100	4.85E-05	0.73	22.42	2.04E-04	817.63	0.95	0.81	1.83E-07	0.18	4.41E+06
2	1.24E-04	0.0100	1.24E-04	1.86	67.27	6.28E-04	2511.49	0.98	0.84	2.86E-07	0.29	2.93E+06
3	1.13E-04	0.0100	1.13E-04	1.71	112.12	1.05E-04	4219.89	0.98	0.90	3.23E-07	0.32	2.80E+06
4	1.24E-04	0.0100	1.24E-04	1.86	156.96	1.40E-03	5582.44	0.93	0.92	1.92E-06	1.92	4.79E+05
5	6.28E-05	0.0101	6.28E-05	0.95	179.39	1.68E-03	6708.44	0.98	0.96	7.13E-07	0.71	1.35E+06
6	6.99E-05	0.0100	6.99E-05	1.05	224.24	2.10E-03	8411.69	0.98	0.97	7.72E-07	0.77	1.25E+06
7	4.69E-05	0.0100	4.69E-05	0.71	269.08	2.49E-03	9946.19	0.97	0.98	1.59E-06	1.59	6.17E+05
8	9.12E-05	0.0100	9.12E-05	1.37	336.35	3.17E-03	12686.31	0.99	0.97	8.48E-07	0.85	1.15E+06

**Table A-16** Phenyl ethanol adsolubilization of DTAB at 0.001 M NaBr, pH 7.0±0.5 and temperature 25±2 °C

Sample	Cs	Silica	q	[q]	Phy(in-f)	Phy(in-f)	Adsolubilized	Degree of adsl	X <sub>adm</sub>	X <sub>aq</sub>	X <sub>aq</sub> (x 10 <sup>-6</sup> )	K <sub>adm</sub>
PG	(M)	(g)	mole/g	molecul e/nm <sup>2</sup>	(mg/l)	Molar	µmole/g (silica)					
1	5.64E-04	0.01	2.25E-03	9.70	124.4	1.02E-03	4071.64	0.25	0.6437	5.46E-05	54.60	11,789.45
2	8.95E-04	0.01	3.58E-03	15.40	156.6	1.28E-03	5126.67	0.16	0.5888	1.23E-04	122.76	4,796.51
3	7.56E-04	0.01	3.02E-03	13.01	172.9	1.42E-03	5661.79	0.09	0.6519	2.66E-04	266.14	2,449.47
4	1.00E-03	0.01	4.00E-03	17.23	390.8	3.19E-03	12795.62	0.11	0.7616	4.89E-04	489.10	1,557.23
5	9.75E-04	0.01	3.90E-03	16.77	312.3	2.56E-03	10225.95	0.05	0.7240	8.65E-04	864.78	837.21
6	1.03E-03	0.01	4.11E-03	17.68	489.1	4.03E-03	16014.61	0.07	0.7958	1.02E-03	1020.74	779.59
7	1.21E-03	0.01	4.83E-03	20.76	372.2	3.05E-03	12187.74	0.04	0.7163	1.40E-03	1401.66	511.06
8	1.32E-03	0.01	5.28E-03	22.70	561.9	4.60E-03	18400.07	0.05	0.7771	1.74E-03	1737.26	447.32
9	9.15E-04	0.01	3.66E-03	15.74	1402	1.15E-03	45908.12	0.09	0.9262	1.98E-03	1977.19	468.43
10	9.55E-04	0.01	3.82E-03	16.43	861.6	7.05E-03	28209.79	0.05	0.8808	2.42E-03	2419.51	364.03
11	7.36E-04	0.01	2.94E-03	12.66	964.3	7.89E-03	31573.08	0.05	0.9147	2.77 E-03	2767.18	330.56

**Table A-17** Phenyl ethanol adsolubilization of PG before polymerization at 0.001 M NaBr, pH 7.0±0.5 and temperature 25±2 °C

Sample	Cs	Silica	q	[q]	Phy(in-f)	Phy(in-f)	Adsolubilized	Degree of adsl	X <sub>adm</sub>	X <sub>aq</sub>	X <sub>aq</sub> (x 10 <sup>-6</sup> )	K <sub>adm</sub>
PG	(M)	(g)	mole/g	Molecule /nm <sup>2</sup>	(mg/l)	Molar	μmole/g (silica)					
1	1.90E-05	0.01	7.60E-05	0.33	41.61	3.41E-04	1362.43	0.17	0.9472	3.03E-05	30.33	31,229.27
2	1.80E-05	0.01	7.20E-05	0.31	84.88	6.95E-04	2778.97	0.10	0.9747	9.69E-05	96.87	10,062.45
3	2.00E-05	0.01	8.00E-05	0.34	100.6	8.24E-04	3294.29	0.07	0.9763	2.04E-04	203.9	4,787.99
4	1.90E-05	0.01	7.60E-05	0.33	141.2	1.16E-03	4624.25	0.05	0.9838	4.17E-04	416.6	2,361.81
5	1.70E-05	0.01	6.80E-05	0.29	133.1	1.09E-03	4356.23	0.03	0.9846	6.36E-04	636.3	1,547.43
6	1.70E-05	0.01	6.80E-05	0.29	187.5	1.53E-03	6139.65	0.03	0.9890	8.83E-04	883.1	1,119.93
7	1.80E-05	0.01	7.20E-05	0.31	864.74	7.08E-03	28312.64	0.10	0.9975	1.15E-03	1147.4	869.30
8	1.90E-05	0.01	7.60E-05	0.33	160.28	1.31E-03	5247.79	0.02	0.9857	1.43E-03	1432.8	687.97
9	1.70E-05	0.01	6.80E-05	0.29	954.22	7.81E-03	31242.28	0.08	0.9978	1.68E-03	1679.7	594.06
10	1.90E-05	0.01	7.60E-05	0.33	1570.44	1.29E-02	51418.17	0.11	0.9985	1.95E-03	1952.5	511.41
11	2.10E-05	0.01	8.40E-05	0.36	283.19	2.32E-03	9271.92	0.02	0.9910	2.50E-03	2504.3	395.73
12	1.93E-05	0.01	7.74E-05	0.33	2257.64	1.84E-02	73918.12	0.11	0.9990	2.58E-03	2577.6	387.55



**Table A-18** Phenyl ethanol adsolubilization of PG after polymerization at 0.001 M NaBr, pH 7.0±0.5 and temperature 25±2 °C

Sample	Cs	Silica	q	[q]	Phy(in-f)	Phy(in-f)	Adsolubilized	Degree of adsl	X <sub>adm</sub>	X <sub>aq</sub>	X <sub>aq</sub> (x 10 <sup>-6</sup> )	K <sub>adm</sub>
PG	(M)	(g)	mole/g	Molecule /nm <sup>2</sup>	(mg/l)	Molar	μmole/g (silica)					
1	1.90E-05	0.01	7.60E-05	0.33	367.83	3.01E-03	12043.14	0.74	0.9937	1.88E-05	18.72	53,072.92
2	1.90E-05	0.01	7.60E-05	0.33	724.96	5.93E-03	23736.05	0.73	0.9968	3.90E-05	39.02	25,544.12
3	1.90E-05	0.01	7.60E-05	0.33	1009.16	8.26E-03	33041.20	0.68	0.9977	7.01E-05	70.07	14,239.51
4	1.80E-05	0.01	7.20E-05	0.31	1328.98	1.09E-02	43512.60	0.67	0.9983	9.59E-05	95.86	10,414.71
5	1.80E-05	0.01	7.20E-05	0.31	2040.89	1.67E-02	66821.29	0.69	0.9989	1.37E-04	136.80	7,302.20
6	2.00E-05	0.01	8.00E-05	0.34	2453.67	2.01E-02	80336.16	0.66	0.9990	1.85E-04	185.34	5,389.99
7	2.00E-05	0.01	8.00E-05	0.34	3766.21	3.08E-02	123310.57	0.61	0.9994	3.56E-04	356.47	2,803.50
8	1.70E-05	0.01	6.80E-05	0.29	6451.36	5.28E-02	211225.79	0.65	0.9997	5.08E-04	507.61	1,969.4
9	1.70E-05	0.01	6.80E-05	0.29	8130.17	6.65E-02	266191.99	0.66	0.9997	6.25E-04	624.72	1,600.31
10	1.80E-05	0.01	7.20E-05	0.31	9909.42	8.11E-02	324447.03	0.67	0.9998	7.27E-04	727.03	1,375.16
11	1.90E-05	0.01	7.60E-05	0.33	11157.06	9.13E-02	365296.17	0.64	0.9998	9.08E-04	907.51	1,101.69

จุฬาลงกรณ์มหาวิทยาลัย

**Table A – 19** Zeta potential measurement for PG before polymerization

No. of measurement	Surfactant Concentration (M)					
	6.0E-06	1.0E-05	3.0E-05	1.0E-04	3.0E-04	7.0E-03
1	-30.84	-23.23	9.609	30.42	35.09	37.85
2	-37.43	-23.11	12.27	31.53	30.24	31.92
3	-32.77	-23.33	10.17	30.71	39.07	35.14
4	-34.42	-25.46	11.03	33.42	34.03	30.79
5	-36.32	-25.17	8.937	31.74	31.85	38.28
6	-36.03	-22.14	11.36	29.44	39.44	41.58
7	-35.80	-27.66	12.74	28.55	35.56	37.17
8	-31.60	-20.92	12.85	32.21	40.10	34.11
9	-35.27	-28.63	10.25	29.21	39.75	30.32
10	-34.08	-23.69	10.95	27.33	41.66	38.62
Average value	-34.55	-23.74	11.02	30.34	36.68	35.58
Standard deviation	1.84	2.42	1.32	1.80	3.87	3.75

**Table A – 20** Zeta potential measurement for PM before polymerization

No. of measurement	Surfactant Concentration (M)				
	1.0E-05	1.0E-04	3.0E-04	1.0E-02	3.0E-02
1	-37.06	-32.85	-29.98	32.6	39.08
2	-38.13	-36.85	-28.99	30.16	42.43
3	-36.37	-37.67	-30.98	32.85	38.83
4	-35.46	-33.42	-26.36	30.21	36.32
5	-33.78	-33.28	-29.00	29.60	36.53
6	-30.82	-33.65	-29.43	29.86	43.82
7	-34.17	-31.43	-28.94	30.45	38.67
8	-32.81	-34.75	-25.69	31	39.44
9	-31.92	-34.64	-29.38	33.03	38.22
10	-38.00	-34.96	-29.71	32.58	35.88
Average value	-35.52	-33.97	-28.85	31.23	38.92
Standard deviation	2.63	2.01	1.61	1.37	2.56

**Table A – 21** Zeta potential measurement for DTAB before polymerization

No. of measurement	Surfactant Concentration (M)					
	1.0E-05	1.0E-04	1.0E-03	3.0E-03	1.0E-02	3.0E-02
1	-35.53	-40.12	-21.89	-10.88	51.42	54.58
2	-33.28	-47.19	-20.00	-11.70	49.60	56.27
3	-34.75	-34.35	-22.67	-10.68	51.72	52.28
4	-35.89	-42.12	-21.67	-13.14	46.74	56.22
5	-38.42	-34.77	-22.10	-12.33	44.74	50.15
6	-36.16	-34.90	-23.00	-12.56	43.32	53.13
7	-40.42	-33.45	-24.46	-11.95	47.35	52.00
8	-42.00	-39.07	-20.00	-12.00	45.18	55.98
9	-39.00	-36.07	-22.67	-11.40	45.90	50.35
10	-33.11	-35.98	-21.61	-12.33	47.82	54.29
Average value	-36.86	-37.80	-22.01	-11.90	47.38	53.53
Standard deviation	2.99	4.33	1.34	0.76	2.81	2.31

**Table A – 22** Zeta potential measurement for PG after polymerization

No. of measurement	Surfactant Concentration (M)					
	1.00E-06	1.00E-05	3.00E-05	1.00E-04	3.00E-04	7.00E-03
1	-36.35	-30.10	-29.03	-13.13	15.48	15.63
2	-36.44	-29.15	-24.59	-16.64	8.921	12.29
3	-35.81	-28.68	-23.09	-15.17	12.23	13.94
4	-35.89	-28.00	-21.82	-15.17	9.213	13.28
5	-32.21	-30.28	-23.32	-13.82	6.562	13.45
6	-34.25	-28.68	-21.85	-12.83		14.11
7	-33.70	-31.59	-22.82	-17.04		12.31
8	-32.98	-29.71	-23.65	-11.30		
9	-33.23	-28.57		-15.00		
10	-31.19	-27.63		-12.52		
Average value	-34.21	-29.24	-23.77	-14.29	10.48	13.57
Standard deviation	1.85	1.19	2.31	1.80	3.44	1.15

**Table A – 23** Zeta potential measurement for PM after polymerization

No. of measurement	Surfactant Concentration (M)				
	1.00E-05	1.00E-04	3.00E-04	1.00E-02	3.00E-02
1	-37.21	-28.34	-20.63	12.46	19.19
2	-37.83	-24.67	-21.25	12.51	17.17
3	-32.69	-28.47	-18.87	11.55	17.95
4	-34.30	-28.60	-18.88	10.33	18.29
5	-36.85	-31.85	-19.68	10.64	21.31
6	-34.64	-32.29	-19.50	12.44	15.53
7	-31.75	-28.13	-16.76	11.32	16.65
8	-36.25	-29.44	-16.45		
9	-37.28	-28.31	-15.73		
10	-36.31	-29.71	-17.85		
Average value	-35.51	-28.98	-18.56	11.66	18.18
Standard deviation	2.07	2.12	1.83	0.98	1.79

**Table A – 24** Zeta potential measurement for DTAB after polymerization

No. of measurement	Surfactant Concentration (M)					
	1.00E-05	1.00E-04	1.00E-03	3.00E-03	1.00E-02	3.00E-02
1	-35.53	-40.12	-21.89	-10.88	51.42	54.58
2	-33.28	-47.19	-20.00	-11.70	49.60	56.27
3	-34.75	-34.35	-22.67	-10.68	51.72	52.28
4	-35.89	-42.12	-21.67	-13.14	46.74	56.22
5	-38.42	-34.77	-22.10	-12.33	44.74	50.15
6	-36.16	-34.90	-23.00	-12.56	43.32	53.13
7	-40.42	-33.45	-24.46	-11.95	47.35	52.00
8	-42.00	-39.07	-20.00	-12.00	45.18	55.98
9	-39.00	-36.07	-22.67	-11.40	45.90	50.35
10	-33.11	-35.98	-21.61	-12.33	47.82	54.29
Average value	-36.86	-37.80	-22.01	-11.90	47.38	53.53
Standard deviation	2.99	4.33	1.34	0.76	2.81	2.31

**Table A – 25** Zeta potential measurement for PG before polymerization and after washing

No. of measurement	Surfactant Concentration (M)				
	6.00E-06	1.00E-05	3.00E-05	1.00E-04	7.00E-04
1	-30.77	-27.53	-39.75	25.17	15.22
2	-36.25	-25.75	-48.59	29.57	15.14
3	-35.51	-29.09	-49.17	29.90	18.65
4	-41.09	-28.42	-46.51	29.43	14.24
5	-33.53	-25.89	-47.03	27.81	19.39
6	-40.14	-23.11	-44.19	23.91	18.96
7	-31.32	-29.71	-40.27	25.28	18.44
8	-40.27	-24.46	-44.40	25.01	13.29
9	-39.75	-24.99	-41.53	26.41	20.50
10	-41.71	-23.91	-41.71	26.80	19.37
Average value	-37.03	-26.29	-44.32	26.93	17.32
Standard deviation	4.12	2.28	3.43	2.15	2.56

**Table A – 26** Zeta potential measurement for PM before polymerization and after washing

No. of measurement	Surfactant Concentration (M)					
	3.00E-05	1.00E-04	2.00E-04	1.00E-03	1.00E-02	3.00E-02
1	-32.21	-36.96	-25.56	-22.22	-13.48	5.72
2	-41.09	-35.80	-30.53	-22.61	-9.187	4.10
3	-40.14	-46.14	-29.46	-23.48	-23.24	4.09
4	-45.57	-38.67	-27.53	-24.85	-21.37	10.98
5	-35.51	-41.10	-29.46	-25.90	-12.79	6.945
6	-41.10	-34.35	-25.26	-23.11	-20.239	8.92
7	-33.53	-39.33	-30.10	-21.21	-21.71	10.95
8	-39.33	-42.58	-33.36	-20.48	-22.18	8.296
9	-42.58	-43.77	-29.46	-19.87	-18.63	7.414
10	-41.09	-45.74	-24.25	-20.48	-19.20	6.71
Average value	-39.22	-40.44	-28.50	-22.42	-18.22	7.412
Standard deviation	4.19	4.11	2.81	1.98	4.74	2.45

**Table A – 27** Zeta potential measurement for DTAB before polymerization and after washing

No. of measurement	Surfactant Concentration (M)				
	1.00E-05	1.00E-04	1.00E-03	1.00E-02	3.00E-02
1	-36.07	-35.51	-30.67	-35.43	-42.77
2	-34.53	-40.63	-33.53	-33.32	-42.64
3	-36.82	-41.47	-42.87	-31.02	-41.71
4	-44.19	-47.35	-36.44	-48.35	-33.82
5	-50.12	-44.19	-35.88	-37.80	-35.74
6	-35.51	-49.33	-37.82	-38.99	-36.74
7	-40.63	-44.53	-37.62	-37.80	-32.03
8	-41.47	-40.29	-39.34	-37.17	-36.82
9	-44.53	-41.12	-38.89	-40.04	-38.72
10	-44.00	-48.02	-32.13	-36.98	-40.28
Average value	-40.43	-43.29	-36.52	-37.58	-38.13
Standard deviation	5.21	4.59	3.65	4.87	3.72

**Table A – 28** Zeta potential measurement for PG after polymerization and after washing

No. of measurement	Surfactant Concentration (M)				
	6.00E-06	1.00E-05	3.00E-05	3.00E-04	7.00E-04
1	-23.64	-12.85	-21.18	25.50	35.02
2	-20.71	-18.84	-27.39	27.74	32.93
3	-18.64	-22.91	-24.03	28.00	27.78
4	-24.74	-21.05	-21.92	27.45	25.57
5	-21.16	-20.40	-24.03	25.86	32.58
6	-24.54	-21.72	-34.12	24.20	34.11
7	-23.73	-25.32	-33.21	26.49	28.00
8	-25.39	-26.83	-16.33	24.77	25.86
9	-21.21	-19.24	-27.32	25.14	25.11
10	-21.40	-26.44	-19.21	25.53	30.37
Average value	-22.52	-21.56	-24.88	26.07	29.73
Standard deviation	2.19	4.19	5.74	1.30	3.75

**Table A – 29** Zeta potential measurement for PM after polymerization and after washing

No. of measurement	Surfactant Concentration (M)				
	6.00E-05	1.00E-04	2.00E-04	1.00E-02	3.00E-02
1	-26.17	-20.85	-17.67	6.882	11.64
2	-25.22	-22.42	-22.64	8.630	9.140
3	-25.80	-23.73	-15.73	11.06	8.898
4	-26.74	-28.08	-23.09	11.51	7.757
5	-31.70	-22.93	-19.63	9.914	8.843
6	-29.15	-27.50	-20.67	10.53	9.984
7	-31.92	-22.57	-21.71	10.88	9.328
8	-26.02	-25.97	-18.94	21.74	10.32
9	-27.45	-26.96	-17.91	19.54	11.46
10	-31.43	-30.37	-15.07	24.72	10.15
Average value	-28.38	-25.14	-19.49	14.14	9.75
Standard deviation	2.72	3.07	2.87	6.12	1.21

**Table A – 30** Zeta potential measurement for DTAB after polymerization and after washing

No. of measurement	Surfactant Concentration (M)				
	1.00E-05	1.00E-04	1.00E-03	1.00E-02	3.00E-02
1	-38.57	-31.25	-28.24	-33.40	-22.57
2	-35.46	-37.58	-27.63	-35.52	-21.35
3	-44.50	-36.10	-34.69	-28.29	-23.33
4	-33.65	-36.16	-31.70	-26.67	-21.61
5	-36.02	-32.69	-31.03	-25.98	-20.35
6	-39.24	-30.82	-29.47	-28.05	-21.51
7	-34.57	-37.36	-27.63	-26.67	-19.32
8	-34.30	-39.69	-30.47	-32.03	-21.085
9	-35.67	-39.24	-28.53	-37.58	-20.22
10	-39.92	-37.15	-29.92	-30.01	-20.93
Average value	-37.04	-35.98	-29.84	-30.47	-20.78
Standard deviation	3.52	3.05	2.13	4.29	1.85

**Table A – 31** Summary of contact angle measurement result for PG

Sample	Contact angle								Temp
	Beginning				Ending				
	1	2	3	Average	1	2	3	Average	
Blank	12.66	14.02	10.09	12.26	N/A	N/A	N/A	N/A	22.45
NP1	61.02	65.56	68.08	64.89	56.11	60.08	52.78	56.32	22.77
NP2	63.33	74.53	75.28	71.05	60.84	62.59	59.67	61.03	22.61
P1	64.25	67.34	67.33	66.31	59.90	55.68	56.84	57.47	21.82
P2	68.00	73.53	78.86	73.46	42.55	45.93	50.72	46.4	22.29
NPW1	74.75	69.65	71.25	71.88	62.35	56.28	58.24	58.96	22.93
NPW2	58.78	60.90	57.39	59.02	46.43	52.12	45.35	47.97	22.29
PW1	62.50	65.81	65.01	64.44	53.78	55.83	49.65	53.09	22.77
PW2	63.14	62.40	65.11	63.55	39.11	40.27	45.94	41.77	22.77
SI1	66.36	62.66	66.70	65.24	55.55	49.88	51.89	52.44	22.61
SE1	82.04	59.53	64.31	68.63	49.82	43.05	53.36	48.74	22.13
SI2	65.23	62.58	64.31	64.04	53.34	51.39	53.36	52.70	22.61
SE2	71.40	76.84	81.08	76.44	50.78	56.60	53.64	53.67	21.82

  
 ศูนย์วิจัยทรัพยากร  
 จุฬาลงกรณ์มหาวิทยาลัย



**Table A – 32** Surface Roughness for PG

Sample	Scan Size (μm)	Fluid Condition					Solid condition				
		Rq (nm)	Ra (nm)	Rmax (nm)	Rz (nm)	Surface area (μm <sup>2</sup> )	Rq (nm)	Ra (nm)	Rmax (nm)	Rz (nm)	Surface area (μm <sup>2</sup> )
Blank mica	100	17.6	13.9	115	46.8	10001	37.2	27.8	325	325	10000
	100	13.6	10.6	93.1	39	10000	118	87.2	695	332	10050
	100						83.4	59.6	618	187	10001
	50	15.7	13.5	70.7	70.7	2500	12.3	9.75	71.2	46.9	2500
	50	10.7	8.75	55	36.5	2500					
	10	3.15	2.78	12.3	7.23	100	4.3	3.61	18.3	2.87	100
	10	5.27	4.38	22	12.4	100					
NP1	100	69.1	46.7	1123	806	10011	133	75.5	1084	310	10131
	100	68.8	47	479	171	10000	141	81	1079	349	10064
	50	35.9	22	442	189	2508	48.4	23.6	648	224	2521
	50	52.1	27.6	916	242	2541	61.9	37.2	667	304	2524
	10	8.91	6.16	199	6.53	100	31.1	13	232	10.8	101
	10						26.2	10.5	228	9.68	101
NPW1	100	64.1	29.3	1245	519	10030	86.8	37.4	1031	126	10171
	100	56.9	23.2	1204	300	10018	94.5	31.5	1094	42.4	2522
	50	32.8	13.7	540	184	2508	137	57.1	1581	101	2615
	50	35.5	17.3	639	291	2513					
	50	7.4	32.5	1189	359	2516	4.29	3.24	64.3	3.34	100
	10	2.46	1.98	33.9	2.84	100	48.5	19.8	459	5.2	102
	10	7.9	2.39	207	4.53	100	9.16	3.75	200	11.5	101

Sample	Scan Size ( $\mu\text{m}$ )	Fluid Condition					Solid condition				
		Rq (nm)	Ra (nm)	Rmax (nm)	Rz (nm)	Surface area ( $\mu\text{m}^2$ )	Rq (nm)	Ra (nm)	Rmax (nm)	Rz (nm)	Surface area ( $\mu\text{m}^2$ )
P1	100	124	83.9	1533	699	10142	166	132	1084	265	10272
	100						175	144	1110	336	10392
	50	110	68.1	931	740	2551	204	167	1214	499	2772
	50	119	76.1	1093	666	2553	200	161	1114	635	2702
	10	165	109	1098	564	108	151	101	934	934	108
	10	102	58.8	673	673	100	126	80.3	861	530	106
PW1	100	92.2	64.2	1411	573	10091	153	119	1221	311	10294
	100	84.8	59.2	787	486	10062	188	144	1693	419	10397
	50	61.1	34.2	688	261	2519	136	102	845	501	2570
	50	57.8	29.4	708	442	2521	91.6	67	626	321	250
	10	18	13.4	122	47.5	100	65	36.6	409	409	101
	10	34.2	14.2	445	18.3	101	59.2	29.9	547	117	102
NP2	100	76.44	48.8	996	49.8	10006	141	69.9	1836	615	10104
	50	10.8	8.98	78.9	13	2500	61.1	29.7	728	418	2507
	50	36.1	19	554	76	2504					
	50	26.4	13.7	585	298	2503					
	20						68.7	45.2	561	386	401
	100	56.1	39.3	696	123	10038	1281	65.6	1658	592	10084
NPW2	100	66.5	49.8	1111	114	10041	145	88	1568	147	10131
	50	53.4	38.5	491	89.8	2513	78.9	52.7	973	198	2529
	50	63	42.2	582	158	2521	124	59.8	1487	99.7	2528
	10	54.7	40.6	415	202	102	86	76.1	423	297	110
	10	43.5	34.8	230	116	101					

Sample	Scan Size (μm)	Fluid Condition					Solid condition				
		Rq (nm)	Ra (nm)	Rmax (nm)	Rz (nm)	Surface area (μm <sup>2</sup> )	Rq (nm)	Ra (nm)	Rmax (nm)	Rz (nm)	Surface area (μm <sup>2</sup> )
	10	42.4	32.9	226	116	101					
P2	100	531	431	2347	800	11671	318	249	2516	426	10000
	100	490	381	2615	1023	11244					
	100	366	272	2435	495	1038					
	50	514	431	2471	845	3925	296	215	1944	358	2500
	50	343	248	2049	1212	2635	308	249	1875	363	2883
	50	264	203	1744	345	2601					
	50	394	296	1919	1196	2618	326	267	1850	435	360
	10	243	170	1408	509	105	359	304	1613	592	421
	10	85.6	53.2	640	164	101	318	252	1854	355	344
PW2	100	549	447	2417	944	13292	546	465	2694	598	12364
	100						570	478	2393	772	12374
	50	536	449	2279	709	4102	471	390	2108	688	3120
	50	503	443	1752	944	3913	449	365	1985	603	2897
	10	248	189	1283	1042	118	286	225	1386	119	131
	10	338	262	1781	1151	129	270	211	1537	119	124
	10						241	182	1316	338	118
SI1	100	80.7	46.6	913	322	10061	121	81.5	1054	275	10185
	100	80.7	47.3	1159	346	10059	145	101	1276	321	10231
	50	88.4	53.6	740	340	2535	178	131	1180	298	2634
	50	100	60.1	947	242	2527	123	78.1	914	268	2575
	10	131	88.3	998	211	107	114	72.1	707	116	104
	10	71	71	980	238	105	115	82.4	723	104	105
SE1	100	349	281	1915	509	10512	361	286	2419	428	10998

Sample	Scan Size (μm)	Fluid Condition					Solid condition				
		Rq (nm)	Ra (nm)	Rmax (nm)	Rz (nm)	Surface area (μm <sup>2</sup> )	Rq (nm)	Ra (nm)	Rmax (nm)	Rz (nm)	Surface area (μm <sup>2</sup> )
	100	392	310	2399	850	10000	357	283	2507	630	11121
	50	414	359	1634	545	2500	225	174	1396	345	2752
	50	474	387	2529	892	2775	308	247	1783	456	3058
	10	376	321	1588	905	122	363	296	2003	645	116
	10	363	319	1307	1196	119	374	306	1790	819	120
SI2	100	228	167	1645	863	10350	365	299	2098	692	11603
	100	251	184	2054	1091	10435	328	264	1976	527	11197
	50	281	205	1803	994	2788	282	241	1374	350	2801
	50	225	162	1389	939	2663	247	212	1433	441	2783
	10	237	186	1452	1008	124	224	174	1186	547	113
	10						161	89.3	1071	1071	107
SE2	100	325	261	1882	378	10460	328	261	1971	409	10756
	100	365	292	2194	598	10501	294	232	2053	476	10545
	50	342	284	1534	464	2723	358	293	1822	471	2786
	50	421	344	2338	661	2709	358	294	1752	434	2806
	50						265	217	1473	365	2727
	10	364	295	1947	787	127	360	284	2088	639	134
	10	294	242	1666	126	658	319	252	1809	1001	125

จุฬาลงกรณ์มหาวิทยาลัย

**Table A – 33** Force curve result for sample SE1

Separation, Z ( $\mu\text{m}$ )	Deflection (V)	$\Omega$	x	d	Force (N/m)	Force after offset (N/m)	Slope	Displacement (nm)
1	5.726	0.029	162.9655	10.5069	11.04906	17.02949	-48.9315	0
0.998	5.659	0.029	160.7241	10.43793	10.8971	16.87752	-48.9516	-0.02004
0.996	5.614	0.029	159.2414	10.36897	10.79657	16.77699	-48.9202	0.011347
0.994	5.568	0.029	157.7241	10.3	10.6937	16.67412	-48.8911	0.0404
0.992	5.521	0.029	156.1724	10.23103	10.58849	16.56892	-48.8644	0.067116
0.99	5.474	0.029	154.6207	10.16207	10.48328	16.46371	-48.8377	0.093831
0.988	5.426	0.029	153.0345	10.0931	10.37574	16.35617	-48.8133	0.118208
0.986	5.379	0.029	151.4828	10.02414	10.27053	16.25096	-48.7866	0.144923
0.984	5.331	0.029	149.8966	9.955172	10.16299	16.14341	-48.7622	0.1693
0.982	5.282	0.029	148.2759	9.886207	10.0531	16.03353	-48.7402	0.191339
0.98	5.231	0.029	146.5862	9.817241	9.938545	15.91897	-48.7228	0.208703
0.979	5.183	0.029	144.9655	9.782759	9.828662	15.80909	-48.7667	0.164781
0.977	5.134	0.029	143.3448	9.713793	9.718779	15.69921	-48.7447	0.18682
0.975	5.087	0.029	141.7931	9.644828	9.613572	15.594	-48.718	0.213535
0.973	5.035	0.029	140.069	9.575862	9.496676	15.4771	-48.7029	0.228561
0.971	4.986	0.029	138.4483	9.506897	9.386793	15.36722	-48.6809	0.2506
0.969	4.936	0.029	136.7931	9.437931	9.274572	15.255	-48.6612	0.270301
0.967	4.887	0.029	135.1724	9.368966	9.16469	15.14512	-48.6392	0.292341
0.965	4.835	0.029	133.4483	9.3	9.047793	15.02822	-48.6241	0.307366
0.963	4.785	0.029	131.7931	9.231034	8.935572	14.916	-48.6044	0.327067
0.961	4.735	0.029	130.1379	9.162069	8.823352	14.80378	-48.5847	0.346769
0.959	4.682	0.029	128.3793	9.093103	8.704117	14.68454	-48.5721	0.359456

Separation, Z ( $\mu\text{m}$ )	Deflection (V)	$\Omega$	x	d	Force (N/m)	Force after offset (N/m)	Slope	Displacement (nm)
0.957	4.631	0.029	126.6897	9.024138	8.589559	14.56999	-48.5547	0.37682
0.955	4.58	0.029	125	8.955172	8.475	14.45543	-48.5373	0.394183
0.953	4.529	0.029	123.3103	8.886207	8.360441	14.34087	-48.52	0.411546
0.951	4.475	0.029	121.5172	8.817241	8.238869	14.2193	-48.5096	0.421896
0.949	4.423	0.029	119.7931	8.748276	8.121972	14.1024	-48.4946	0.436921
0.947	4.37	0.029	118.0345	8.67931	8.002738	13.98317	-48.4819	0.449609
0.945	4.315	0.029	116.2069	8.610345	7.878828	13.85926	-48.4739	0.457621
0.943	4.261	0.029	114.4138	8.541379	7.757255	13.73768	-48.4635	0.46797
0.941	4.209	0.029	112.6897	8.472414	7.640359	13.62079	-48.4485	0.482996
0.939	4.156	0.029	110.931	8.403448	7.521124	13.50155	-48.4358	0.495683
0.938	4.102	0.029	109.1034	8.368966	7.397214	13.37764	-48.4938	0.437734
0.936	4.05	0.029	107.3793	8.3	7.280317	13.26074	-48.4788	0.452759
0.934	3.996	0.029	105.5862	8.231034	7.158745	13.13917	-48.4684	0.463109
0.932	3.942	0.029	103.7931	8.162069	7.037172	13.0176	-48.4581	0.473458
0.93	3.888	0.029	102	8.093103	6.9156	12.89603	-48.4477	0.483808
0.928	3.837	0.029	100.3103	8.024138	6.801041	12.78147	-48.4303	0.501171
0.926	3.782	0.029	98.48276	7.955172	6.677131	12.65756	-48.4223	0.509183
0.924	3.727	0.029	96.65517	7.886207	6.553221	12.53365	-48.4143	0.517195
0.922	3.672	0.029	94.82759	7.817241	6.42931	12.40974	-48.4063	0.525206
0.92	3.616	0.029	92.96552	7.748276	6.303062	12.28349	-48.4006	0.53088
0.918	3.564	0.029	91.24138	7.67931	6.186166	12.16659	-48.3856	0.545905
0.916	3.509	0.029	89.41379	7.610345	6.062255	12.04268	-48.3776	0.553917
0.914	3.454	0.029	87.58621	7.541379	5.938345	11.91877	-48.3696	0.561929
0.912	3.396	0.029	85.65517	7.472414	5.807421	11.78785	-48.3686	0.562927
0.91	3.341	0.029	83.82759	7.403448	5.68351	11.66394	-48.3606	0.570938

Separation, Z ( $\mu\text{m}$ )	Deflection (V)	$\Omega$	x	d	Force (N/m)	Force after offset (N/m)	Slope	Displacement (nm)
0.908	3.286	0.029	82	7.334483	5.5596	11.54003	-48.3526	0.57895
0.906	3.232	0.029	80.2069	7.265517	5.438028	11.41846	-48.3422	0.5893
0.904	3.174	0.029	78.27586	7.196552	5.307103	11.28753	-48.3412	0.590297
0.902	3.118	0.029	76.41379	7.127586	5.180855	11.16128	-48.3355	0.595971
0.9	3.061	0.029	74.51724	7.058621	5.052269	11.0327	-48.3322	0.599307
0.898	3.002	0.029	72.55172	6.989655	4.919007	10.89943	-48.3335	0.597967
0.896	2.947	0.029	70.72414	6.92069	4.795097	10.77552	-48.3255	0.605978
0.895	2.892	0.029	68.86207	6.886207	4.668848	10.64928	-48.3858	0.545691
0.893	2.835	0.029	66.96552	6.817241	4.540262	10.52069	-48.3825	0.549027
0.891	2.779	0.029	65.10345	6.748276	4.414014	10.39444	-48.3768	0.554701
0.889	2.719	0.029	63.10345	6.67931	4.278414	10.25884	-48.3805	0.551023
0.887	2.662	0.029	61.2069	6.610345	4.149828	10.13026	-48.3772	0.554359
0.885	2.606	0.029	59.34483	6.541379	4.023579	10.00401	-48.3715	0.560032
0.883	2.548	0.029	57.41379	6.472414	3.892655	9.873083	-48.3705	0.56103
0.881	2.492	0.029	55.55172	6.403448	3.766407	9.746834	-48.3648	0.566704
0.879	2.435	0.029	53.65517	6.334483	3.637821	9.618248	-48.3615	0.57004
0.877	2.378	0.029	51.75862	6.265517	3.509234	9.489662	-48.3581	0.573375
0.875	2.32	0.029	49.82759	6.196552	3.37831	9.358738	-48.3571	0.574373
0.873	2.261	0.029	47.86207	6.127586	3.245048	9.225476	-48.3585	0.573033
0.871	2.203	0.029	45.93103	6.058621	3.114124	9.094552	-48.3575	0.574031
0.869	2.148	0.029	44.10345	5.989655	2.990214	8.970641	-48.3495	0.582043
0.867	2.09	0.029	42.17241	5.92069	2.85929	8.839717	-48.3485	0.583041
0.865	2.031	0.029	40.2069	5.851724	2.726028	8.706455	-48.3498	0.581701
0.863	1.972	0.029	38.24138	5.782759	2.592766	8.573193	-48.3511	0.58036
0.861	1.914	0.029	36.31034	5.713793	2.461841	8.442269	-48.3502	0.581358

Separation, Z ( $\mu\text{m}$ )	Deflection (V)	$\Omega$	x	d	Force (N/m)	Force after offset (N/m)	Slope	Displacement (nm)
0.859	1.854	0.029	34.31034	5.644828	2.326241	8.306669	-48.3538	0.57768
0.857	1.794	0.029	32.31034	5.575862	2.190641	8.171069	-48.3575	0.574002
0.855	1.733	0.029	30.27586	5.506897	2.052703	8.033131	-48.3635	0.567986
0.854	1.673	0.029	28.24138	5.472414	1.914766	7.895193	-48.4355	0.496009
0.852	1.614	0.029	26.27586	5.403448	1.781503	7.761931	-48.4368	0.494669
0.85	1.555	0.029	24.31034	5.334483	1.648241	7.628669	-48.4382	0.493329
0.848	1.496	0.029	22.34483	5.265517	1.514979	7.495407	-48.4395	0.491989
0.846	1.436	0.029	20.34483	5.196552	1.379379	7.359807	-48.4432	0.488311
0.844	1.375	0.029	18.31034	5.127586	1.241441	7.221869	-48.4492	0.482295
0.842	1.316	0.029	16.34483	5.058621	1.108179	7.088607	-48.4506	0.480955
0.84	1.257	0.029	14.37931	4.989655	0.974917	6.955345	-48.4519	0.479615
0.838	1.196	0.029	12.34483	4.92069	0.836979	6.817407	-48.4579	0.473599
0.836	1.137	0.029	10.37931	4.851724	0.703717	6.684145	-48.4593	0.472259
0.834	1.079	0.029	8.448276	4.782759	0.572793	6.553221	-48.4583	0.473257
0.832	1.02	0.029	6.482759	4.713793	0.439531	6.419959	-48.4596	0.471917
0.83	0.96	0.029	4.482759	4.644828	0.303931	6.284359	-48.4633	0.468239
0.828	0.9	0.029	2.482759	4.575862	0.168331	6.148759	-48.4669	0.464561
0.826	0.841	0.029	0.517241	4.506897	0.035069	6.015497	-48.4683	0.463221
0.824	0.782	0.029	-1.44828	4.437931	-0.09819	5.882234	-48.4696	0.461881
0.822	0.723	0.029	-3.41379	4.368966	-0.23146	5.748972	-48.471	0.460541
0.82	0.663	0.029	-5.41379	4.3	-0.36706	5.613372	-48.4746	0.456863
0.818	0.603	0.029	-7.41379	4.231034	-0.50266	5.477772	-48.4783	0.453185
0.816	0.544	0.029	-9.37931	4.162069	-0.63592	5.34451	-48.4797	0.451845
0.814	0.485	0.029	-11.3448	4.093103	-0.76918	5.211248	-48.481	0.450505
0.813	0.426	0.029	-13.3448	4.058621	-0.90478	5.075648	-48.5506	0.380866



Separation, Z ( $\mu\text{m}$ )	Deflection (V)	$\Omega$	x	d	Force (N/m)	Force after offset (N/m)	Slope	Displacement (nm)
0.811	0.365	0.029	-15.3793	3.989655	-1.04272	4.93771	-48.5567	0.37485
0.809	0.307	0.029	-17.3103	3.92069	-1.17364	4.806786	-48.5557	0.375848
0.807	0.246	0.029	-19.3448	3.851724	-1.31158	4.668848	-48.5617	0.369832
0.805	0.187	0.029	-21.3103	3.782759	-1.44484	4.535586	-48.563	0.368492
0.803	0.127	0.029	-23.3103	3.713793	-1.58044	4.399986	-48.5667	0.364814
0.801	0.069	0.029	-25.2414	3.644828	-1.71137	4.269062	-48.5657	0.365811
0.799	0.009	0.029	-27.2414	3.575862	-1.84697	4.133462	-48.5694	0.362133
0.797	-0.05	0.029	-29.2069	3.506897	-1.98023	4.0002	-48.5707	0.360793
0.795	-0.109	0.029	-31.1724	3.437931	-2.11349	3.866938	-48.5721	0.359453
0.793	-0.168	0.029	-33.1379	3.368966	-2.24675	3.733676	-48.5734	0.358113
0.791	-0.227	0.029	-35.1034	3.3	-2.38001	3.600414	-48.5747	0.356773
0.789	-0.286	0.029	-37.069	3.231034	-2.51328	3.467152	-48.5761	0.355433
0.787	-0.345	0.029	-39.0345	3.162069	-2.64654	3.33389	-48.5774	0.354093
0.785	-0.403	0.029	-40.9655	3.093103	-2.77746	3.202966	-48.5764	0.355091
0.783	-0.464	0.029	-43	3.024138	-2.9154	3.065028	-48.5824	0.349075
0.781	-0.522	0.029	-44.931	2.955172	-3.04632	2.934103	-48.5814	0.350073
0.779	-0.582	0.029	-46.931	2.886207	-3.18192	2.798503	-48.5851	0.346395
0.777	-0.64	0.029	-48.8621	2.817241	-3.31285	2.667579	-48.5841	0.347393
0.775	-0.697	0.029	-50.7586	2.748276	-3.44143	2.538993	-48.5808	0.350728
0.773	-0.754	0.029	-52.6552	2.67931	-3.57002	2.410407	-48.5774	0.354064
0.771	-0.813	0.029	-54.6207	2.610345	-3.70328	2.277145	-48.5788	0.352724
0.77	-0.87	0.029	-56.5517	2.575862	-3.83421	2.146221	-48.6437	0.287761
0.768	-0.929	0.029	-58.5172	2.506897	-3.96747	2.012959	-48.6451	0.286421
0.766	-0.986	0.029	-60.4138	2.437931	-4.09606	1.884372	-48.6418	0.289757
0.764	-1.044	0.029	-62.3448	2.368966	-4.22698	1.753448	-48.6408	0.290755

Separation, Z ( $\mu\text{m}$ )	Deflection (V)	$\Omega$	x	d	Force (N/m)	Force after offset (N/m)	Slope	Displacement (nm)
0.762	-1.102	0.029	-64.2759	2.3	-4.3579	1.622524	-48.6398	0.291752
0.76	-1.16	0.029	-66.2069	2.231034	-4.48883	1.4916	-48.6388	0.29275
0.758	-1.217	0.029	-68.1034	2.162069	-4.61741	1.363014	-48.6354	0.296086
0.756	-1.275	0.029	-70.0345	2.093103	-4.74834	1.23209	-48.6344	0.297084
0.754	-1.332	0.029	-71.931	2.024138	-4.87692	1.103503	-48.6311	0.30042
0.752	-1.389	0.029	-73.8276	1.955172	-5.00551	0.974917	-48.6278	0.303756
0.75	-1.446	0.029	-75.7241	1.886207	-5.1341	0.846331	-48.6244	0.307091
0.748	-1.505	0.029	-77.6897	1.817241	-5.26736	0.713069	-48.6258	0.305751
0.746	-1.564	0.029	-79.6552	1.748276	-5.40062	0.579807	-48.6271	0.304411
0.744	-1.621	0.029	-81.5517	1.67931	-5.52921	0.451221	-48.6238	0.307747
0.742	-1.676	0.029	-83.3793	1.610345	-5.65312	0.32731	-48.6158	0.315759
0.74	-1.733	0.029	-85.2759	1.541379	-5.7817	0.198724	-48.6124	0.319094
0.738	-1.791	0.029	-87.2069	1.472414	-5.91263	0.0678	-48.6114	0.320092
0.736	-1.849	0.029	-89.1379	1.403448	-6.04355	-0.06312	-48.6104	0.32109
0.734	-1.903	0.029	-90.931	1.334483	-6.16512	-0.1847	-48.6001	0.33144
0.732	-1.962	0.029	-92.8966	1.265517	-6.29839	-0.31796	-48.6014	0.3301
0.73	-2.018	0.029	-94.7586	1.196552	-6.42463	-0.44421	-48.5957	0.335773
0.729	-2.074	0.029	-96.6552	1.162069	-6.55322	-0.57279	-48.6584	0.273148
0.727	-2.128	0.029	-98.4483	1.093103	-6.67479	-0.69437	-48.648	0.283498
0.725	-2.185	0.029	-100.345	1.024138	-6.80338	-0.82295	-48.6447	0.286834
0.723	-2.241	0.029	-102.207	0.955172	-6.92963	-0.9492	-48.639	0.292507
0.721	-2.299	0.029	-104.138	0.886207	-7.06055	-1.08012	-48.638	0.293505
0.719	-2.352	0.029	-105.897	0.817241	-7.17979	-1.19936	-48.6253	0.306193
0.717	-2.409	0.029	-107.793	0.748276	-7.30837	-1.32794	-48.622	0.309529
0.715	-2.466	0.029	-109.69	0.67931	-7.43696	-1.45653	-48.6186	0.312864

Separation, Z ( $\mu\text{m}$ )	Deflection (V)	$\Omega$	x	d	Force (N/m)	Force after offset (N/m)	Slope	Displacement (nm)
0.713	-2.52	0.029	-111.483	0.610345	-7.55853	-1.5781	-48.6083	0.323214
0.711	-2.575	0.029	-113.31	0.541379	-7.68244	-1.70201	-48.6003	0.331226
0.709	-2.63	0.029	-115.138	0.472414	-7.80635	-1.82592	-48.5923	0.339237
0.707	-2.684	0.029	-116.931	0.403448	-7.92792	-1.9475	-48.5819	0.349587
0.705	-2.736	0.029	-118.655	0.334483	-8.04482	-2.06439	-48.5669	0.364612
0.703	-2.79	0.029	-120.448	0.265517	-8.16639	-2.18597	-48.5565	0.374962
0.701	-2.843	0.029	-122.207	0.196552	-8.28563	-2.3052	-48.5439	0.387649
0.699	-2.894	0.029	-123.897	0.127586	-8.40019	-2.41976	-48.5265	0.405013
0.697	-2.946	0.029	-125.621	0.058621	-8.51708	-2.53666	-48.5115	0.420038
0.695	-2.987	0.029	-126.966	-0.01034	-8.60826	-2.62783	-48.4707	0.460781
0.693	-3.008	0.029	-127.621	-0.07931	-8.65268	-2.67226	-48.3832	0.548282
0.691	-2.857	0.029	-122.345	-0.14828	-8.29498	-2.31455	-47.8936	1.037908

ศูนย์วิทยทรัพยากร  
จุฬาลงกรณ์มหาวิทยาลัย

**Table A – 34** Force curve result for sample SE2

Separation ( $\mu\text{m}$ )	Deflection (V)	$\Omega$	x	d	Force (N/m)	Force after offset (N/m)	Slope	Displacement (nm)
1	5.726	0.029	162.9655	10.5069	11.04906	17.02949	-48.9315	0
0.998	5.659	0.029	160.7241	10.43793	10.8971	16.87752	-48.9516	-0.02004
0.996	5.614	0.029	159.2414	10.36897	10.79657	16.77699	-48.9202	0.011347
0.994	5.568	0.029	157.7241	10.3	10.6937	16.67412	-48.8911	0.0404
0.992	5.521	0.029	156.1724	10.23103	10.58849	16.56892	-48.8644	0.067116
0.99	5.474	0.029	154.6207	10.16207	10.48328	16.46371	-48.8377	0.093831
0.988	5.426	0.029	153.0345	10.0931	10.37574	16.35617	-48.8133	0.118208
0.986	5.379	0.029	151.4828	10.02414	10.27053	16.25096	-48.7866	0.144923
0.984	5.331	0.029	149.8966	9.955172	10.16299	16.14341	-48.7622	0.1693
0.982	5.282	0.029	148.2759	9.886207	10.0531	16.03353	-48.7402	0.191339
0.98	5.231	0.029	146.5862	9.817241	9.938545	15.91897	-48.7228	0.208703
0.979	5.183	0.029	144.9655	9.782759	9.828662	15.80909	-48.7667	0.164781
0.977	5.134	0.029	143.3448	9.713793	9.718779	15.69921	-48.7447	0.18682
0.975	5.087	0.029	141.7931	9.644828	9.613572	15.594	-48.718	0.213535
0.973	5.035	0.029	140.069	9.575862	9.496676	15.4771	-48.7029	0.228561
0.971	4.986	0.029	138.4483	9.506897	9.386793	15.36722	-48.6809	0.2506
0.969	4.936	0.029	136.7931	9.437931	9.274572	15.255	-48.6612	0.270301
0.967	4.887	0.029	135.1724	9.368966	9.16469	15.14512	-48.6392	0.292341
0.965	4.835	0.029	133.4483	9.3	9.047793	15.02822	-48.6241	0.307366
0.963	4.785	0.029	131.7931	9.231034	8.935572	14.916	-48.6044	0.327067
0.961	4.735	0.029	130.1379	9.162069	8.823352	14.80378	-48.5847	0.346769
0.959	4.682	0.029	128.3793	9.093103	8.704117	14.68454	-48.5721	0.359456

Separation ( $\mu\text{m}$ )	Deflection (V)	$\Omega$	x	d	Force (N/m)	Force after offset (N/m)	Slope	Displacement (nm)
0.957	4.631	0.029	126.6897	9.024138	8.589559	14.56999	-48.5547	0.37682
0.955	4.58	0.029	125	8.955172	8.475	14.45543	-48.5373	0.394183
0.953	4.529	0.029	123.3103	8.886207	8.360441	14.34087	-48.52	0.411546
0.951	4.475	0.029	121.5172	8.817241	8.238869	14.2193	-48.5096	0.421896
0.949	4.423	0.029	119.7931	8.748276	8.121972	14.1024	-48.4946	0.436921
0.947	4.37	0.029	118.0345	8.67931	8.002738	13.98317	-48.4819	0.449609
0.945	4.315	0.029	116.2069	8.610345	7.878828	13.85926	-48.4739	0.457621
0.943	4.261	0.029	114.4138	8.541379	7.757255	13.73768	-48.4635	0.46797
0.941	4.209	0.029	112.6897	8.472414	7.640359	13.62079	-48.4485	0.482996
0.939	4.156	0.029	110.931	8.403448	7.521124	13.50155	-48.4358	0.495683
0.938	4.102	0.029	109.1034	8.368966	7.397214	13.37764	-48.4938	0.437734
0.936	4.05	0.029	107.3793	8.3	7.280317	13.26074	-48.4788	0.452759
0.934	3.996	0.029	105.5862	8.231034	7.158745	13.13917	-48.4684	0.463109
0.932	3.942	0.029	103.7931	8.162069	7.037172	13.0176	-48.4581	0.473458
0.93	3.888	0.029	102	8.093103	6.9156	12.89603	-48.4477	0.483808
0.928	3.837	0.029	100.3103	8.024138	6.801041	12.78147	-48.4303	0.501171
0.926	3.782	0.029	98.48276	7.955172	6.677131	12.65756	-48.4223	0.509183
0.924	3.727	0.029	96.65517	7.886207	6.553221	12.53365	-48.4143	0.517195
0.922	3.672	0.029	94.82759	7.817241	6.42931	12.40974	-48.4063	0.525206
0.92	3.616	0.029	92.96552	7.748276	6.303062	12.28349	-48.4006	0.53088
0.918	3.564	0.029	91.24138	7.67931	6.186166	12.16659	-48.3856	0.545905
0.916	3.509	0.029	89.41379	7.610345	6.062255	12.04268	-48.3776	0.553917
0.914	3.454	0.029	87.58621	7.541379	5.938345	11.91877	-48.3696	0.561929
0.912	3.396	0.029	85.65517	7.472414	5.807421	11.78785	-48.3686	0.562927
0.91	3.341	0.029	83.82759	7.403448	5.68351	11.66394	-48.3606	0.570938

Separation ( $\mu\text{m}$ )	Deflection (V)	$\Omega$	x	d	Force (N/m)	Force after offset (N/m)	Slope	Displacement (nm)
0.908	3.286	0.029	82	7.334483	5.5596	11.54003	-48.3526	0.57895
0.906	3.232	0.029	80.2069	7.265517	5.438028	11.41846	-48.3422	0.5893
0.904	3.174	0.029	78.27586	7.196552	5.307103	11.28753	-48.3412	0.590297
0.902	3.118	0.029	76.41379	7.127586	5.180855	11.16128	-48.3355	0.595971
0.9	3.061	0.029	74.51724	7.058621	5.052269	11.0327	-48.3322	0.599307
0.898	3.002	0.029	72.55172	6.989655	4.919007	10.89943	-48.3335	0.597967
0.896	2.947	0.029	70.72414	6.92069	4.795097	10.77552	-48.3255	0.605978
0.895	2.892	0.029	68.86207	6.886207	4.668848	10.64928	-48.3858	0.545691
0.893	2.835	0.029	66.96552	6.817241	4.540262	10.52069	-48.3825	0.549027
0.891	2.779	0.029	65.10345	6.748276	4.414014	10.39444	-48.3768	0.554701
0.889	2.719	0.029	63.10345	6.67931	4.278414	10.25884	-48.3805	0.551023
0.887	2.662	0.029	61.2069	6.610345	4.149828	10.13026	-48.3772	0.554359
0.885	2.606	0.029	59.34483	6.541379	4.023579	10.00401	-48.3715	0.560032
0.883	2.548	0.029	57.41379	6.472414	3.892655	9.873083	-48.3705	0.56103
0.881	2.492	0.029	55.55172	6.403448	3.766407	9.746834	-48.3648	0.566704
0.879	2.435	0.029	53.65517	6.334483	3.637821	9.618248	-48.3615	0.57004
0.877	2.378	0.029	51.75862	6.265517	3.509234	9.489662	-48.3581	0.573375
0.875	2.32	0.029	49.82759	6.196552	3.37831	9.358738	-48.3571	0.574373
0.873	2.261	0.029	47.86207	6.127586	3.245048	9.225476	-48.3585	0.573033
0.871	2.203	0.029	45.93103	6.058621	3.114124	9.094552	-48.3575	0.574031
0.869	2.148	0.029	44.10345	5.989655	2.990214	8.970641	-48.3495	0.582043
0.867	2.09	0.029	42.17241	5.92069	2.85929	8.839717	-48.3485	0.583041
0.865	2.031	0.029	40.2069	5.851724	2.726028	8.706455	-48.3498	0.581701
0.863	1.972	0.029	38.24138	5.782759	2.592766	8.573193	-48.3511	0.58036
0.861	1.914	0.029	36.31034	5.713793	2.461841	8.442269	-48.3502	0.581358

Separation ( $\mu\text{m}$ )	Deflection (V)	$\Omega$	x	d	Force (N/m)	Force after offset (N/m)	Slope	Displacement (nm)
0.859	1.854	0.029	34.31034	5.644828	2.326241	8.306669	-48.3538	0.57768
0.857	1.794	0.029	32.31034	5.575862	2.190641	8.171069	-48.3575	0.574002
0.855	1.733	0.029	30.27586	5.506897	2.052703	8.033131	-48.3635	0.567986
0.854	1.673	0.029	28.24138	5.472414	1.914766	7.895193	-48.4355	0.496009
0.852	1.614	0.029	26.27586	5.403448	1.781503	7.761931	-48.4368	0.494669
0.85	1.555	0.029	24.31034	5.334483	1.648241	7.628669	-48.4382	0.493329
0.848	1.496	0.029	22.34483	5.265517	1.514979	7.495407	-48.4395	0.491989
0.846	1.436	0.029	20.34483	5.196552	1.379379	7.359807	-48.4432	0.488311
0.844	1.375	0.029	18.31034	5.127586	1.241441	7.221869	-48.4492	0.482295
0.842	1.316	0.029	16.34483	5.058621	1.108179	7.088607	-48.4506	0.480955
0.84	1.257	0.029	14.37931	4.989655	0.974917	6.955345	-48.4519	0.479615
0.838	1.196	0.029	12.34483	4.92069	0.836979	6.817407	-48.4579	0.473599
0.836	1.137	0.029	10.37931	4.851724	0.703717	6.684145	-48.4593	0.472259
0.834	1.079	0.029	8.448276	4.782759	0.572793	6.553221	-48.4583	0.473257
0.832	1.02	0.029	6.482759	4.713793	0.439531	6.419959	-48.4596	0.471917
0.83	0.96	0.029	4.482759	4.644828	0.303931	6.284359	-48.4633	0.468239
0.828	0.9	0.029	2.482759	4.575862	0.168331	6.148759	-48.4669	0.464561
0.826	0.841	0.029	0.517241	4.506897	0.035069	6.015497	-48.4683	0.463221
0.824	0.782	0.029	-1.44828	4.437931	-0.09819	5.882234	-48.4696	0.461881
0.822	0.723	0.029	-3.41379	4.368966	-0.23146	5.748972	-48.471	0.460541
0.82	0.663	0.029	-5.41379	4.3	-0.36706	5.613372	-48.4746	0.456863
0.818	0.603	0.029	-7.41379	4.231034	-0.50266	5.477772	-48.4783	0.453185
0.816	0.544	0.029	-9.37931	4.162069	-0.63592	5.34451	-48.4797	0.451845
0.814	0.485	0.029	-11.3448	4.093103	-0.76918	5.211248	-48.481	0.450505
0.813	0.426	0.029	-13.3448	4.058621	-0.90478	5.075648	-48.5506	0.380866

Separation ( $\mu\text{m}$ )	Deflection (V)	$\Omega$	x	d	Force (N/m)	Force after offset (N/m)	Slope	Displacement (nm)
0.811	0.365	0.029	-15.3793	3.989655	-1.04272	4.93771	-48.5567	0.37485
0.809	0.307	0.029	-17.3103	3.92069	-1.17364	4.806786	-48.5557	0.375848
0.807	0.246	0.029	-19.3448	3.851724	-1.31158	4.668848	-48.5617	0.369832
0.805	0.187	0.029	-21.3103	3.782759	-1.44484	4.535586	-48.563	0.368492
0.803	0.127	0.029	-23.3103	3.713793	-1.58044	4.399986	-48.5667	0.364814
0.801	0.069	0.029	-25.2414	3.644828	-1.71137	4.269062	-48.5657	0.365811
0.799	0.009	0.029	-27.2414	3.575862	-1.84697	4.133462	-48.5694	0.362133
0.797	-0.05	0.029	-29.2069	3.506897	-1.98023	4.0002	-48.5707	0.360793
0.795	-0.109	0.029	-31.1724	3.437931	-2.11349	3.866938	-48.5721	0.359453
0.793	-0.168	0.029	-33.1379	3.368966	-2.24675	3.733676	-48.5734	0.358113
0.791	-0.227	0.029	-35.1034	3.3	-2.38001	3.600414	-48.5747	0.356773
0.789	-0.286	0.029	-37.069	3.231034	-2.51328	3.467152	-48.5761	0.355433
0.787	-0.345	0.029	-39.0345	3.162069	-2.64654	3.33389	-48.5774	0.354093
0.785	-0.403	0.029	-40.9655	3.093103	-2.77746	3.202966	-48.5764	0.355091
0.783	-0.464	0.029	-43	3.024138	-2.9154	3.065028	-48.5824	0.349075
0.781	-0.522	0.029	-44.931	2.955172	-3.04632	2.934103	-48.5814	0.350073
0.779	-0.582	0.029	-46.931	2.886207	-3.18192	2.798503	-48.5851	0.346395
0.777	-0.64	0.029	-48.8621	2.817241	-3.31285	2.667579	-48.5841	0.347393
0.775	-0.697	0.029	-50.7586	2.748276	-3.44143	2.538993	-48.5808	0.350728
0.773	-0.754	0.029	-52.6552	2.67931	-3.57002	2.410407	-48.5774	0.354064
0.771	-0.813	0.029	-54.6207	2.610345	-3.70328	2.277145	-48.5788	0.352724
0.77	-0.87	0.029	-56.5517	2.575862	-3.83421	2.146221	-48.6437	0.287761
0.768	-0.929	0.029	-58.5172	2.506897	-3.96747	2.012959	-48.6451	0.286421
0.766	-0.986	0.029	-60.4138	2.437931	-4.09606	1.884372	-48.6418	0.289757
0.764	-1.044	0.029	-62.3448	2.368966	-4.22698	1.753448	-48.6408	0.290755



Separation ( $\mu\text{m}$ )	Deflection (V)	$\Omega$	x	d	Force (N/m)	Force after offset (N/m)	Slope	Displacement (nm)
0.762	-1.102	0.029	-64.2759	2.3	-4.3579	1.622524	-48.6398	0.291752
0.76	-1.16	0.029	-66.2069	2.231034	-4.48883	1.4916	-48.6388	0.29275
0.758	-1.217	0.029	-68.1034	2.162069	-4.61741	1.363014	-48.6354	0.296086
0.756	-1.275	0.029	-70.0345	2.093103	-4.74834	1.23209	-48.6344	0.297084
0.754	-1.332	0.029	-71.931	2.024138	-4.87692	1.103503	-48.6311	0.30042
0.752	-1.389	0.029	-73.8276	1.955172	-5.00551	0.974917	-48.6278	0.303756
0.75	-1.446	0.029	-75.7241	1.886207	-5.1341	0.846331	-48.6244	0.307091
0.748	-1.505	0.029	-77.6897	1.817241	-5.26736	0.713069	-48.6258	0.305751
0.746	-1.564	0.029	-79.6552	1.748276	-5.40062	0.579807	-48.6271	0.304411
0.744	-1.621	0.029	-81.5517	1.67931	-5.52921	0.451221	-48.6238	0.307747
0.742	-1.676	0.029	-83.3793	1.610345	-5.65312	0.32731	-48.6158	0.315759
0.74	-1.733	0.029	-85.2759	1.541379	-5.7817	0.198724	-48.6124	0.319094
0.738	-1.791	0.029	-87.2069	1.472414	-5.91263	0.0678	-48.6114	0.320092
0.736	-1.849	0.029	-89.1379	1.403448	-6.04355	-0.06312	-48.6104	0.32109
0.734	-1.903	0.029	-90.931	1.334483	-6.16512	-0.1847	-48.6001	0.33144
0.732	-1.962	0.029	-92.8966	1.265517	-6.29839	-0.31796	-48.6014	0.3301
0.73	-2.018	0.029	-94.7586	1.196552	-6.42463	-0.44421	-48.5957	0.335773
0.729	-2.074	0.029	-96.6552	1.162069	-6.55322	-0.57279	-48.6584	0.273148
0.727	-2.128	0.029	-98.4483	1.093103	-6.67479	-0.69437	-48.648	0.283498
0.725	-2.185	0.029	-100.345	1.024138	-6.80338	-0.82295	-48.6447	0.286834
0.723	-2.241	0.029	-102.207	0.955172	-6.92963	-0.9492	-48.639	0.292507
0.721	-2.299	0.029	-104.138	0.886207	-7.06055	-1.08012	-48.638	0.293505
0.719	-2.352	0.029	-105.897	0.817241	-7.17979	-1.19936	-48.6253	0.306193
0.717	-2.409	0.029	-107.793	0.748276	-7.30837	-1.32794	-48.622	0.309529
0.715	-2.466	0.029	-109.69	0.67931	-7.43696	-1.45653	-48.6186	0.312864

**Table A-35** Summary of FTIR result for PG at variation of polymerization time

Wave number (cm <sup>-1</sup> )	Percent transmission versus polymerization time (min)				
	0	15	120	360	960
400	2.836	2.310	1.866	1.459	0.970
500	2.842	2.316	1.869	1.460	0.970
600	3.105	2.475	2.160	1.778	1.299
700	3.224	2.469	2.171	1.772	1.252
800	2.998	2.457	2.183	1.761	1.277
900	3.159	2.603	2.237	1.775	1.312
1000	3.020	2.470	2.159	1.740	1.281
1100	2.514	1.836	1.690	1.452	0.866
1200	2.574	1.951	1.870	1.546	1.002
1300	3.084	2.106	1.935	1.562	1.050
1400	3.164	2.561	2.175	1.699	1.265
1500	3.179	2.592	2.181	1.695	1.273
1600	3.138	2.597	2.153	1.679	1.262
1700	3.149	2.583	2.150	1.670	1.248
1800	3.178	2.632	2.174	1.677	1.263
1900	3.166	2.627	2.168	1.669	1.257
2000	3.160	2.624	2.158	1.660	1.249
2100	3.161	2.626	2.152	1.654	1.243
2200	3.155	2.623	2.148	1.648	1.237
2300	3.160	2.637	2.144	1.646	1.236
2400	3.140	2.609	2.134	1.634	1.220
2500	3.131	2.603	2.127	1.628	1.213
2600	3.119	2.593	2.119	1.621	1.204
2700	3.106	2.582	2.111	1.615	1.196
2800	3.089	2.565	2.099	1.607	1.185
2900	3.055	2.499	2.069	1.592	1.161
3000	3.035	2.495	2.065	1.588	1.156
3100	2.993	2.457	2.043	1.577	1.140
3200	2.923	2.389	1.998	1.557	1.107
3300	2.870	2.333	1.954	1.538	1.080
3400	2.784	2.250	1.864	1.506	1.036
3500	2.808	2.273	1.881	1.511	1.042
3600	2.901	2.365	1.966	1.540	1.084
3700	2.987	2.450	2.030	1.561	1.115
3800	2.997	2.458	2.031	1.560	1.114
3900	2.990	2.453	2.027	1.557	1.109
4000	2.986	2.448	2.026	1.555	1.106

## Appendix D

### *Journal articles*

- 1) Asnachinda, E., Khaodhiar, S., and Sabatini, D. A. (2009) **Effect of Ionic Head Group on Admicelle Formation by Polymerizable Surfactants.** J Surfactants Deterg. Published online.  
(<http://www.springerlink.com/content/8710056235202v30/fulltext.pdf>).
- 2) Asnachinda, E., O'Haver, J. H., Sabatini, D. A., and Khoadhiar, S. **“Atomic Force Microscopy and Contact Angle Measurement Studied of Polymerizable Gemini Surfactant Admicelle on Mica”** Accepted (July, 2009) at Journal of Applied Polymer Science.
- 3) Asnachinda, E., Khaodhiar, S., and Sabatini, D. A. **“Styrene and Phenylethanol Adsolubilization of Polymerizable Gemini Surfactant”** submitted at Journal of Surfactants and Detergents (July, 2009).
- 4) Attaphong, C., Asnachinda, E., Charoensaeng, A., Khaodhiar, S., and Sabatini, D. A. **“Adsorption and Adsolubilization of Polymerizable Surfactants and Aluminum oxide Molecules and Extended Surfactants”** submitted (July, 2009) at Colloid and Interface Science.

**Conferences:**

- 1) Attaphong, C., Asnachinda E., Charoensaeng, A., Khaodhiar S., and Sabatini D. A. **“Adsorption and Adsolubilization Using Polymerizable Surfactants onto Aluminum Oxide Surface”**. The 98<sup>th</sup> American Oil and Chemists’ Society (AOCS) Annual Meeting and Expo, St. Quebec city, Canada, May, 2007.
- 2) Asnachinda, E., Khaodhiar, S., and Sabatini, D. A. **“Effect of Ionic Head Group on Admicelle Formation of Polymerizable Surfactants”** The 99<sup>th</sup> American Oil and Chemists’ Society (AOCS) Annual Meeting and Expo, Seattle, USA, May, 2008.
- 3) Asnachinda, E., O’Haver, J., Sabatini, D. A., and Khaodhiar, S., **“Adsorption, Adsolubilization and Corresponding AFM Studies for Polymerizable Gemini Surfactants”** The 100<sup>th</sup> American Oil and Chemists’ Society (AOCS) Annual Meeting and Expo, Orlando, USA, May, 2009.

ศูนย์วิทยทรัพยากร  
จุฬาลงกรณ์มหาวิทยาลัย

## AUTHOR BIOGRAPHY

Miss Emma Asnachinda was born on October 28, 1977, in Leicester, United Kingdom. In year 2000, she graduated in Bachelor of Engineering, Department of Environmental Engineering, Faculty of Engineering at Chiangmai University, Chiangmai, Thailand. Three years later, she received her Master's degree in the Environmental Engineering at Department of Environmental Engineering, Chulalongkorn University, Bangkok, Thailand. She pursued her philosophy of Doctoral Degree studies in National Research Center for Environmental and Hazardous Water Management (NCE-EHWM), Chulalongkorn University in October, 2005, and finished her philosophy of Doctoral Degree in July, 2009.



ศูนย์วิทยทรัพยากร  
จุฬาลงกรณ์มหาวิทยาลัย